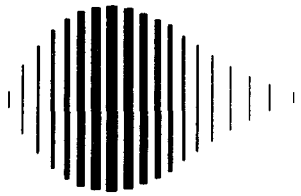

NATIONAL CENTER FOR EARTHQUAKE ENGINEERING RESEARCH

State University of New York at Buffalo

Study of Wire Rope Systems for Seismic Protection of Equipment in Buildings

by

G. F. Demetriades, M. C. Constantinou and A. M. Reinhorn

State University of New York at Buffalo
Department of Civil Engineering
Buffalo, New York 14260

Technical Report NCEER-92-0012

May 20, 1992

This research was conducted at the State University of New York at Buffalo and was partially supported by the National Science Foundation under Grant No. BCS 90-25010 and the New York State Science and Technology Foundation under Grant No. NEC-91029.

NOTICE

This report was prepared by State University of New York at Buffalo as a result of research sponsored by the National Center for Earthquake Engineering Research (NCEER) through grants from the National Science Foundation, the New York State Science and Technology Foundation, and other sponsors. Neither NCEER, associates of NCEER, its sponsors, State University of New York at Buffalo, nor any person acting on their behalf:

a. makes any warranty, express or implied, with respect to the use of any information, apparatus, method, or process disclosed in this report or that such use may not infringe upon privately owned rights; or

b. assumes any liabilities of whatsoever kind with respect to the use of, or the damage resulting from the use of, any information, apparatus, method or process disclosed in this report.

Any opinions, findings, and conclusions or recommendations expressed in this publication are those of the author(s) and do not necessarily reflect the views of NCEER, the National Science Foundation, the New York State Science and Technology Foundation, or other sponsors.

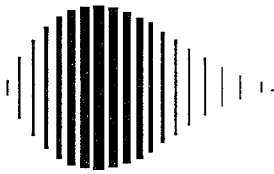

Study of Wire Rope Systems for Seismic Protection of Equipment in Buildings

by

G.F. Demetriades[1], M.C. Constantinou[2] and A.M. Reinhorn[3]

May 20, 1992

Technical Report NCEER-92-0012

NCEER Project Number 91-5211B
and
NSF Grant Number BCS 88-57080

NSF Master Contract Number BCS 90-25010
and
NYSSTF Grant Number NEC-91029

1 Research Assistant, Department of Civil Engineering, State University of New York at Buffalo
2 Associate Professor, Department of Civil Engineering, State University of New York at Buffalo
3 Professor, Department of Civil Engineering, State University of New York at Buffalo

NATIONAL CENTER FOR EARTHQUAKE ENGINEERING RESEARCH
State University of New York at Buffalo
Red Jacket Quadrangle, Buffalo, NY 14261

PREFACE

The National Center for Earthquake Engineering Research (NCEER) was established to expand and disseminate knowledge about earthquakes, improve earthquake-resistant design, and implement seismic hazard mitigation procedures to minimize loss of lives and property. The emphasis is on structures in the eastern and central United States and lifelines throughout the country that are found in zones of low, moderate, and high seismicity.

NCEER's research and implementation plan in years six through ten (1991-1996) comprises four interlocked elements, as shown in the figure below. Element I, Basic Research, is carried out to support projects in the Applied Research area. Element II, Applied Research, is the major focus of work for years six through ten. Element III, Demonstration Projects, have been planned to support Applied Research projects, and will be either case studies or regional studies. Element IV, Implementation, will result from activity in the four Applied Research projects, and from Demonstration Projects.

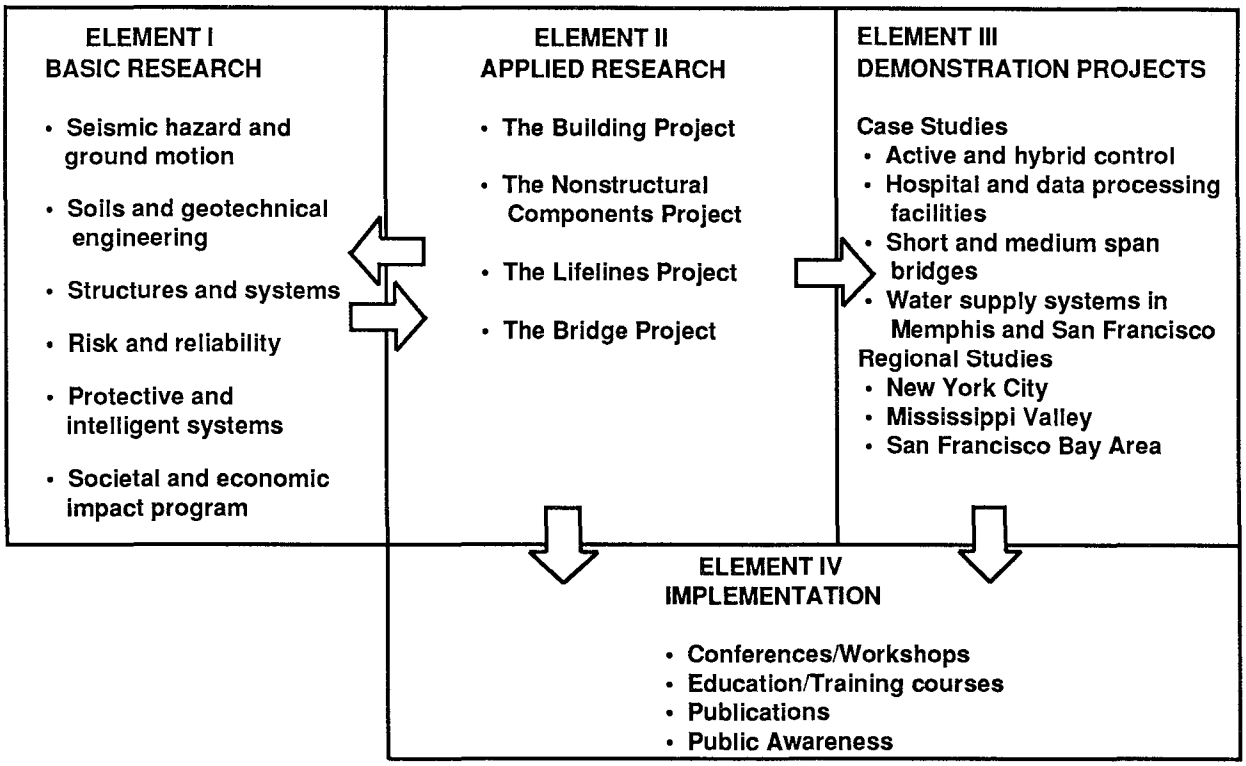

Research tasks in the **Nonstructural Components Project** focus on analytical and experimental investigations of seismic behavior of secondary systems, investigating hazard mitigation through optimization and protection, and developing rational criteria and procedures for seismic design and performance evaluation. Specifically, tasks are being performed to: (1) provide a risk analysis of a selected group of nonstructural elements; (2) improve simplified analysis so that research results can be readily used by practicing engineers; (3) protect sensitive equipment and critical

subsystems using passive, active or hybrid systems; and (4) develop design and performance evaluation guidelines.

The end product of the **Nonstructural Components Project** will be a set of simple guidelines for design, performance evaluation, support design, and protection and mitigation measures in the form of handbooks or computer codes, and software and hardware associated with innovative protection technology.

The **protective and intelligent systems program** constitutes one of the important areas of research in the **Nonstructural Components Project.** Current tasks include the following:

1. Evaluate the performance of full-scale active bracing and active mass dampers already in place in terms of performance, power requirements, maintenance, reliability and cost.
2. Compare passive and active control strategies in terms of structural type, degree of effectiveness, cost and long-term reliability.
3. Perform fundamental studies of hybrid control.
4. Develop and test hybrid control systems.

One of the passive protective systems considered in this program is the wire rope system, which has found wide applications in shock and vibration isolation of equipment. In this report, applications of this type of energy dissipation system to seismic isolation of a selected class of equipment are investigated. Both analytical and experimental work has been carried out, and the results show that stiff wire rope systems may provide some degree of protection of equipment in buildings while allowing very small displacements.

ABSTRACT

Wire rope isolators have found numerous applications in the shock and vibration isolation of military hardware and industrial machinery. In this study, the usefulness of these devices for the seismic protection of equipment in buildings is investigated. Installation methods of entirely supporting equipment on wire rope isolators and of combining them with locked casters are experimentally and analytically studied. It is found that the use of wire rope isolators in stiff configurations may substantially improve the seismic response of equipment in comparison to other installation methods.

Mathematical models for describing the hysteretic behavior of wire rope isolators are developed and experimentally calibrated and verified. Analytical predictions of seismic response are shown to be in good accord with experimental results.

ACKNOWLEDGEMENTS

Financial support has been provided by the National Center of Earthquake Engineering Research (project No. 915211B) and the National Science Foundation (Grant No. BCS 8857080). Aeroflex International, Plainview, New York and SVP Inc., West Milford, New Jersey donated the wire rope isolators used in the study. Part of the study was part of a NCEER - IBM joint project on installation methods for computer equipment.

TABLE OF CONTENTS

SECTION	TITLE	PAGE
1.	INTRODUCTION	1-1
2.	MODELING OF WIRE ROPE ISOLATORS	2-1
2.1	Testing and Modeling in Horizontal Direction	2-2
2.2	Testing and Modeling in Vertical Direction	2-5
3.	EXPERIMENTAL AND ANALYTICAL STUDY OF WIRE ROPE ISOLATION SYSTEMS FOR EQUIPMENT	3-1
3.1	Description of Equipment and Isolation System	3-1
3.2	Instrumentation and Experimental Program	3-2
3.3	Test Results	3-4
3.4	Analytical Investigation of a Very Stiff Wire Rope System	3-8
4.	ANALYTICAL PREDICTION OF RESPONSE	4-1
4.1	Equations of Motion for Large Rotations	4-2
4.2	Equations of Motion for Small Rotations	4-5
4.3	Simplified Analysis Procedure	4-7
4.4	Comparison of Experimental and Analytical Results	4-11
5.	COMBINED WIRE ROPE AND CASTER SUPPORT SYSTEM FOR EQUIPMENT - COMPARATIVE EXPERIMENTAL STUDY	5-1
5.1	Description of Equipment and Support System	5-1
5.2	Experimental Results and Comparison to other Installation Methods	5-3
5.3	Analytical Prediction of Response	5-6
6.	CONCLUSIONS	6-1
7.	REFERENCES	7-1

LIST OF ILLUSTRATIONS

FIGURE	TITLE	PAGE
1-1	(a) 8 - Coil Helical Wire Rope Isolator (b) 4 - Coil Arch Wire Rope Isolator.	1-6
2-1	Geometrical Characteristics of Helical and Arch Wire Rope Isolators.	2-13
2-2	Arrangement for Testing Wire Rope Isolators (No.1 to 4) in Roll Direction.	2-14
2-3	Parameters in Bilinear Model.	2-15
2-4	Comparison of Experimental and Analytical Force - Displacement Loops of Isolator No.1 subjected to Roll Motion.	2-16
2-5	Comparison of Experimental and Analytical Force - Displacement Loops of Isolator No.2 subjected to Roll Motion.	2-17
2-6	Comparison of Experimental and Analytical Force - Displacement Loops of Isolator No.3 subjected to Roll Motion.	2-18
2-7	Arrangement for Testing Wire Rope Isolators (No.5) while Maintaining Constant Height.	2-19
2-8	Comparison of Experimental and Analytical Force - Displacement Loops of Isolator No.5 subjected to Shear Motion.	2-20

LIST OF ILLUSTRATIONS (Cont'd)

FIGURE	TITLE	PAGE
2-9	Arrangement for Testing Wire Rope Isolators in Compression - Tension.	2-21
2-10	Typical Force - Displacement Loop of Wire Rope Isolators in Compression - Tension.	2-22
2-11	Force - Displacement Loops in Compression - Tension for Cyclic Motion.	2-23
2-12	Comparison of Experimental and Analytical Force - Displacement Loops of Isolator No.1 subjected to Compression - Tension.	2-24
2-13	Comparison of Experimental and Analytical Force - Displacement Loops of Isolator No.2 subjected to Compression - Tension.	2-26
2-14	Comparison of Experimental and Analytical Force - Displacement Loops of Isolator No.3 subjected to Compression - Tension.	2-29
2-15	Comparison of Experimental and Analytical Force - Displacement Loops of Isolator No.4 subjected to Compression - Tension.	2-32
3-1	Tested Equipment Cabinet.	3-20
3-2	Views of Isolated Cabinet on Shake Table (a) Transverse View, (b) Isolation System (No.3).	3-21
3-3	Instrumentation Diagram.	3-22

LIST OF ILLUSTRATIONS (Cont'd)

FIGURE	TITLE	PAGE
3-4	Location of Instruments.	3-23
3-5	Time History of Ground Acceleration of Taft N21E Motion and its Acceleration and Displacement Response Spectra.	3-24
3-6	Time History of 5th Floor Acceleration of 7-story Building Excited by Taft N21E Motion and its Acceleration and Displacement Response Spectra.	3-25
3-7	Time History of 7th Floor Acceleration of 7-story Building Excited by Taft N21E Motion and its Acceleration and Displacement Response Spectra.	3-26
3-8	Time History of Ground Acceleration of El Centro S00E Motion and its Acceleration and Displacement Response Spectra.	3-27
3-9	Time History of 5th Floor Acceleration of 7-story Building Excited by El Centro S00E Motion and its Acceleration and Displacement Response Spectra.	3-28
3-10	Time History of 7th Floor Acceleration of 7-story Building Excited by El Centro S00E Motion and its Acceleration and Displacement Response Spectra.	3-29

LIST OF ILLUSTRATIONS (Cont'd)

FIGURE	TITLE	PAGE
3-11	Time History of Ground Acceleration of Pacoima Dam S74W Motion and its Acceleration and Displacement Response Spectra.	3-30
3-12	Displacement Histories of Center of Mass of Isolated Equipment in Pull-Release Tests.	3-31
3-13	Moment-Rotation Loops of Isolated Cabinet in Test with Taft 7th Floor Excitation.	3-32
3-14	Moment-Rotation Loops of System 4.	3-33
4-1	Model of Equipment supported by Wire Rope Isolators.	4-17
4-2	Free Body Diagram of Equipment.	4-18
4-3	Comparison of Experimental and Analytical Time Histories of Horizontal Displacement of Level 1 for Taft Ground Motion.	4-19
4-4	Comparison of Experimental and Analytical Time Histories of Horizontal Displacement of Level 1 for Taft 5th Floor Motion.	4-20
4-5	Comparison of Experimental and Analytical Time Histories of Horizontal Displacement of Level 1 for Taft 7th Floor Motion.	4-21

LIST OF ILLUSTRATIONS (Cont'd)

FIGURE	TITLE	PAGE
4-6	Comparison of Experimental and Analytical Time Histories of Horizontal Displacement of Level 1 for El Centro Ground Motion.	4-22
4-7	Comparison of Experimental and Analytical Time Histories of Horizontal Displacement of Level 1 for El Centro 5th Floor Motion.	4-23
4-8	Comparison of Experimental and Analytical Time Histories of Horizontal Displacement of Level 1 for El Centro 7th Floor Motion.	4-24
4-9	Comparison of Experimental and Analytical Time Histories of Horizontal Displacement of Level 1 for Pacoima Ground Motion.	4-25
4-10	Comparison of Experimental and Analytical Time Histories of Horizontal Displacement of Top for Taft 7th Floor Motion.	4-26
4-11	Comparison of Experimental and Analytical Time Histories of Horizontal Displacement of Top for El Centro Ground Motion.	4-27
4-12	Comparison of Experimental and Analytical Time Histories of Horizontal Displacement of Top for El Centro 7th Floor Motion.	4-27
4-13	Comparison of Experimental and Analytical Time Histories of Horizontal Isolator Displacement for Taft 7th Floor Motion.	4-28

LIST OF ILLUSTRATIONS (Cont'd)

FIGURE	TITLE	PAGE
4-14	Comparison of Experimental and Analytical Time Histories of Horizontal Isolator Displacement for El Centro Ground Motion.	4-29
4-15	Comparison of Experimental and Analytical Time Histories of Horizontal Isolator Displacement for El Centro 7th Floor Motion.	4-29
4-16	Comparison of Experimental and Analytical Time Histories of Vertical Isolator Displacement for Taft 7th Floor Motion.	4-30
4-17	Comparison of Experimental and Analytical Time Histories of Vertical Isolator Displacement for El Centro 7th Floor Motion.	4-31
4-18	Comparison of Experimental and Analytical Time Histories of Horizontal Acceleration of Level 1 for Taft 7th Floor Motion.	4-32
4-19	Comparison of Experimental and Analytical Time Histories of Top Horizontal Acceleration for Taft 7th Floor Motion.	4-32
4-20	Comparison of Experimental and Analytical Time Histories of Horizontal Acceleration of Level 1 for El Centro 7th Floor Motion.	4-33
4-21	Comparison of Experimental and Analytical Time Histories of Top Horizontal Acceleration for El Centro 7th Floor Motion.	4-33

LIST OF ILLUSTRATIONS (Cont'd)

FIGURE	TITLE	PAGE
4-22	Analytical Moment - Rotation Loops of System 1 for Harmonic Excitation.	4-34
5-1	View of IBM 9370 Computer Equipment on Raised Floor and Shake Table.	5-11
5-2	Schematic Representation of IBM 9370 Computer Equipment on Shake Table and Instrumentation Diagram.	5-12
5-3	Response Spectra at Raised Floor of a 5% Damped System for Taft 7th Floor and El Centro 7th Floor Motion.	5-13
5-4	Details of Installation of Wire Rope Isolators with Uplift Restrainer.	5-14
5-5	Response of Frictional Oscillator of Taft 7th Floor at Raised Floor Level.	5-16
5-6	Response of Frictional Oscillator of El Centro 7th Floor at Raised Floor Level.	5-17
5-7	Comparison of Experimental and Analytical Time Histories of Displacement of Casters in Tested IBM Equipment.	5-18

LIST OF TABLES

TABLE	TITLE	PAGE
2-I	Geometrical Characteristics of Tested Wire Rope Isolators.	2-10
2-II	Parameters of Model of Isolators in Roll and Shear Directions.	2-11
2-III	Coefficients in Function F_0 of Model of Wire Rope Isolators in Vertical Direction.	2-12
2-IV	Coefficients of Function F_D of Model of Wire Rope Isolators in Vertical Direction.	2-12
3-I	Characteristics of Earthquake Excitation in Testing Program.	3-10
3-II	Recorded Peak Response of Isolated Equipment for Taft Ground Motion.	3-11
3-III	Recorded Peak Response of Isolated Equipment for Taft 5th Floor Motion.	3-12
3-IV	Recorded Peak Response of Isolated Equipment for Taft 7th Floor Motion.	3-13
3-V	Recorded Peak Response of Isolated Equipment for El Centro Ground Motion.	3-14
3-VI	Recorded Peak Response of Isolated Equipment for El Centro 5th Floor Motion.	3-15

LIST OF TABLES (Cont'd)

TABLE	TITLE	PAGE
3-VII	Recorded Peak Response of Isolated Equipment for El Centro 7th Floor Motion.	3-16
3-VIII	Recorded Peak Response of Isolated Equipment for Pacoima Ground Motion.	3-17
3-IX	Relation Between Quantities in Tables of Response and Recording Instruments.	3-18
3-X	Dynamic Characteristics of Isolated Cabinet as Determined from Pull-Release Tests.	3-18
3-XI	Analytical Peak Response of Equipment System 4 and Experimental Peak Response of Fixed Cabinet.	3-19
4-I	Comparison of Experimental and Analytical Peak Response Values.	4-13
4-II	Properties of System 1 Extracted from Moment - Rotation Loops of Fig. 4-22.	4-15
4-III	Characteristics of System 1 used in Simplified Analysis.	4-16
5-I	Recorded Peak Response of IBM Equipment with Wire Rope Isolators.	5-8
5-II	Comparison of Peak Response of Equipment with Different Installation Methods for Taft 7th Floor Input.	5-9

LIST OF TABLES (Cont'd)

TABLE	TITLE	PAGE
5-III	Comparison of Peak Response of Equipment with Different Installation Methods for El Centro 7th Floor Input.	5-10

SECTION 1

INTRODUCTION

Seismic base isolation is a design technique that is becoming widely accepted and is being studied with continually increasing interest. The principle of seismic isolation is to introduce an interface at the base of a structure that can attenuate the magnitude of the horizontal movement of the ground transmitted to the structure during an earthquake. This results in a significant reduction in floor accelerations, story shears and interstory drifts, thus providing protection to the structure itself as well as to all items and equipment mounted on the structure (Kelly 1982, 1985, 1988; Zayas 1987; Chalhoub 1988, 1990; Tsai 1989; Buckle 1990; Mokha 1990, 1991; Constantinou 1990b, 1991; Manolis 1990; Juhn 1992).

The reduction of the seismic forces imparted to the structural system is achieved by introducing flexibility and energy absorption capability in the isolation system. The introduction of flexibility increases the fundamental period of the isolated structure to values well above the predominant period of the earthquake excitation so that the isolation effect is primarily produced by deflection of the earthquake energy (Kelly 1991). This desirable effect is, however, produced at the expense of large isolation system displacements which are in the range of 8 to 20 in. (200 to 500 mm) for strong earthquake excitation. While the

displacements appear to be large, they are in reality small in comparison to the building dimensions and can be accommodated by the isolation system without, usually, instability problems.

The same principle may be used to isolate and directly protect sensitive equipment housed mainly in conventionally constructed buildings where the high floor accelerations during an earthquake can be catastrophical for them.

However, earthquake motions, when transmitted through conventionally constructed buildings, which in strong excitation respond inelastically, reach the upper floors amplified and with their frequency content spread over a wide range of frequencies (Singh 1988; Lin 1985; Chen 1988). Isolation in this case becomes difficult. To achieve effective isolation, it is necessary to increase the period of the isolated equipment to large values which typically are larger than those required for effective isolation of buildings. This results in displacements which are unacceptably large for single equipment. Furthermore, the construction of very flexible isolation systems for single equipment is impractical because such systems are usually not capable of carring the weight of the supported equipment.

To counteract these problems, the Japanese construction industry developed elaborate isolation systems for computer floors which support a large number of equipment

(Fujita 1991). These systems utilize either low friction sliding bearings, or multi-stage rubber bearings, or pneumatic isolators.

The seismic protection of single equipment may be also achieved not by lengthening their period and thus deflecting the earthquake energy but by absorbing earthquake energy through a stiff and highly energy-dissipative system. Such a system may provide a degree of protection while allowing relatively small displacements. Makris 1992a and 1992b reported experimental results on a system consisting of helical steel springs immersed in highly viscous fluid for seismic protection of equipment. The system was used to support a slender equipment cabinet which was subjected to strong floor seismic motions. The system, which resulted in a frequency of 3.5 Hz in the isolated equipment, was capable of reducing accelerations by a factor of 2 in comparison to the non - isolated equipment, while allowing displacements at the isolation level which did not exceed 0.4 in.(10 mm). This spring - viscous damper system evolved from a widely used vibration isolation system.

Herein another system which is widely used in shock and vibration isolation of equipment is investigated for use as a seismic isolation system. Wire rope isolators are mounting assemblies made of stranded wire rope which is wound in the form of a helix and held between metal retainers (Fig. 1-1a). In a further development, arch wire rope isolators are

formed by two groups of oppositely inclined, arch-like, open - bottom wire rope elements which are clamped between retainer bars (Fig. 1-1b).

Both helical and arch wire rope isolators consist of twisted stainless steel cable. They have flexibility in all three directions, large displacement capacity and inherent damping which results from rubbing and sliding friction between the intertwined cables. Their ability to absorb energy is simultaneous in all three directions. These isolators have found numerous applications in the shock and vibration isolation of industrial and defense equipment, electronic systems, critical machinery and other sensitive equipment.

In applications of shock and vibration isolation, wire rope isolators support the weight of the isolated system. Typically, the isolated system has fundamental frequency of the order of 10 Hz. Their energy dissipation capacity is, in terms of equivalent viscous damping ratio, about 0.1 to 0.2 of critical under small amplitude motion. The aforementioned frequency of about 10 Hz is that of a vertical or a horizontal mode of vibration since, typically, equipment are either squatty or are prevented from undergoing rocking motion. This is accomplished by attaching the equipment to a wall by wire rope isolators.

This study investigates the use of wire rope isolators as a means of providing seismic protection to single slender equipment which are only attached to vibrating floors.

First, helical and arch type wire rope isolators were used to support a slender equipment cabinet in four different configurations. The isolators provided a fundamental frequency (in the rocking mode) in the range of 1 to about 6 Hz in the four systems. Second, helical wire rope isolators were used to provide only restoring force in a computer equipment supported by locked casters. The fundamental frequency in this case was about 3.4 Hz. The isolated equipment were subjected on a shake table to floor excitation which was determined by filtering recorded earthquake motions through an actual 7-story building. Experimental results were also obtained for the equipment being either fixed to the floor or connected to the floor by other commonly used means. It was found that for certain configurations of wire rope isolators, it was possible to achieve substantial reduction of the acceleration transmission to the isolated equipment in comparison to other conventional means of support of the equipment. The results of this study are reported herein. Furthermore, analytical models describing the dynamic behavior of wire rope isolators are developed, calibrated and presented. The models are capable of describing,with good accuracy, the observed dynamic response of the tested equipment.

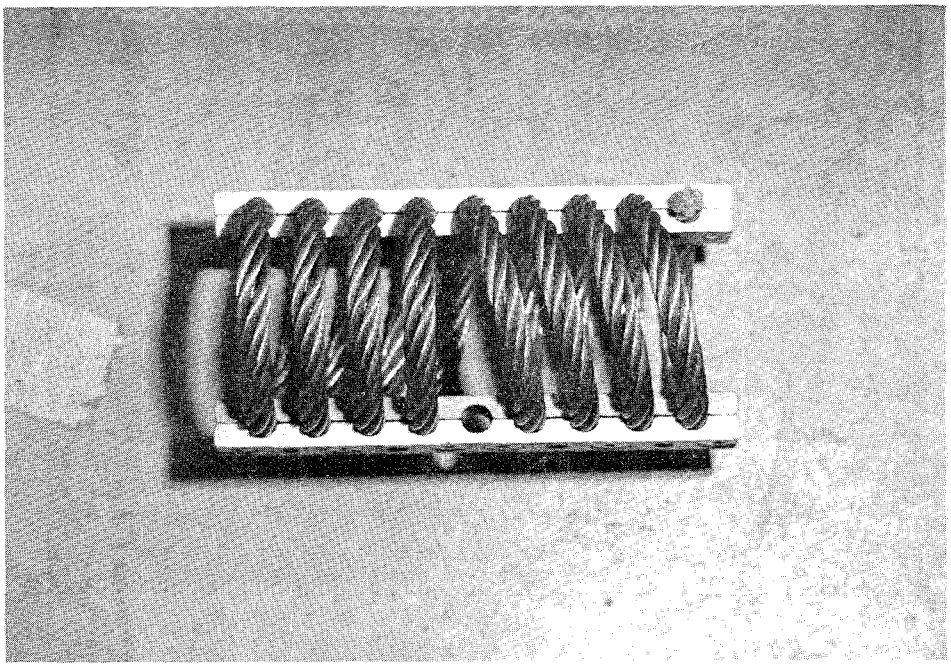

(a)

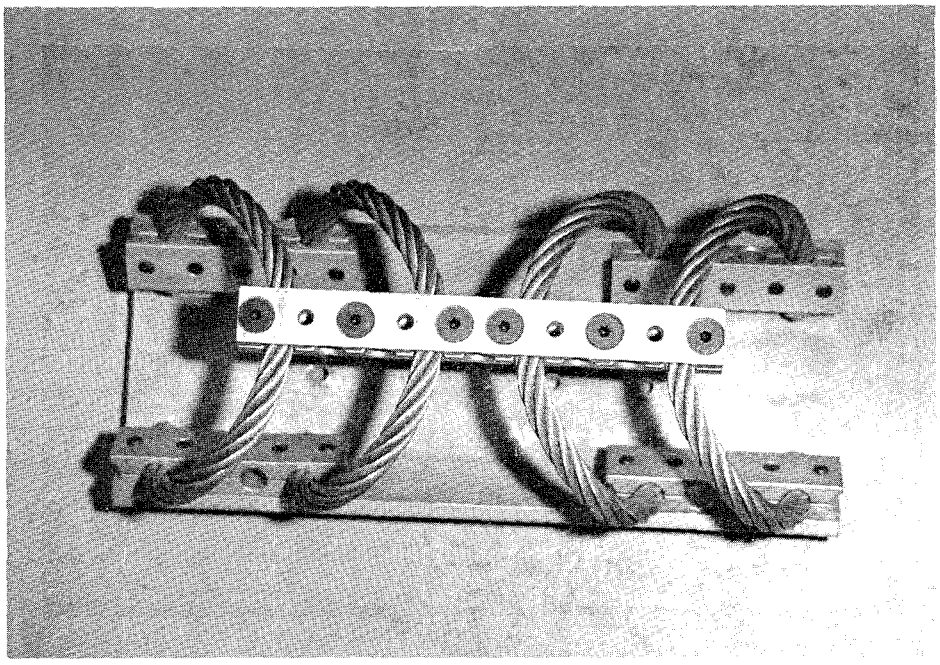

(b)

Figure 1-1 (a) 8-Coil Helical Wire Rope Isolator,
(b) 4-Coil Arch Wire Rope Isolator

SECTION 2

MODELING OF WIRE ROPE ISOLATORS

Wire rope isolators have different response characteristics depending on the diameter of the wire rope, the number of strands, the cable length, the cable twist, the number of cables per section and on the direction of the applied force.

To determine their dynamic characteristics in the horizontal and vertical directions, a series of dynamic tests was conducted on a number of isolators by imposing cyclic sinusoidal motion of specified amplitude, frequency and initial force. In both cases a hydraulic actuator, which was driven in displacement - controlled mode, was used to impose the motion and a load cell that was placed between the isolator and the actuator recorded the applied forces.

Five wire rope isolators were selected for testing. Their geometrical characteristics are presented in Table 2-I with reference to Figure 2-1. The first four of these isolators were later used in the isolation of an equipment cabinet in which the isolators supported its weight. During shake table testing, these isolators were subjected to simultaneous compression/tension and roll motions (see Fig. 2-1). Accordingly, component testing was restricted to only these two directions. The fifth isolator (No.5 in Table 2-I) was used in the isolation of a computer equipment which was

supported by casters. In this application, the isolators were subjected to only shearing motion (see Fig. 2-1) without allowance for vertical motion. They were, accordingly, tested only in that direction.

Wire rope isolators exhibit non-linear hysteretic behavior. In applications in which the isolators carry the weight of the isolated equipment, they are subjected to simultaneous motions in all three directions. It is, thus, expected that the forces which develop in these three directions exhibit interaction. In modeling the behavior of the isolators, it was assumed that this interaction is not important and that each isolator may be modeled by three hysteretic non-interacting spring elements placed along the three principal directions (vertical, roll and shear).

2.1 Testing and Modeling in Horizontal Direction.

Isolators No. 1 to 4 (Table 2-I) were tested in the roll direction by the arrangement of Figure 2-2. The arrangement could impose motion in the roll direction while allowing for some limited displacement in the vertical direction. This resembled the behavior of the isolators in actual use in which they are allowed to reduce in height during horizontal deformation. However, the arrangement could not precisely simulate the actual conditions, so that some stiffening of the isolators was observed at large horizontal displacements. This stiffening was disregarded in the modeling.

Tests were conducted by imposing five cycles of motion of frequencies of 0.1, 1, 2 and 5 Hz and amplitude of 0.25, 0.5 and 0.75 inches (6.4, 12.7 and 19.1 mm). Recorded force -displacement loops showed stable hysteretic behavior for all five cycles, symmetry and independency to frequency.

The recorded behavior represented classical hysteretic behavior and could be easily modeled by the smooth bilinear hysteretic model of Bouc, 1971. The model, in its more general form of Wen, 1976 is

$$F = \alpha \frac{F_y}{Y} U + (1-\alpha) F_y Z \qquad (2\text{-}1)$$

where F = force, U = displacement and Z is a hysteretic dimensionless quantity given by the following differential equation :

$$Y\dot{Z} + \gamma |\dot{U}| Z |Z|^{n-1} + \beta \dot{U} |Z|^n - A\dot{U} = 0 \qquad (2\text{-}2)$$

In the above equations α, β, γ, A and n are dimensionless quantities that control the shape of the hysteretic loop, and F_y and Y are the yield force and yield displacement, respectively. A dot denotes differentiation with respect to time.

It should be noted that for A = 1 and $\beta+\gamma=1$, Constantinou and Adnane, 1987 have shown that the model

collapses to a model of viscoplasticity that was proposed by Ozdemir, 1976. For the analytical modeling of wire rope isolators, the values of β= 0.1, γ=0.9, A=1 and n=1 were used. Appropriate values for the yield displacement, Y, were evaluated from the experimental results with F_y and α calculated in each case by the following equations:

$$F_y = Q + K_x Y \tag{2-3}$$

$$\alpha = \frac{K_x Y}{F_y} \tag{2-4}$$

where Q is the characteristic strength and K_x is the stiffness in the roll direction according to the bilinear model depicted in Figure 2-3. It should be noted that α represents the ratio of post-yielding to pre-yielding stiffnesses.

The parameters of the model in the roll direction of isolators No.1 to 4 are given in Table 2-II. Comparisons of experimental and analytical force - displacement loops are presented in Figures 2-4 to 2-6. It may seen that the analytical model predicts well the experimental results.

Testing of isolator No.5 was conducted with a different arrangement which maintained constant height of the isolator during deformation in shear. Figure 2-7 shows the testing arrangement. Two isolators were connected to a plate which was driven by an actuator. Results for a single isolator were obtained by dividing the recorded force by two. The

behavior in shear of isolator No.5 was qualitatively the same as that of the other isolators in roll. The model of equations 2-1 and 2-2 reproduced well the experimental response as illustrated in Figure 2-8. The parameters of the model are given in Table 2-II.

2.2 Testing and Modeling in Vertical Direction.

All isolators were tested in the vertical (compression - tension) direction by the arrangement of Figure 2-9. The hysteretic behavior of the isolators in the vertical direction exhibited asymmetry due to different stiffnesses in tension and in compression. Figure 2-10 provides evidence for this behavior. The shown force - displacement loop in compression -tension is for isolator No.3. In compression, the isolator exhibits essentially elastoplastic behavior while in tension it exhibits an increasingly stiffening behavior. Figure 2-11 shows loops of the same isolator when subjected to cyclic motion at frequencies ranging from 0.1 to 5 Hz. The differences on the tension side among the various loops are due primarily to the inertia effects of the testing arrangement and the fact that the amplitude of 0.5 inch (12.7 mm) was not achieved in all cycles. It should be noted that energy dissipation, as expressed by the difference between the loading and unloading branches of the loops, is different in tension than it is in compression.

Hysteretic models for describing asymmetric behavior of the type shown in Figures 2-10 and 2-11 could be derived by a modification of the model of equations 2-1 and 2-2. The force - displacement relation is written in the form

$$F = F_O(U) + F_D(U)\,Z \tag{2-5}$$

in which F_0 represents the displacement (U) - dependent skeleton curve and $F_D(U)$ is the also displacement - dependent half difference between the loading and unloading branches of the loop. Z is a hysteretic dimensionless quantity taking values in the interval [-1, 1] and is described by equation 2-2. The two parts of equation 2-5 describe, respectively, stiffness and hysteretic energy dissipation.

Experimental force - displacement loops, like the one of Figure 2-10, indicated that functions F_0 and F_D could be expressed in the form:

$$F_O(U) = Q_1.[A_0 - \exp(\sum_{n=1}^{N} a_n.U^n)] \tag{2-6}$$

$$F_D(U) = Q_2.\exp[\sum_{m=0}^{M} b_m.U^m)] \tag{2-7}$$

in which Q_1, A_0, a_n, N, Q_2, M and b_m are coefficients derived from regression analysis of experimental results for each isolator. Values of these coefficients for the tested wire rope isolators are presented in Tables 2-III and 2-IV.

For a complete description of the model of equations 2-2 and 2-5 to 2-7 it is required that parameters β, γ, A and n in equation 2-2 are determined. For this, an investigation of equation 2-2 is in order. Analytical solutions of this equation are possible for the ascending and, separately, for the descending branches of the Z - U loop. Concentrating on the ascending branch for which Z and $\dot{U}$ are larger than zero, we write equation 2-2 in the form

$$\dot{Z} + (\beta + \gamma) Z^n \left(\frac{\dot{U}}{Y}\right) = A\left(\frac{\dot{U}}{Y}\right) \tag{2-8}$$

The solution is (Kamke 1959)

$$Z = \left(-\frac{A}{\beta + \gamma}\right)^{\frac{1}{n}} . y(t) \tag{2-9}$$

$$\int \frac{dy}{1 + y^n} = A\left(-\frac{\beta + \gamma}{A}\right)^{\frac{1}{n}} \left(\frac{U}{Y}\right) + C \tag{2-10}$$

where C is a constant of integration. Furthermore, equation 2-8 may be written as

$$Y \frac{dZ}{dU} = A - (\beta + \gamma) Z^n \tag{2-11}$$

from where in the limit $\frac{dZ}{dU} = 0$ the maximum value of Z is obtained

$$Z_{max} = \left(\frac{A}{\beta+\gamma}\right)^{\frac{1}{n}} \qquad (2\text{-}12)$$

The solution for the descending branch is given by equations 2-9 and 2-10 but with Z replaced by -Z and $\beta+\gamma$ by - $(\beta+\gamma)$.

Equations 2-9 and 2-10 reveal that the model of equation 2-2 is rate - independent, i.e. independent of the value of velocity. Rather, only the sign of velocity determines the ascending and descending branches. Furthermore, equation 2-12 restricts the values of constants A, β and γ to A = $\beta+\gamma$ so that Z_{max} = 1. Explicit expressions for Z are possible only for n=1 or 2:

$$Z = \frac{A}{\beta+\gamma}\left\{1 - \exp\left[-(\beta+\gamma)\frac{U}{Y}\right]\right\} + C, \quad \text{for} \quad n = 1 \qquad (2\text{-}13)$$

$$Z = \left(\frac{A}{\beta+\gamma}\right)^{\frac{1}{2}} \tanh\left[(\beta+\gamma)^2 \frac{U}{Y}\right] + C, \qquad \text{for} \quad n = 2 \qquad (2\text{-}14)$$

For A = $\beta+\gamma$ as required for Z_{max} = 1, equations 2-13 and 2-14 show that Z represents a smooth approximation to the unit step function. Increasing values of n result in approximations that are closer to the step function with the case $n \to \infty$ presumably reproducing the step function itself. Interestingly, the actual values of constants β and γ do not play any role. Rather, only their sum plays a role.

Based on the conclusions of this analytical solution and comparisons of experimental and analytical compression - tension loops, the following values were selected : A=3.0,

β=0.0, γ=3.0 (A = β+ γ) and n=1. Values of displacement quantity Y were different for each isolator as shown in Table 2-IV. Comparisons of experimental and analytical force - displacement loops of the four isolators in compression - tension mode are presented in Figures 2-12 to 2-15. Each of these loops is for a specific initial compression force imposed to the isolator prior to initiation of the cyclic motion and for five cycles of motion. The loops for the stiff isolator No.4 are for small amplitudes of displacement. Evidently the analytical model predicts the experimental behavior with good accuracy.

Table 2-I - Geometrical Characteristics of Tested Wire Rope Isolators (1 in.= 25.4 mm)

DESIGNATION	TYPE	TESTING DIRECTION	NUMBER OF COILS	DIAMETER OF ROPE (inch)	L (inch)	W (inch)	H (inch)
ISOLATOR 1	ARCH	COMPR/ROLL	2	0.500	11.25	4.60	4.75
ISOLATOR 2	HELICAL	"	8	0.500	7.00	5.60	4.90
ISOLATOR 3	ARCH	"	4	0.500	11.25	4.60	4.75
ISOLATOR 4	HELICAL	"	8	0.625	10.50	6.00	4.70
ISOLATOR 5	HELICAL	SHEAR	8	0.375	8.50	4.13	3.00

Table 2-II - Parameters of Model of Isolators in Roll and Shear Directions

(1 in.= 25.4 mm, 1 Kip = 4.46 kN)

	DIRECTION	K_x (Kip/in)	Y (inch)	Q (Kip)	F_y (Kip)	α
ISOLATOR 1	ROLL	0.172	0.010	0.013	0.0147	0.1169
ISOLATOR 2	ROLL	0.171	0.010	0.028	0.0294	0.0581
ISOLATOR 3	ROLL	0.365	0.015	0.030	0.0355	0.1543
ISOLATOR 4	ROLL	0.684	0.015	0.100	0.1103	0.0931
ISOLATOR 5	SHEAR	0.240	0.010	0.014	0.0164	0.1463

Table 2-III - Coefficients in Function F_0 of Model of Wire Rope Isolators in Vertical Direction (1 in.= 25.4 mm, 1 Kip = 4.46 kN)

	Q_1 (Kip)	A_0	N	a_1 (in^{-1})	a_2 (in^{-2})	a_3 (in^{-3})
ISOLATOR 1	-0.290	1.00	3	1.7860	0.3510	0.202
ISOLATOR 2	-0.790	1.04	3	0.8523	-0.0367	0.151
ISOLATOR 3	-0.470	1.00	1	2.0797	-	-
ISOLATOR 4	-0.905	1.00	3	1.3120	-0.5730	0.336

Table 2-IV - Coefficients of Function F_D of Model of Wire Rope Isolators in Vertical Direction (1 in.= 25.4 mm, 1 Kip = 4.46 kN)

	Coefficients of Function F_D						Y (in)
	Q_2 (Kip)	M	b_0	b_1 (in^{-1})	b_2 (in^{-2})	b_3 (in^{-3})	
ISOLATOR 1	0.001	3	3.555	1.5734	1.132	0.252	0.100
ISOLATOR 2	0.001	1	4.701	0.6496	-	-	0.100
ISOLATOR 3	0.001	1	4.090	0.8960	-	-	0.100
ISOLATOR 4	0.001	1	5.882	1.2300	-	-	0.055

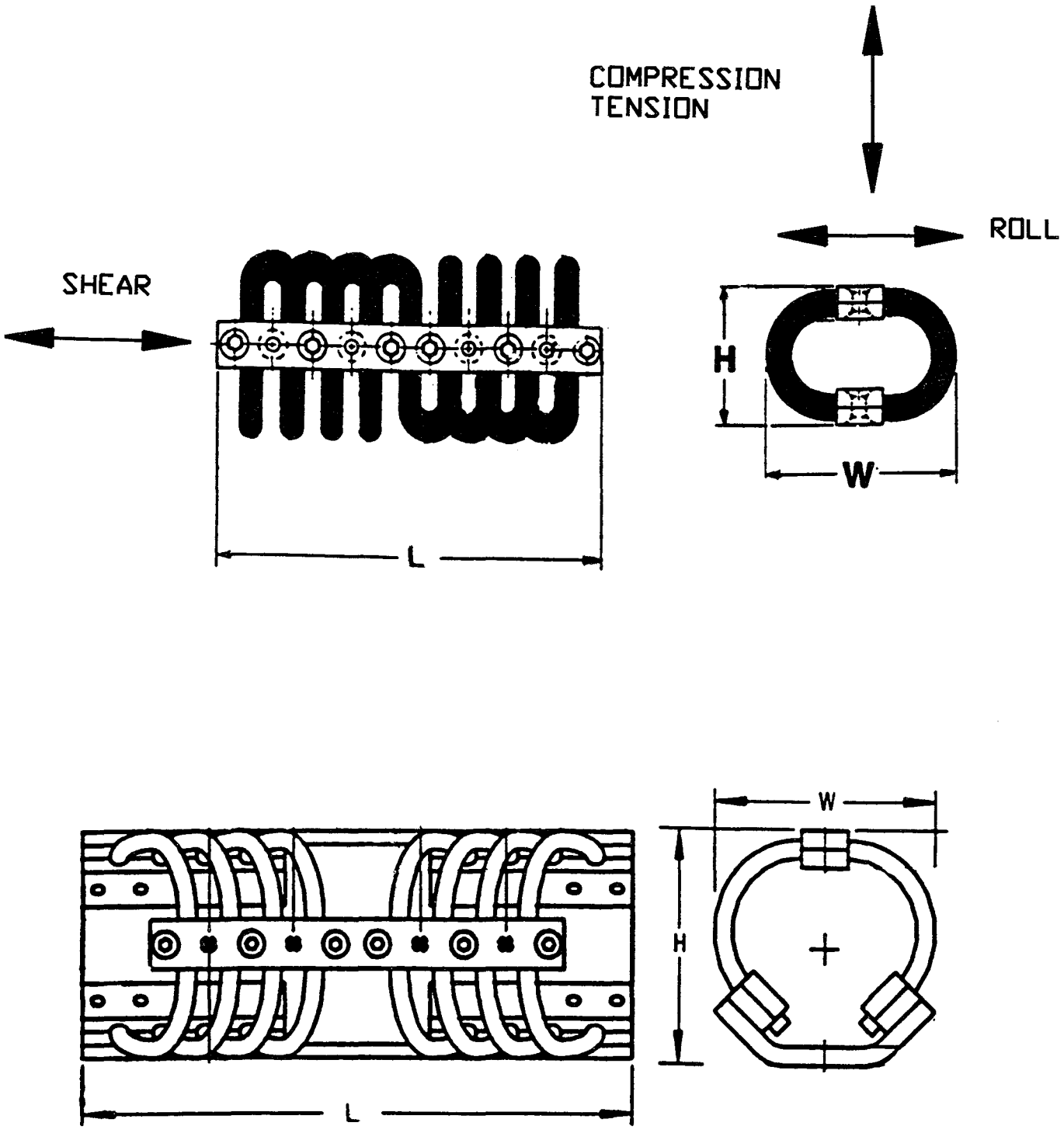

Figure 2-1 Geometrical Characteristics of Helical and Arch Wire Rope Isolators.

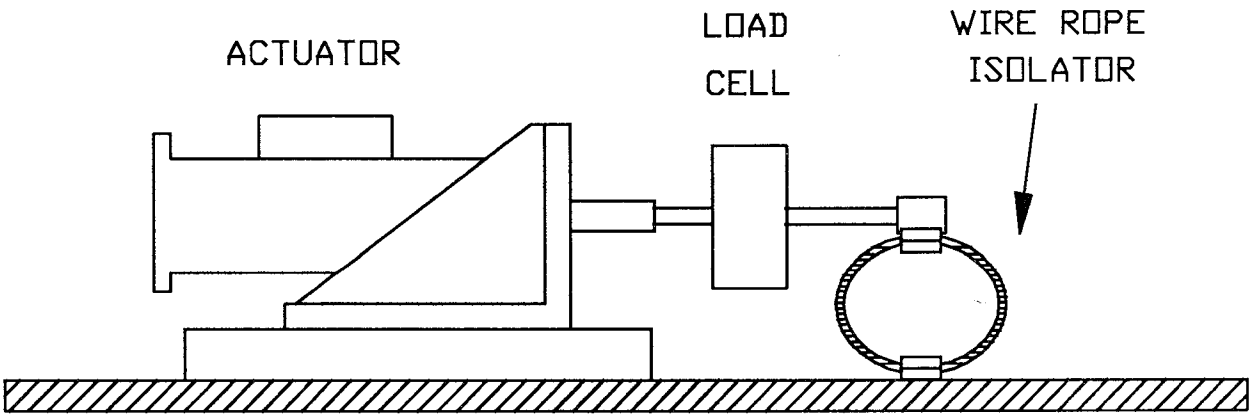

Figure 2-2 Arrangement for Testing Wire Rope Isolators (No.1 to 4) in Roll Direction.

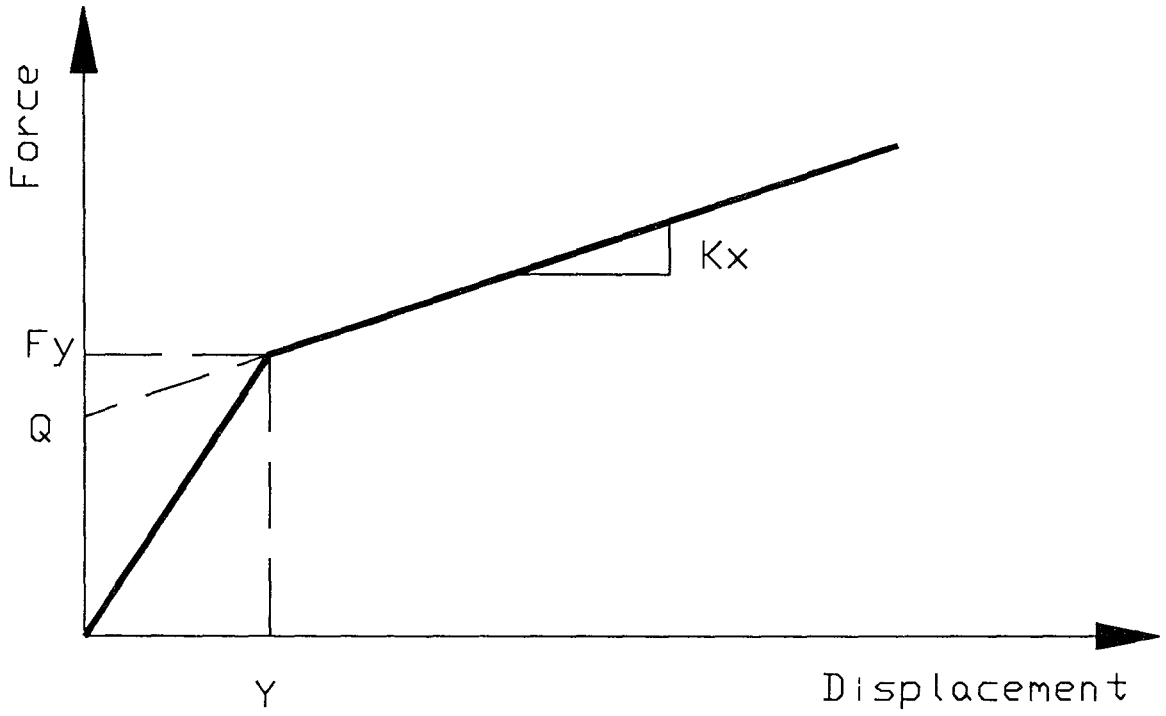

Figure 2-3 Parameters in Bilinear Model.

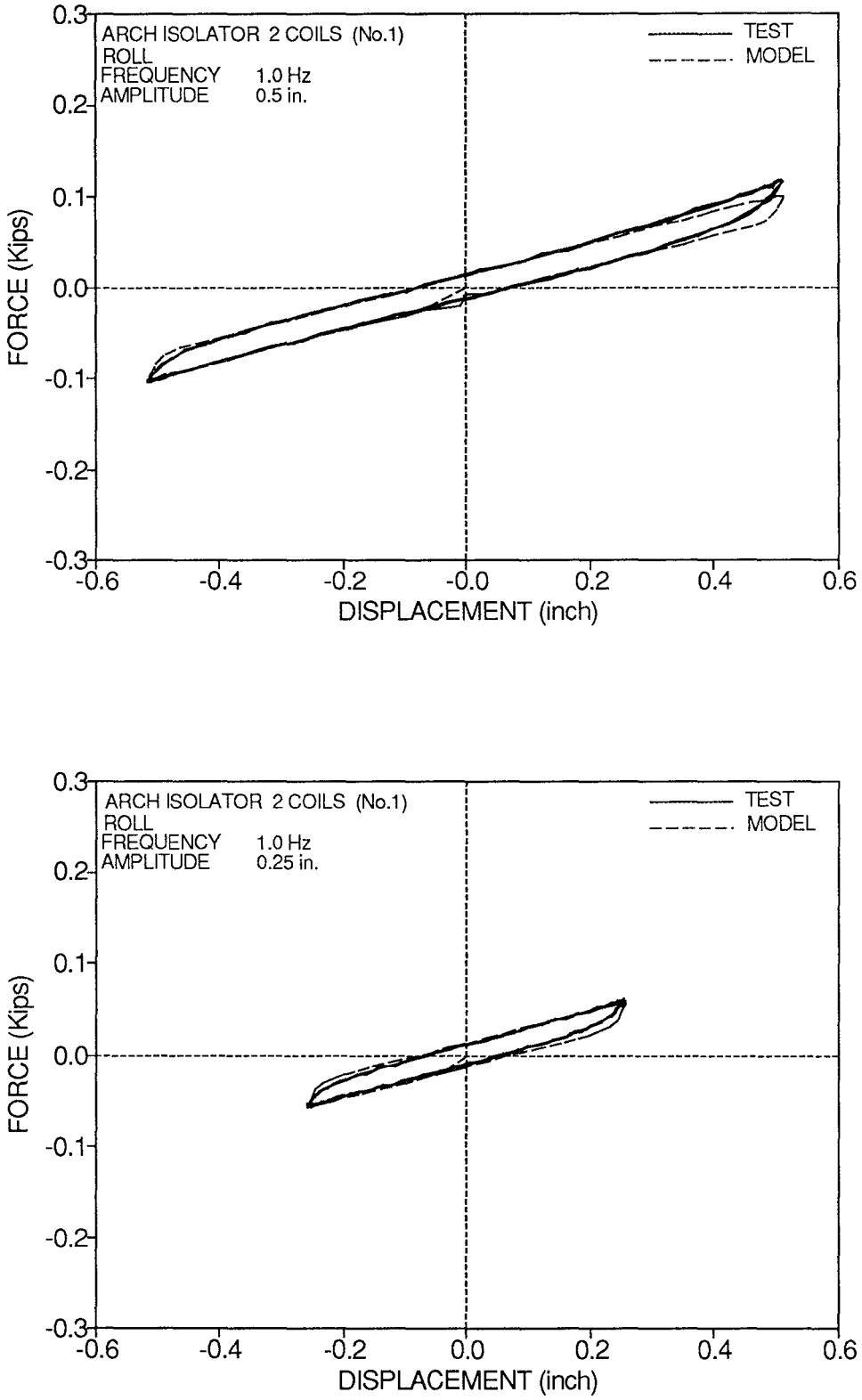

Figure 2-4 Comparison of Experimental and Analytical Force - Displacement Loops of Isolator No.1 subjected to Roll Motion (1 in.= 25.4 mm, 1 Kip= 4.46 kN).

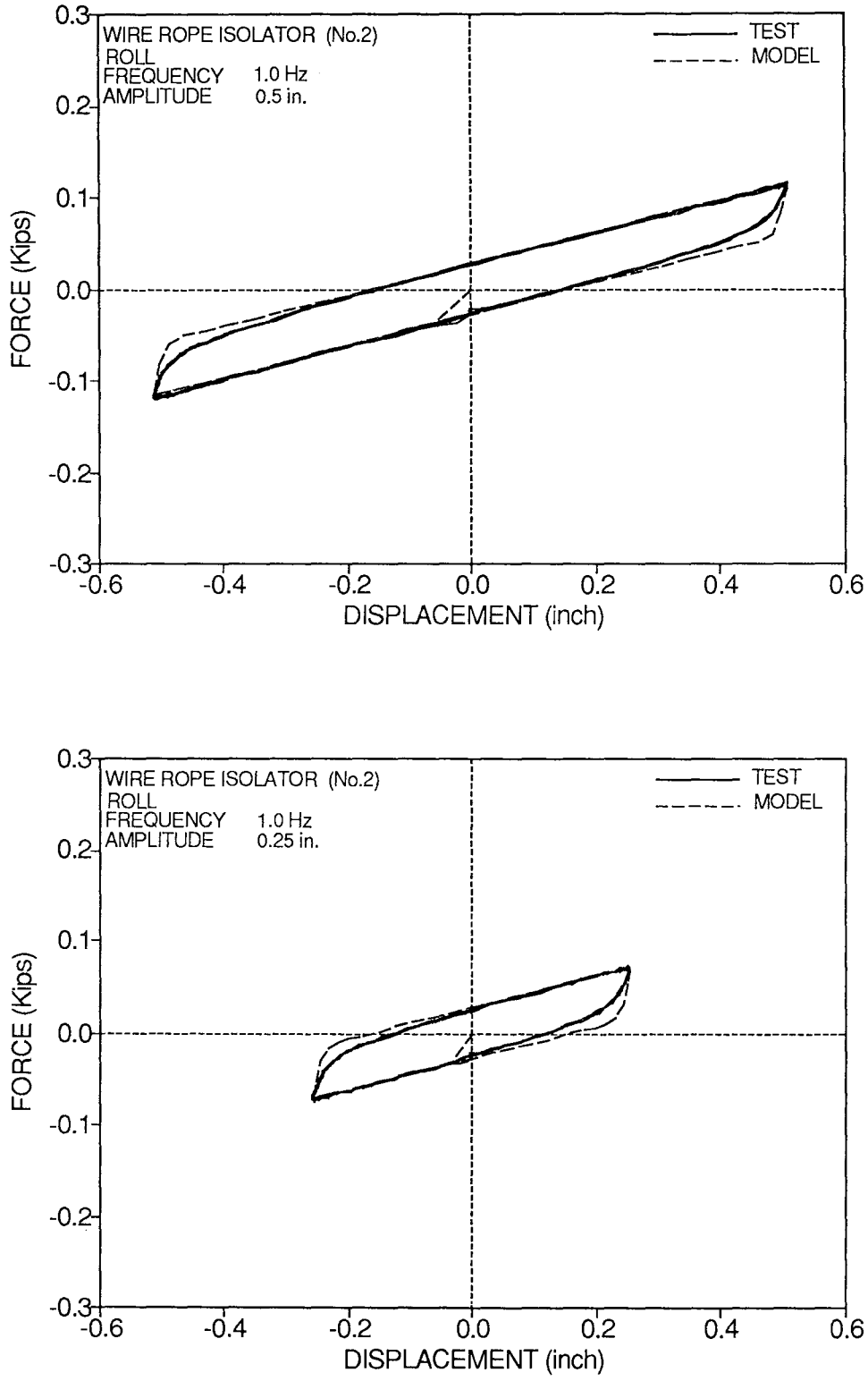

Figure 2-5 Comparison of Experimental and Analytical Force - Displacement Loops of Isolator No.2 subjected to Roll Motion (1 in.= 25.4 mm, 1 Kip= 4.46 kN).

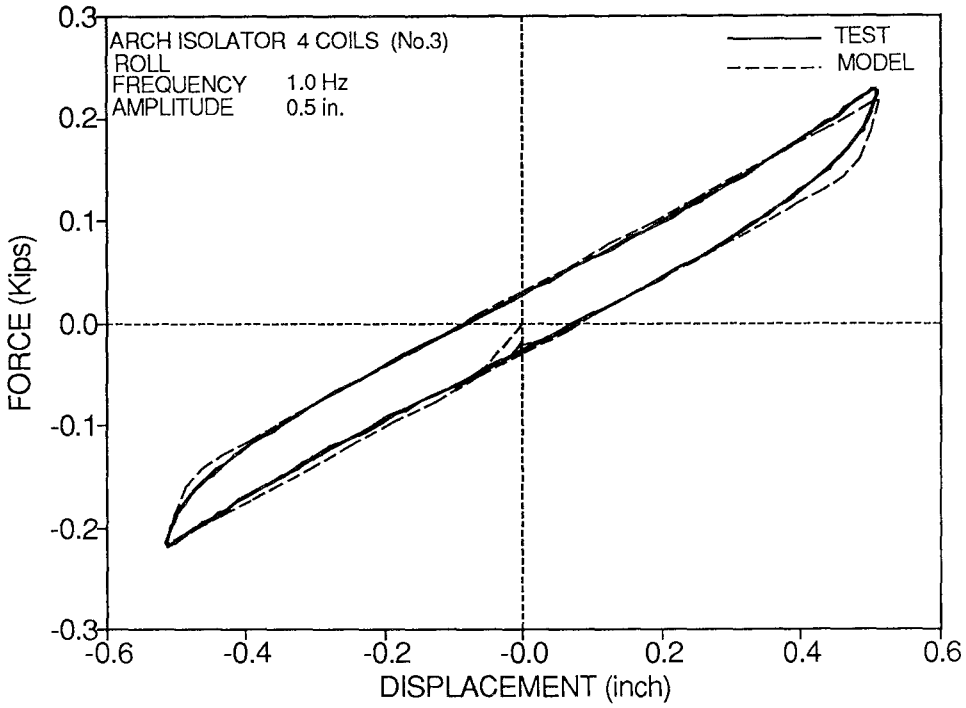

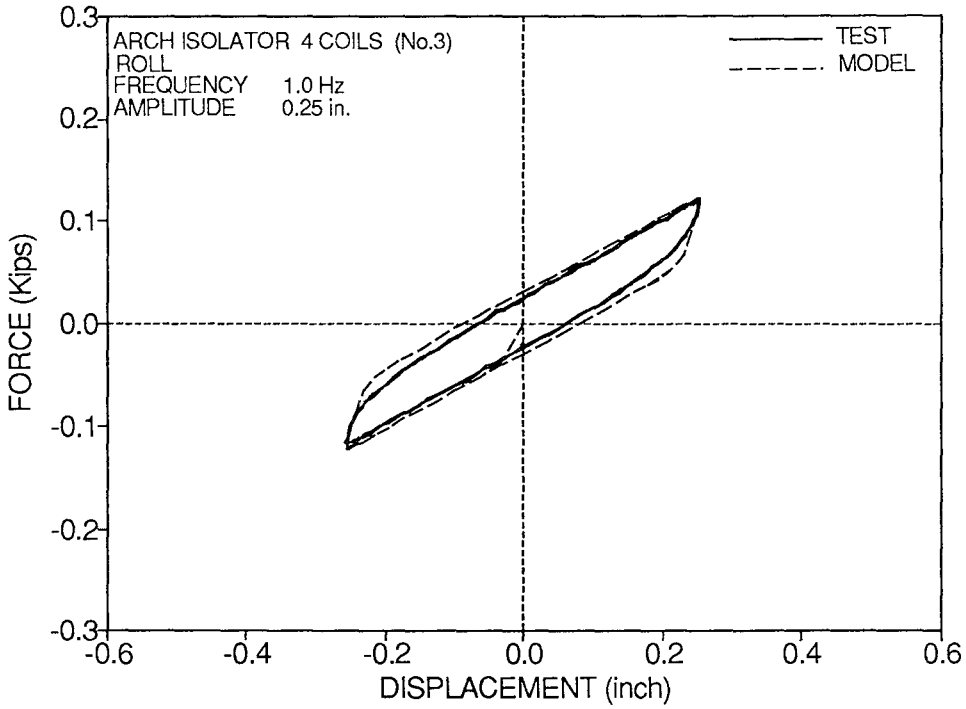

Figure 2-6 Comparison of Experimental and Analytical Force - Displacement Loops of Isolator No.3 subjected to Roll Motion (1 in.= 25.4 mm, 1 Kip= 4.46 kN).

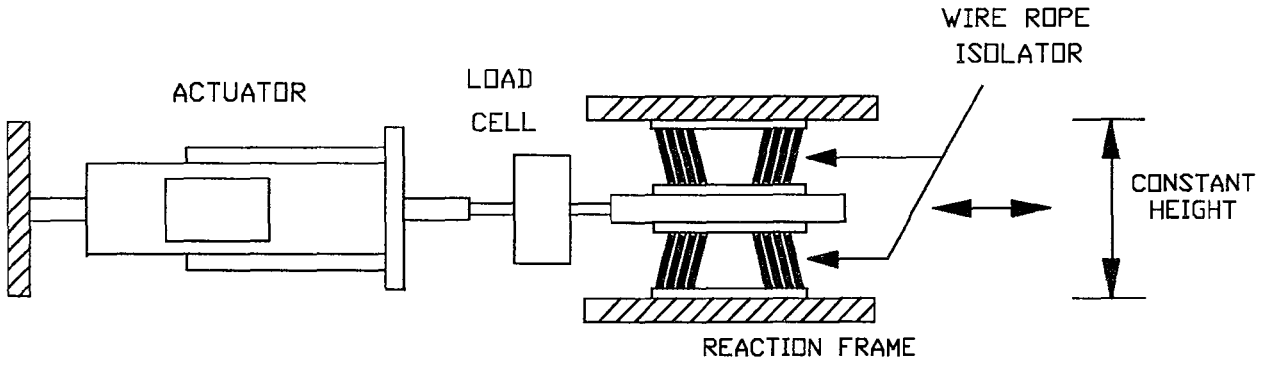

Figure 2-7 Arrangement for Testing Wire Rope Isolators (No.5) while Maintaining Constant Height.

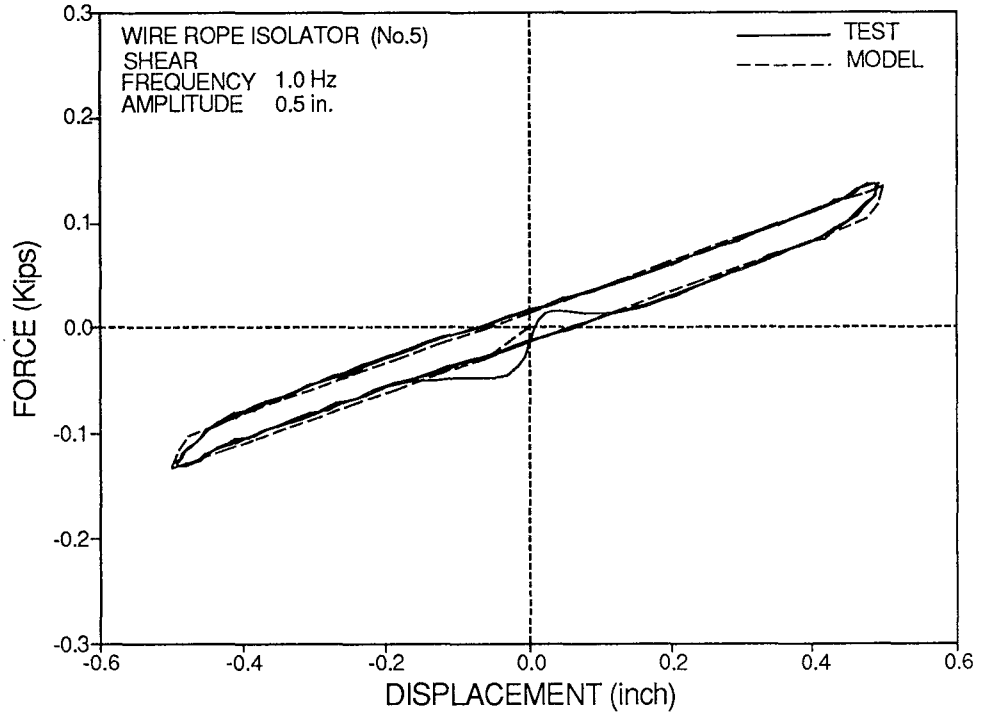

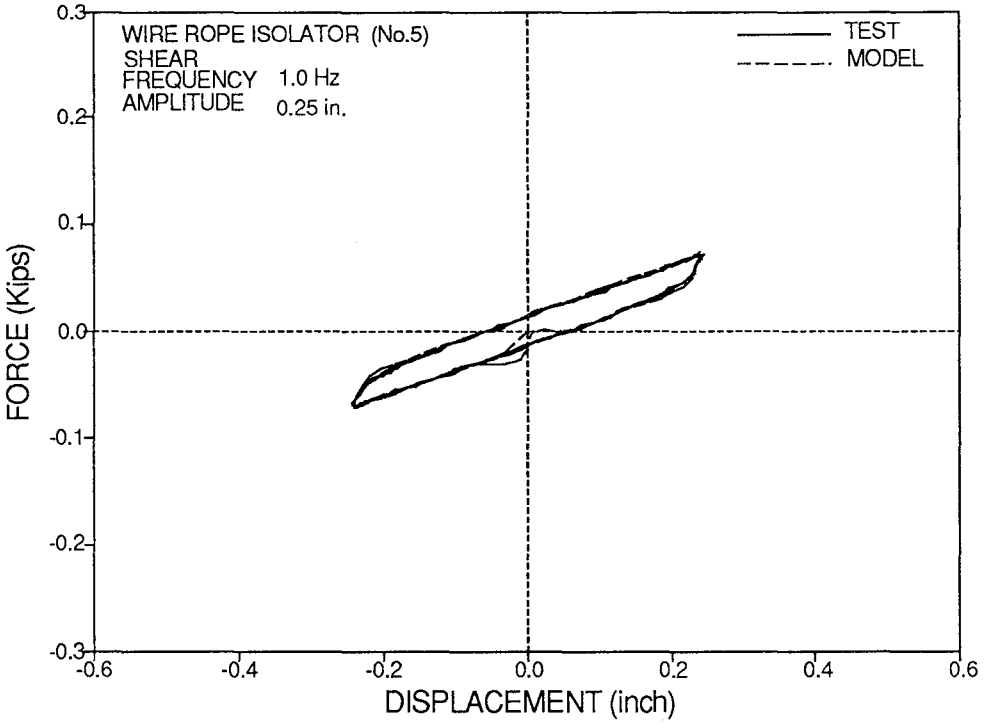

Figure 2-8 Comparison of Experimental and Analytical Force - Displacement Loops of Isolator No.5 subjected to Shear Motion (1 in.= 25.4 mm, 1 Kip= 4.46 kN).

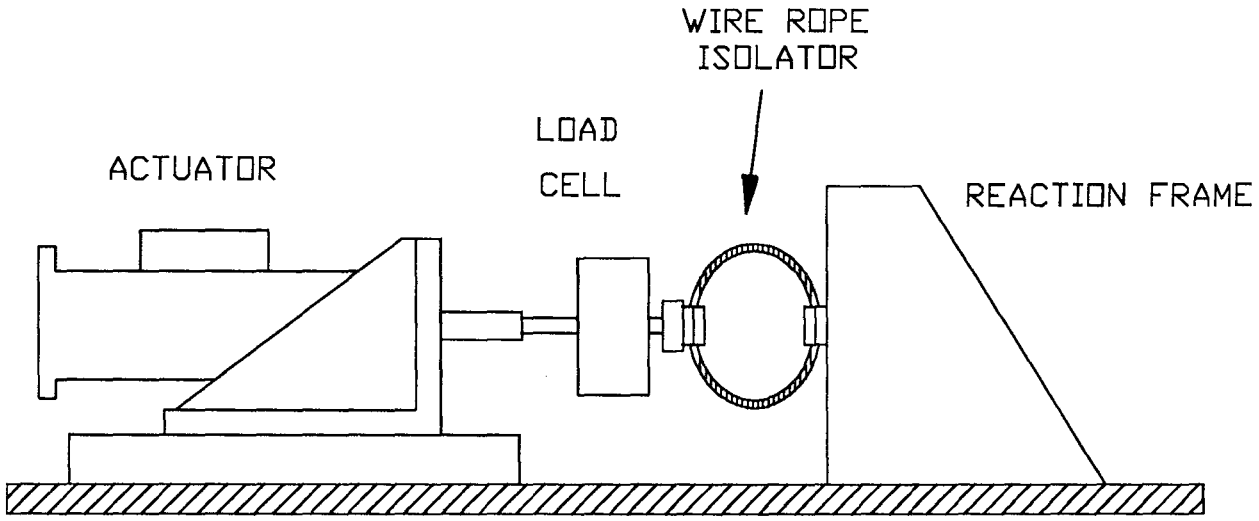

Figure 2-9 Arrangement for Testing Wire Rope Isolators in Compression - Tension.

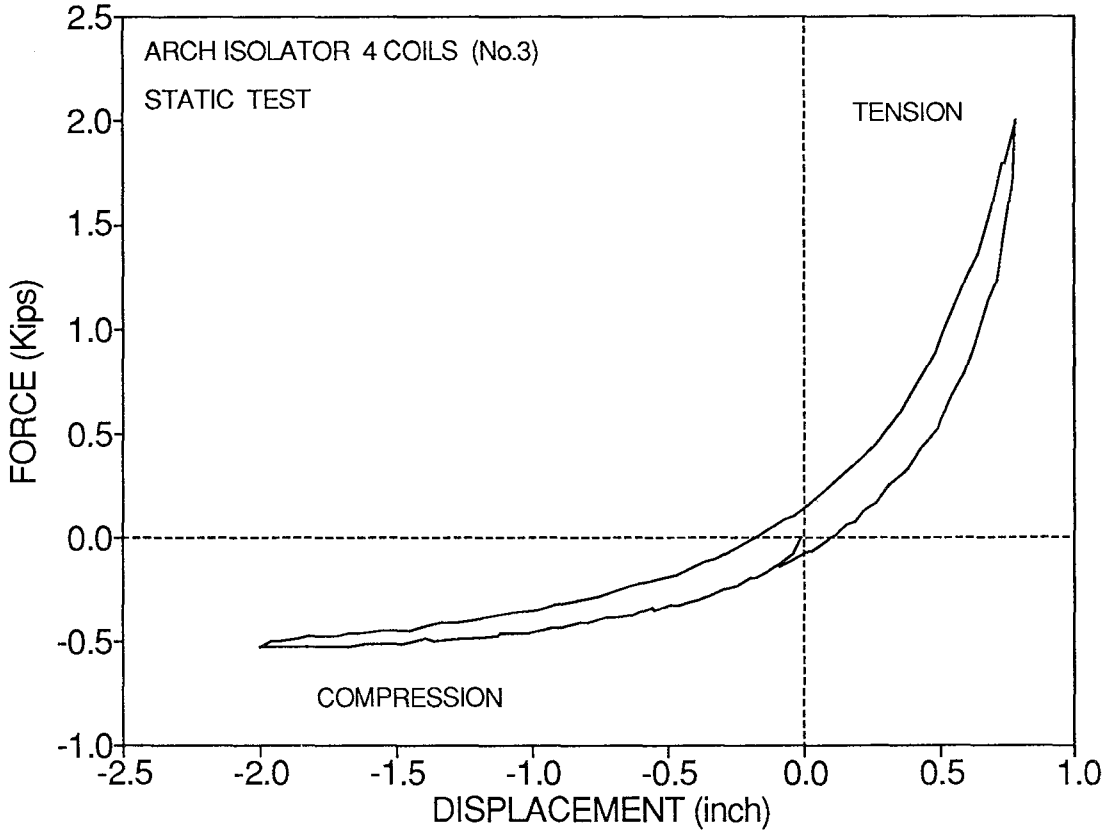

Figure 2-10 Typical Force - Displacement Loop of Wire Rope Isolators in Compression - Tension (1 in.= 25.4 mm, 1 Kip= 4.46 kN).

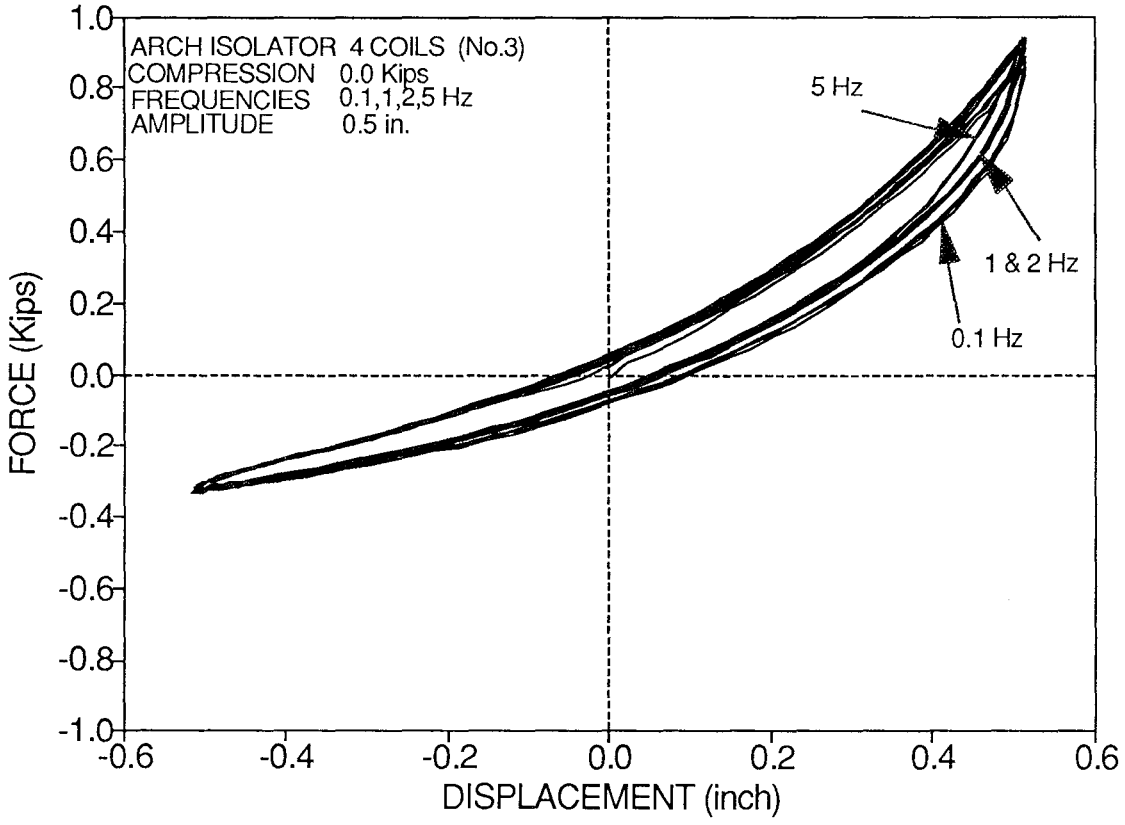

Figure 2-11 Force - Displacement Loops in Compression - Tension for Cyclic Motion (1 in.= 25.4 mm, 1 Kip= 4.46 kN).

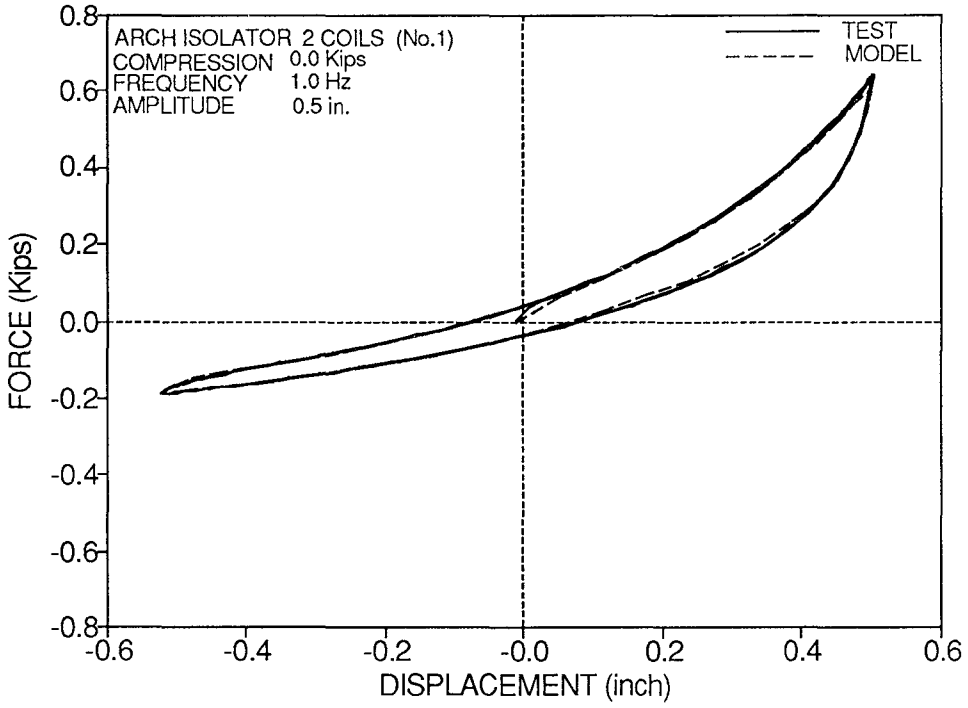

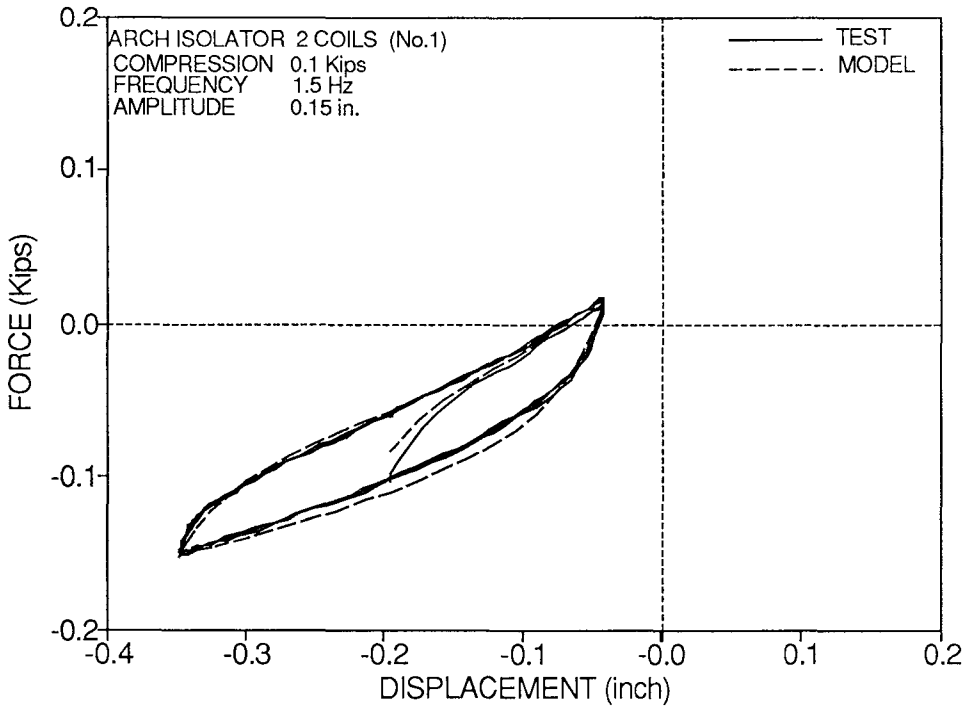

Figure 2-12 Comparison of Experimental and Analytical Force - Displacement Loops of Isolator No.1 subjected to Compression-Tension (1 in.= 25.4 mm, 1 Kip= 4.46 kN).

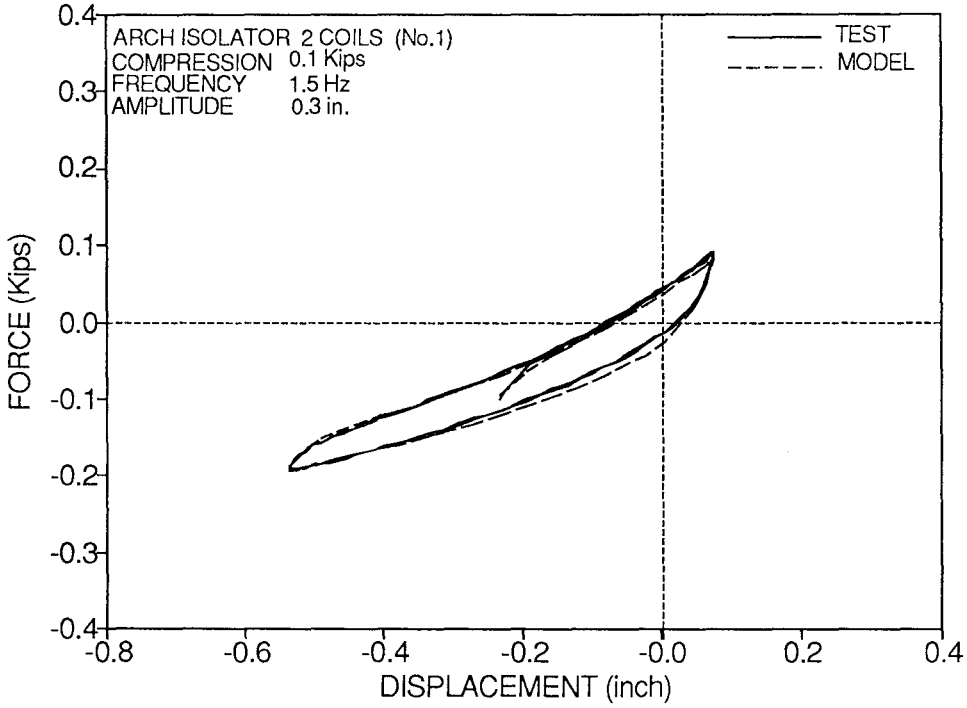

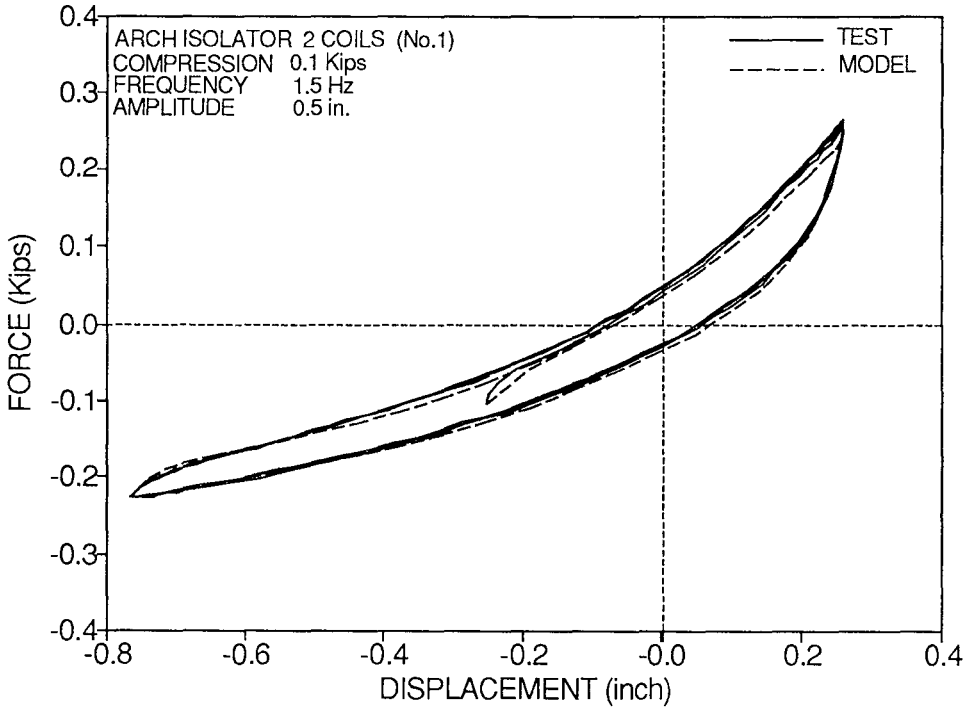

Figure 2-12 Continued.

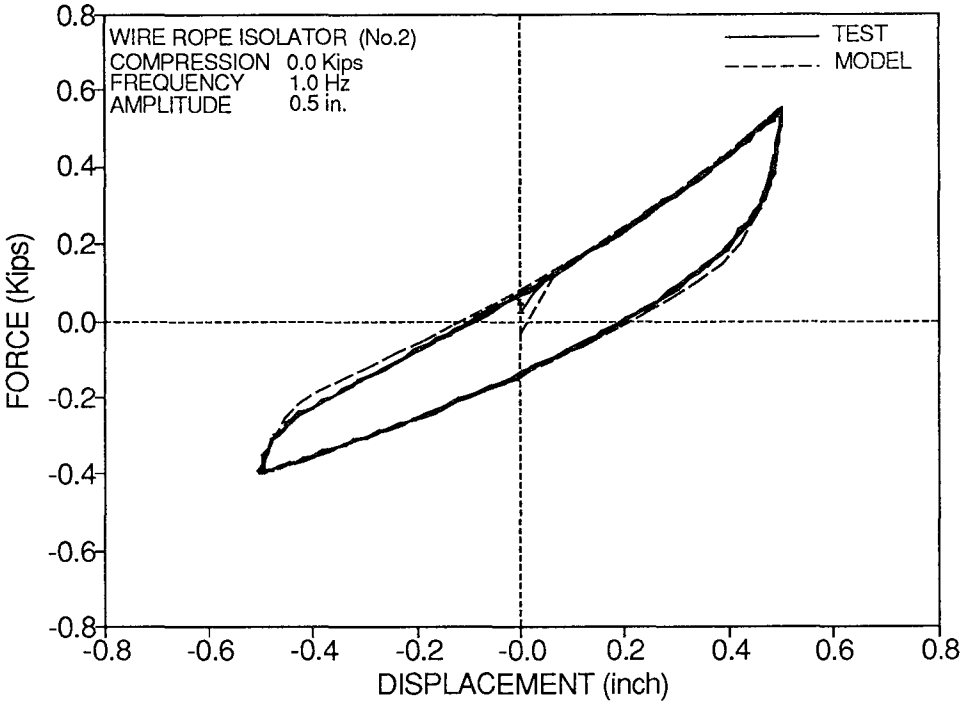

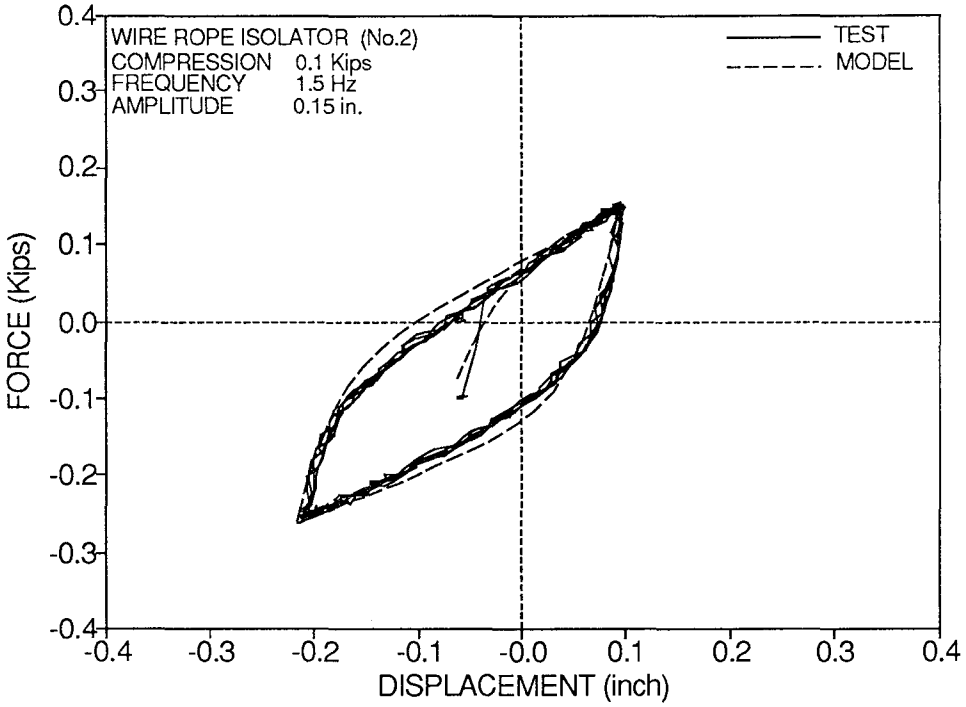

Figure 2-13 Comparison of Experimental and Analytical Force - Displacement Loops of Isolator No.2 subjected to Compression-Tension (1 in.= 25.4 mm, 1 Kip= 4.46 kN).

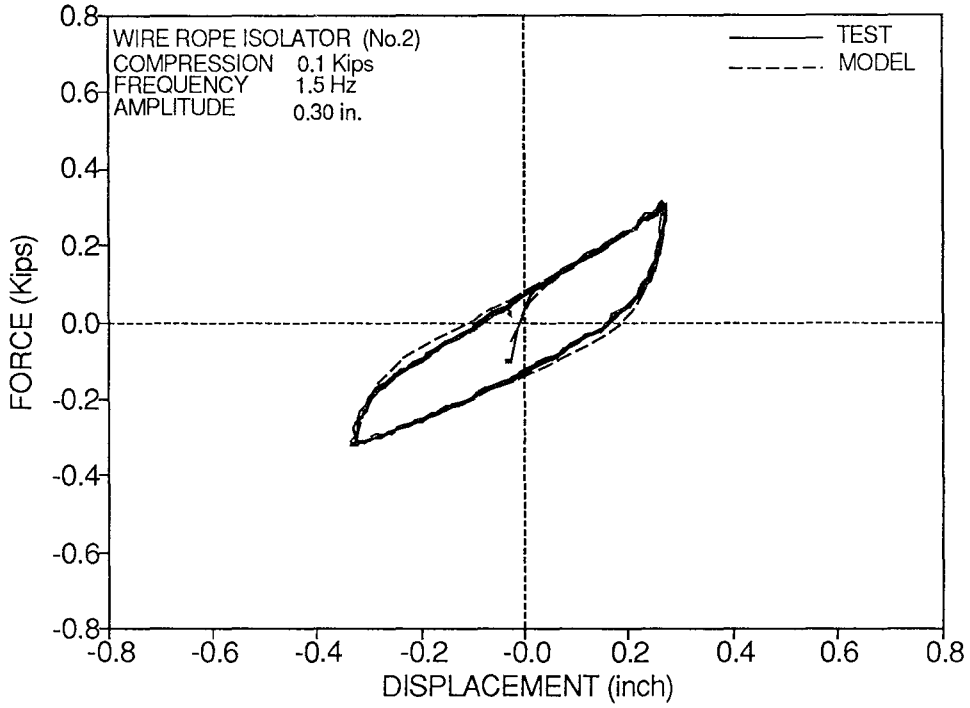

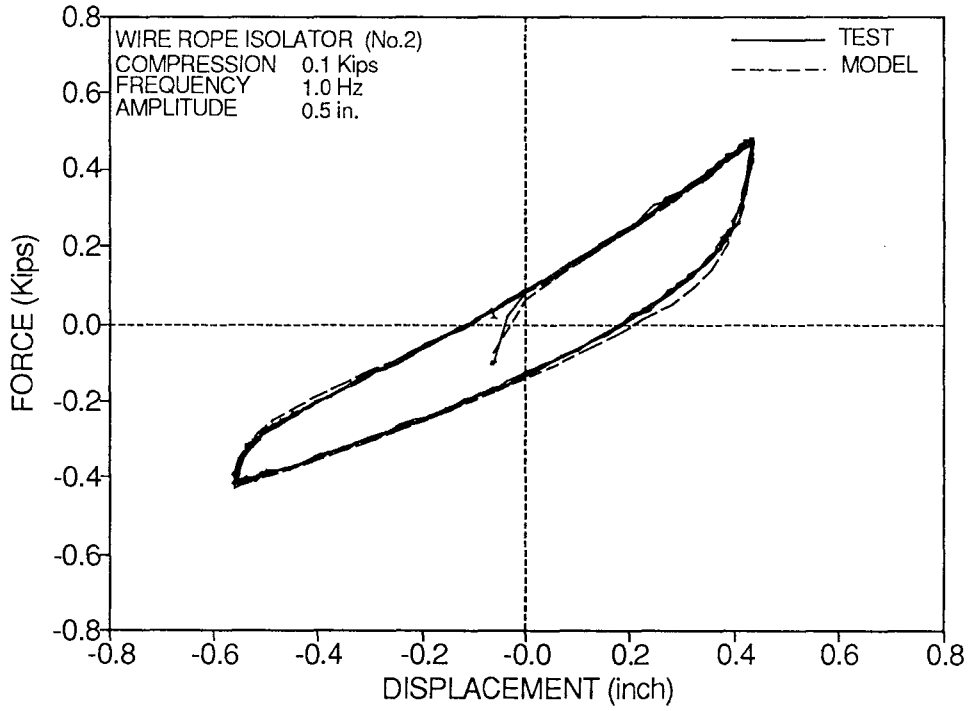

Figure 2-13 Continued.

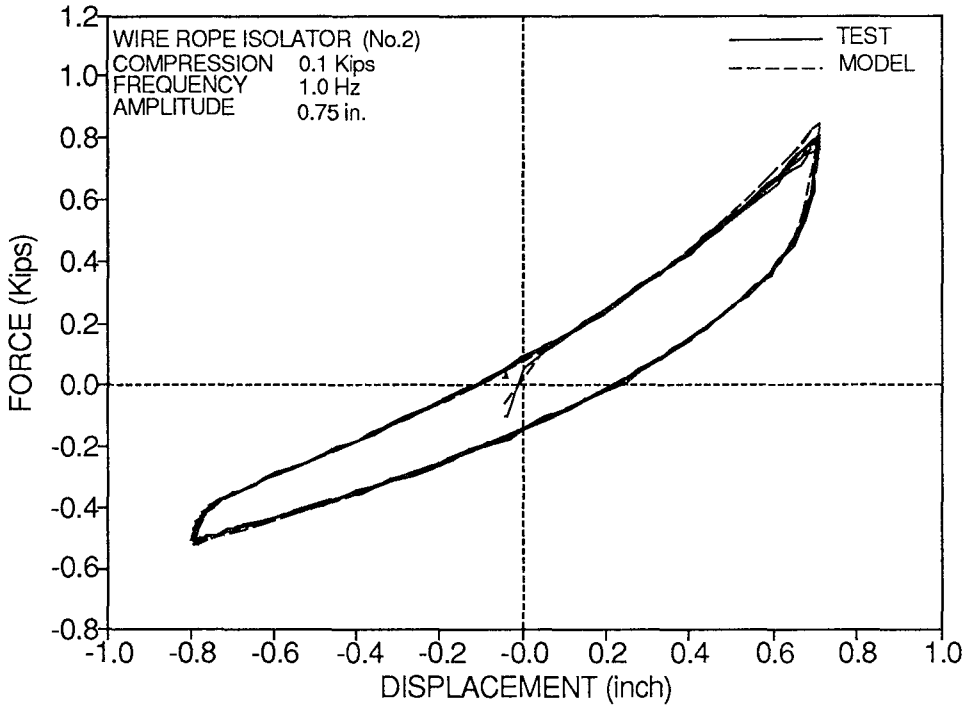

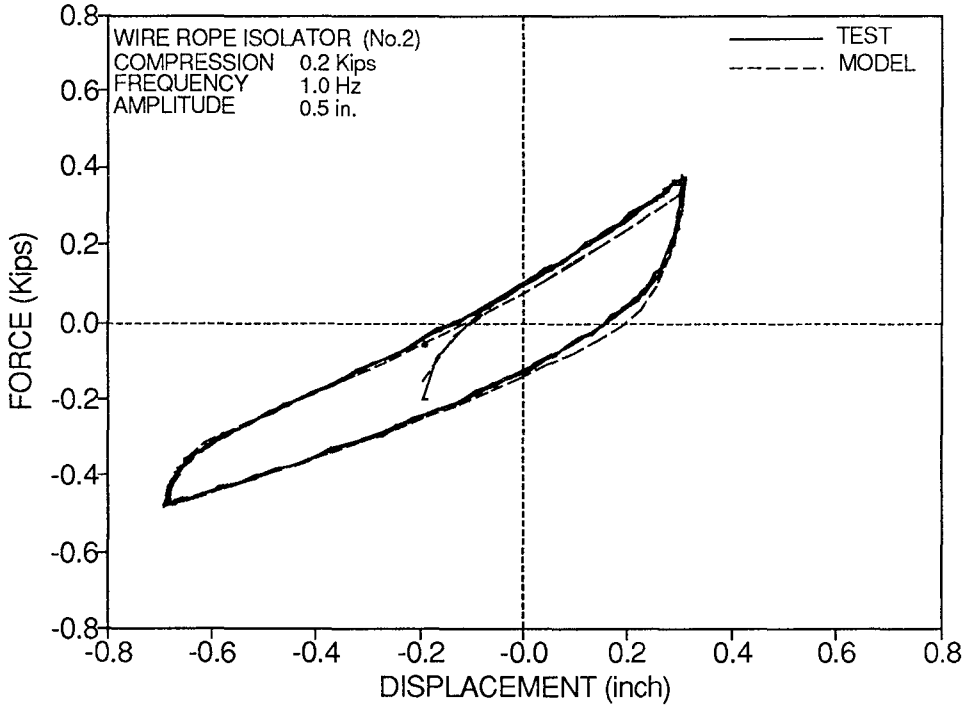

Figure 2-13 Continued.

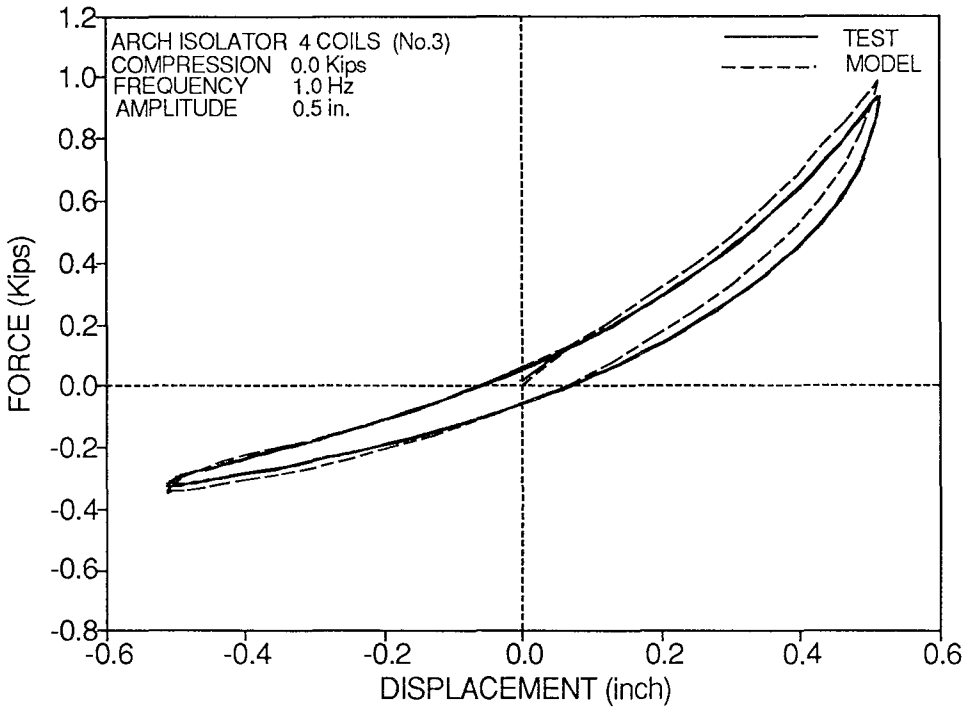

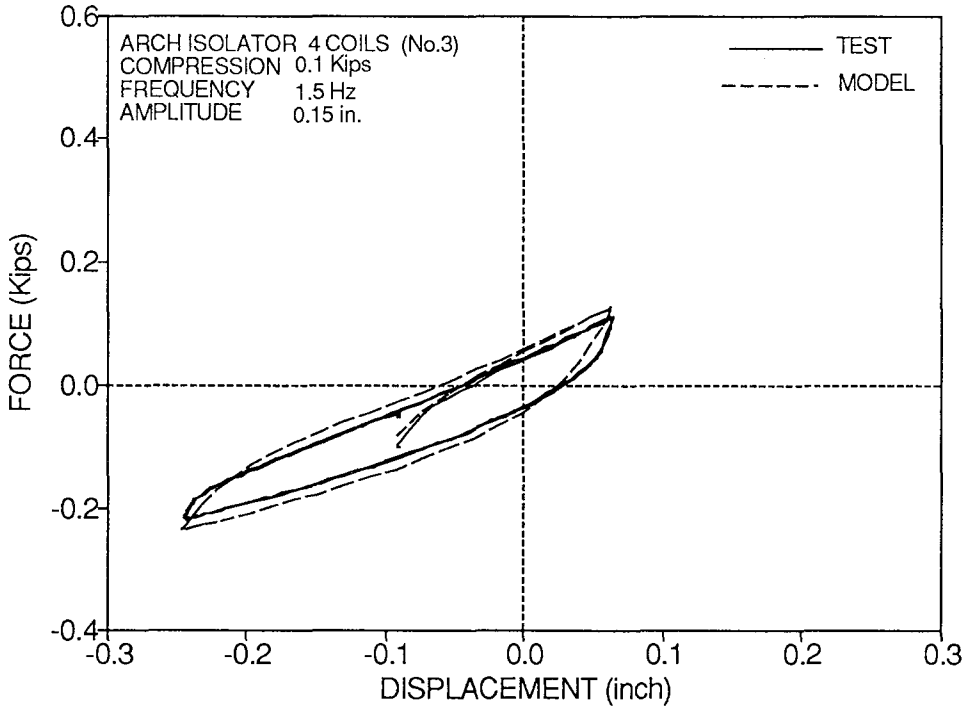

Figure 2-14 Comparison of Experimental and Analytical Force - Displacement Loops of Isolator No.3 subjected to Compression-Tension (1 in.= 25.4 mm, 1 Kip= 4.46 kN).

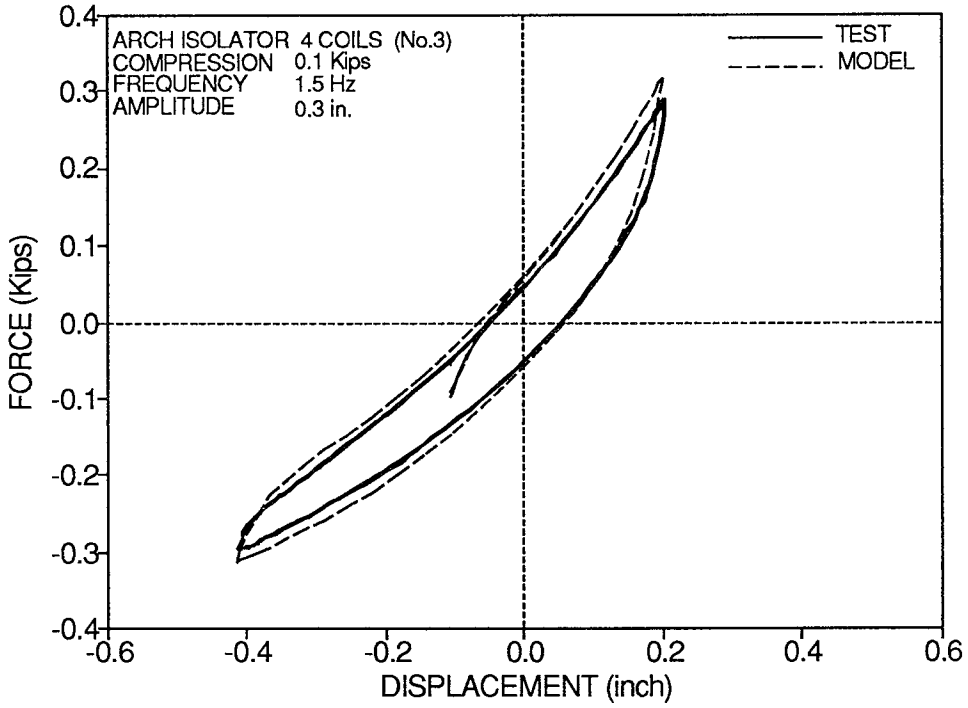

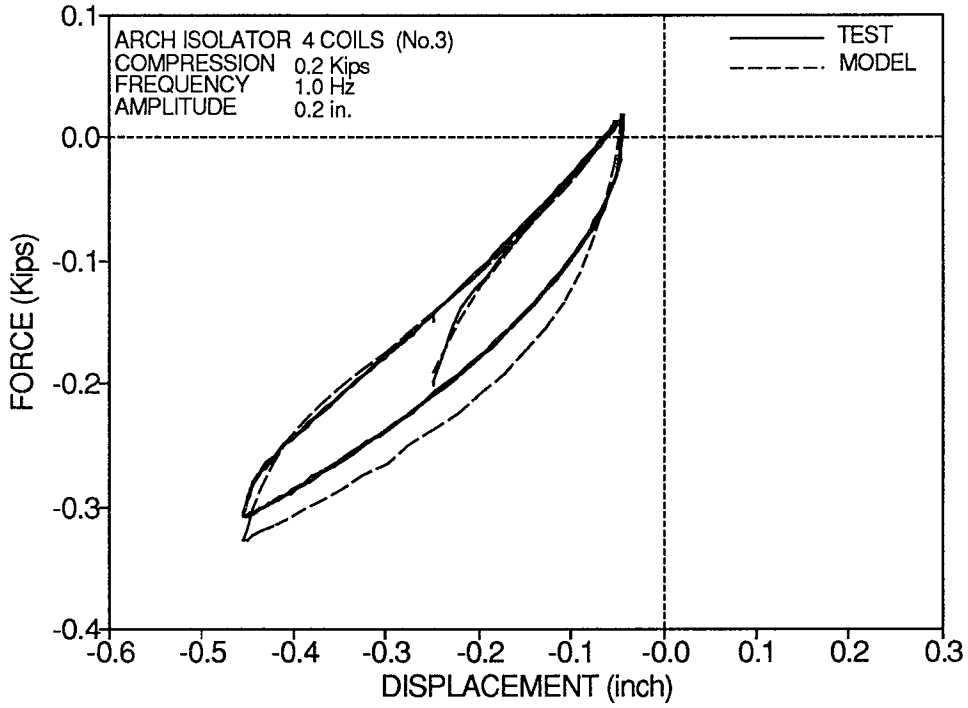

Figure 2-14 Continued.

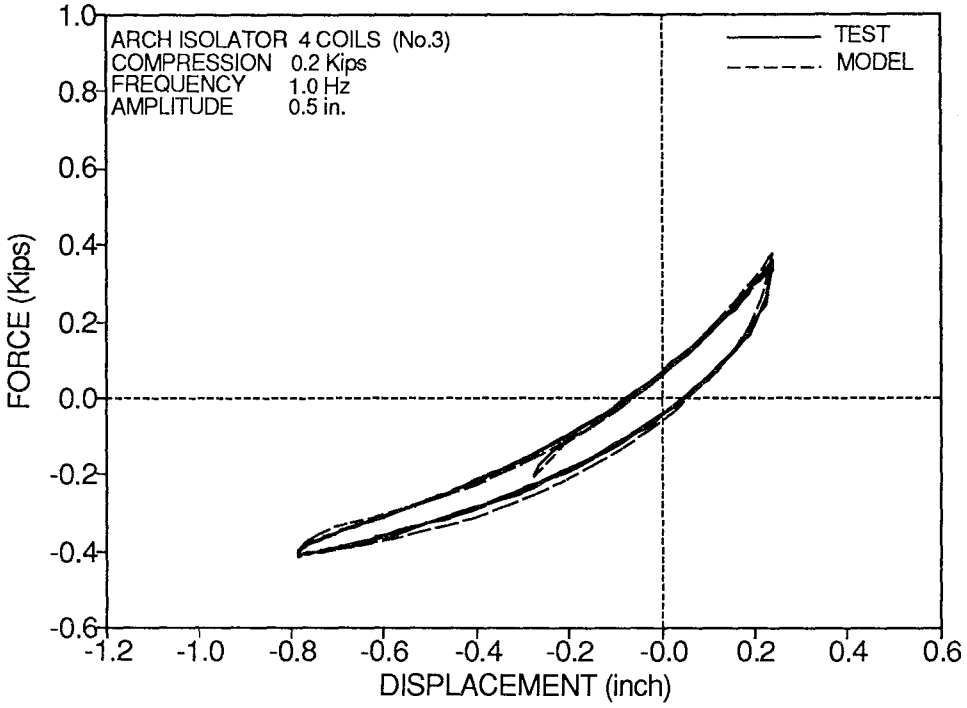

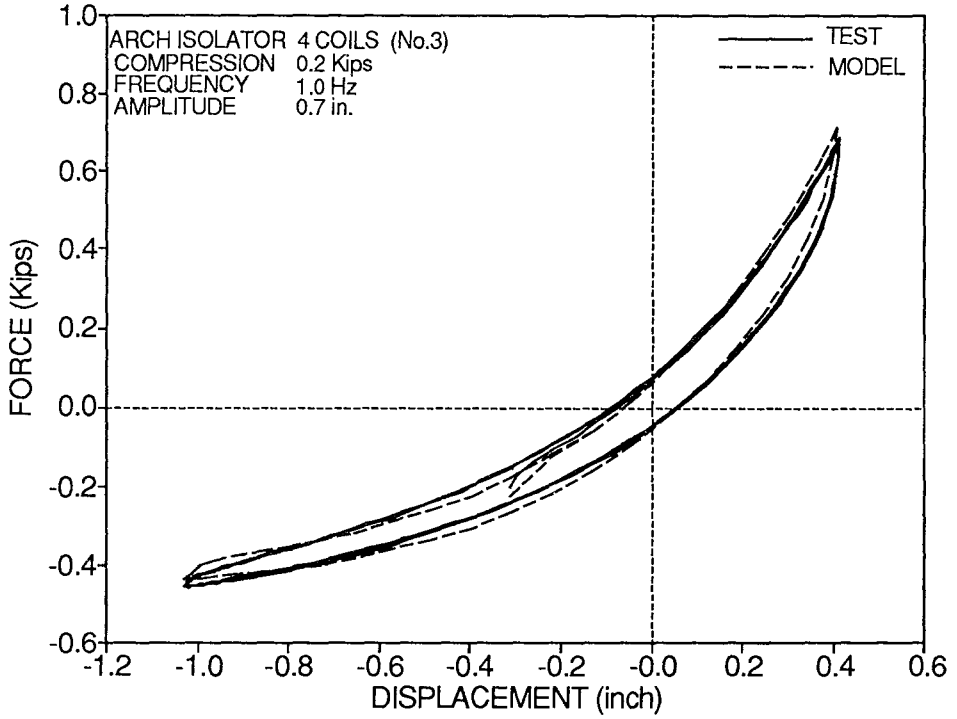

Figure 2-14 Continued.

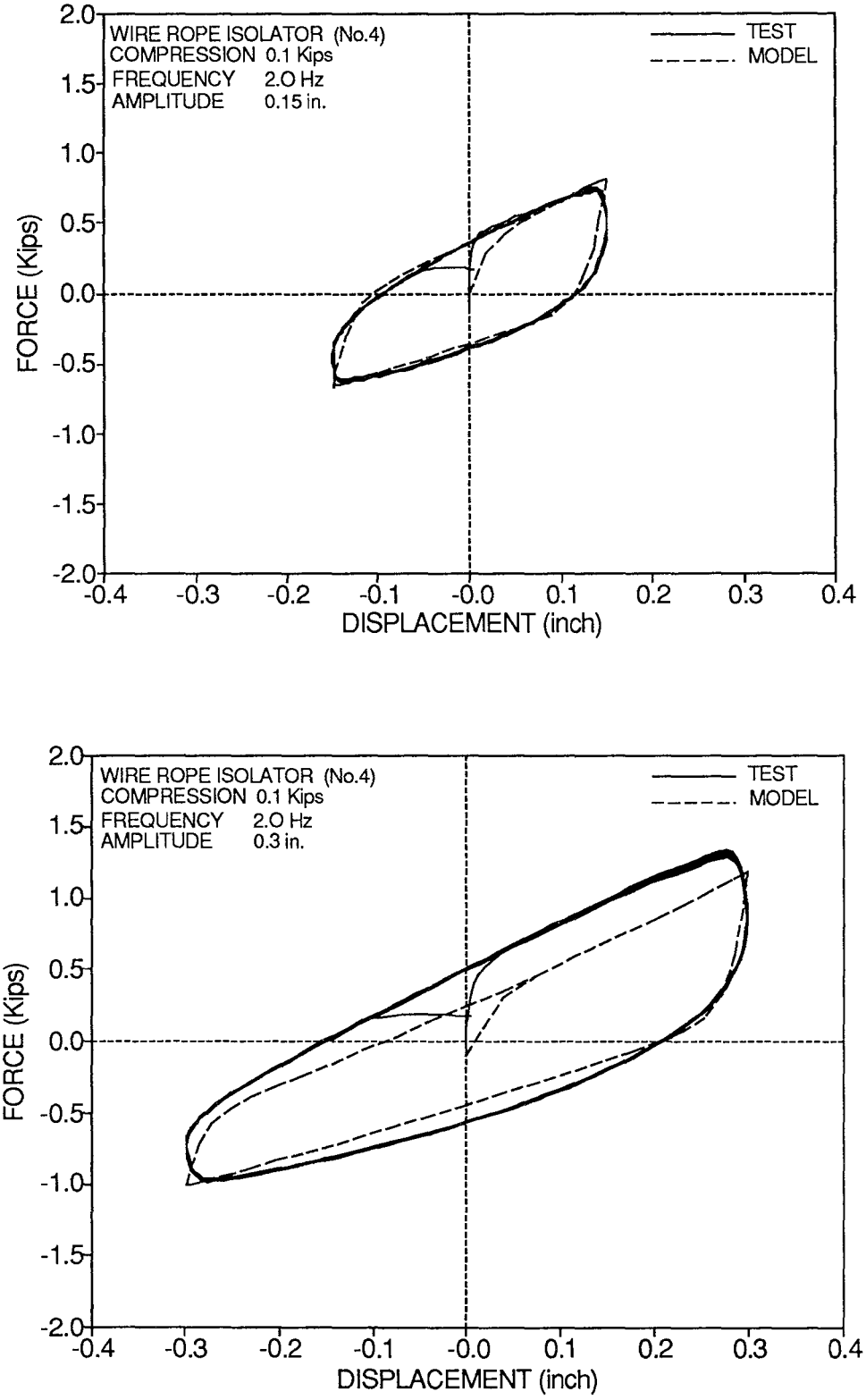

Figure 2-15 Comparison of Experimental and Analytical Force - Displacement Loops of Isolator No.4 subjected to Compression-Tension (1 in.= 25.4 mm, 1 Kip= 4.46 kN).

SECTION 3

EXPERIMENTAL AND ANALYTICAL STUDY OF WIRE ROPE ISOLATION SYSTEMS FOR EQUIPMENT

To determine the effectiveness of wire rope isolation systems, as well as to verify the validity of the mathematical models developed for wire rope isolators, an equipment cabinet was tested on the shake table. It was subjected to floor earthquake motions under isolated and non-isolated conditions. In all tested systems, the cabinet was supported by four wire rope isolators. Due to its slender configuration, the cabinet could undergo substantial rocking motion. Three systems of different stiffness characteristics were tested, while a forth one was only analyzed. The results of the experimental and analytical studies are presented in this section. However, the analytical modeling is described in section 4.

Another experimental study with a different configuration of wire rope isolators and different equipment is described in section 5.

3.1 Description of Equipment and Isolation System

The tested equipment is shown in Figure 3-1. The equipment is 74 in.(1880 mm) in height and has plan dimensions of 22 in. by 30 in.(559 mm by 762 mm). It consists of five horizontal diaphragms (isolator level, levels 1, 2, 3 and top level) which are connected together by side walls, only in the

longitudinal direction. Its weight is 400 lbs (1784 N) and the center of mass was determined to be at the height of level 1 and at the geometric center of the cabinet's plan. The radius of gyration of the equipment about a horizontal axis passing through the center of mass and parallel to the longitudinal direction of the cabinet was determined to be 22.83 in. (580 mm).

In the three tested configurations and the one analyzed configuration, the isolation system consisted of four wire rope isolators placed at a distance of 18.25 in. (463.6 mm) in the transverse direction as shown in Figure 3-1. Seismic excitation was applied in the vertical and transverse directions so that the isolators were subjected to combined vertical and roll motions. The four isolation systems are identified as systems 1, 2, 3 and 4. System 1 consisted of isolators No.1 (Table 2-I), system 2 consisted of isolators No.2 and so forth.

Views of the isolated cabinet (system 2 with helical wire isolators No.2) on the shake table are shown in Figure 3-2.

3.2 Instrumentation and Experimental Program

The instrumentation consisted of twenty one channels. Fifteen of these channels, nine accelerometers and six displacement transducers, monitored the response of the equipment, and the rest, three accelerometers and three displacement transducers, monitored the shake table response.

Figures 3-3 and 3-4 show the instrumentation diagram.

The equipment was tested in its transverse direction under isolated and non - isolated (fixed) conditions. Identification tests of the non - isolated equipment gave a fundamental frequency of 10.3 Hz and viscous damping ratio of 0.6% in the transverse direction. The earthquake excitation consisted of the 1952 Taft (Kern County, CA, Taft Lincoln School tunnel, component N21E and vertical), 1940 El Centro (Imperial Valley, CA, component S00E and vertical) and 1971 Pacoima Dam (San Fernando, CA component S74W and vertical) records. The characteristics of these earthquake motions are listed in Table 3-I. The Taft and El Centro motions were filtered through an actual 7-story building in an attempt to generate floor motions.

The 7-story building is the reinforced concrete building tested using the full-scale pseudo-dynamic testing facility at Tsukuba, Japan under the U.S. - Japan cooperative research program (Okamoto 1985). Available information and experimental data for this structure enabled the development of a detailed inelastic model for the structure using program IDARC (Park 1987). The computed time histories of acceleration at the 5th and 7th floors of this structure were used as input to the shake table without any time scaling. The very small weight of the equipment in relation to that of a typical floor ($\approx$1/1000) let us neglect equipment-structure interaction in the analysis.

Figures 3-5 to 3-11 show the horizontal components of ground and floor acceleration histories (as produced by the shake table) and their acceleration and displacement spectra. The vertical components of acceleration were transmitted through the structure unchanged. One may note the considerable amplification and filtering of the horizontal components of the ground motions at the higher floors of the structure. The 5%-damped acceleration spectra of the upper floor motions show considerable amplification in the range of 0.4 to 0.8 secs, the range which contains the fundamental period of the yielding 7-story structure. The spectra of the 7th floor El Centro motion are consistent with published floor response spectra for the design of equipment (Chen 1988). The motions used in this experimental program are identical to those used by Makris 1992a and 1992b in testing of the same cabinet with another isolation system.

3.3 Test Results

The recorded peak response of the cabinet under isolated and non - isolated (fixed) conditions is presented in Tables 3-I to 3-VIII. The values listed in these tables were recorded by the instruments listed in Table 3-IX. An immediate observation is made in the results of Tables 3-II to 3-VIII: systems 2 and 3 were not effective. The accelerations of the cabinet in these two systems were in most cases higher than in the fixed cabinet. However, system 2 was effective in reducing

accelerations by factors of the order of two in the strongest motions (Taft 7th floor, El Centro 7th floor and Pacoima).

In explaining this behavior, the dynamic characteristics of the three systems were determined in free vibration tests. Time histories of the horizontal displacement of the center of mass of the isolated cabinet are shown in Figure 3-12. From these displacement histories it was possible to determine the effective period of free vibration and the corresponding equivalent viscous damping ratio for systems 1 and 3 from the data of the first half cycle of motion. The damping ratio was determined by the logarithmic decrement method (Clough 1975). These dynamic properties, which are amplitude dependent due to the nonlinear hysteretic behavior of wire rope isolators, are listed in Table 3-X. The values of period indicate that system 3 (4-coil isolator) is about twice as stiff as system 1 (2-coil isolator). Moreover, system 1 has significantly more capability to dissipate energy than system 3. This is primarily the reason for the better performance of system 1.

Evidence for this may be obtained by comparing the experimental responses of the two systems for the Taft 7th floor excitation (Table 3-IV). The two systems undergo displacements at the center of mass of 2.2 and 4.5 in.(56 and 114 mm), respectively, thus within the range in which the free vibration results are valid. From the response spectra of the input motion (Fig. 3-7) and using the dynamic characteristics

of Table 3-X it is easily demonstrated that the response of system 3 is about twice as much as that of system 1.

The higher energy dissipation capability of system 1 may be also demonstrated by comparing the moment-rotation relations of the two systems in the Taft 7th floor test. The isolated cabinet responds primarily in rocking (compare values of horizontal and vertical isolator displacements in Tables 3-II to 3-VIII). Accordingly, its dynamic characteristics may be determined from the relation between the moment exerted to the base by the isolators, M, and the rotation, θ, of the base. Using the experimental histories of vertical isolator displacement, equations 2-2 and 2-5 to 2-7 were numerically integrated to obtain the time histories of vertical force exerted to the base by each isolator. Denoting as a the half distance between isolators (see Figs. 3-1 and 3-3) we have

$$M = 2(F_S - F_N)a \tag{3-1}$$

$$\theta = \frac{U_S - U_N}{2a} \tag{3-2}$$

where F_S, U_S are the force and displacement of the isolator located at the south side (see Fig. 3-3) and F_N, U_N are the force and displacement of the isolator located at the north side. Figure 2-13 shows the M - θ loops for systems 1 and 3 in the Taft 7th floor test. It is interesting to note that these loops exhibit symmetric hysteretic behavior, unlike the force - displacement loops of individual isolators (see Fig. 2-11).

The dynamic characteristics of effective period of free vibration, T, and equivalent viscous damping ratio, ξ, are determined from

$$T = 2\pi\left(\frac{I}{K_r}\right)^{1/2} \tag{3-3}$$

$$\xi = \frac{W_D}{4\pi W_S} \tag{3-4}$$

where K_r = rotational stiffness from the slope of the M-θ relation, I = moment of inertia of the cabinet about an axis passing through the center of the isolation system ($I = mr^2 + mh^2$), W_D = energy under the moment-rotation loop and W_S = strain energy stored at maximum displacements (Clough 1975). These characteristics are T = 0.93 secs, ξ = 0.11 for system 1 and T = 0.62 secs, ξ = 0.05 for system 3. Periods are lower than those determined in free vibration testing (Table 3-X) because the horizontal flexibility of the isolators was not accounted for. The damping ratios are almost identical to those determined in free vibration tests.

The preceding analysis of experimental results and discussion demonstrates that damping in wire rope isolators is dependent on the amplitude of deformation. At large deformations, as those expected in strong floor earthquake motions, damping ratio may be insufficient. This is the reason for the ineffectiveness of the tested systems 2 and 3. Even system 1, which was effective in reducing accelerations, had

equivalent damping ratio of about 0.1 of critical which is regarded as moderately high. The possibility of further improvement of damping capability by use of very stiff wire rope isolators is analytically investigated in the next subsection of this report.

3.4 Analytical Investigation of a Very Stiff Wire Rope System

In an attempt to understand the behavior of very stiff wire rope systems, a system consisting of four helical wire rope isolators of the type No.4 (see Fig. 2-15 and Table 2-I and section 2 for description) was analytically studied. The isolators were assumed placed as in the tested systems. The analysis was performed by numerical integration of the governing constitutive and dynamic equilibrium equations as described in section 4. Calculated peak response values for horizontal excitation only are listed in Table 3-XI and compared to the corresponding experimental values for the fixed equipment.

The analytical results certainly contain some error since the flexibility of the cabinet was not considered in the analysis. The contribution of the flexibility of the cabinet may be important in the analysis of very stiff wire rope systems. Assuming that the analytical results are correct, we observe that the wire rope system resulted in some improvement of the seismic performance of the cabinet for all input motions. Concentrating on two of the cases in Table 3-XI (Taft 7th floor and Pacoima ground) we plot the moment-rotation

loops of the system (Fig. 3-14) from where the dynamic characteristics (equations 3-3 and 3-4) are determined to be: $T = 0.14$ secs, $\xi = 0.23$ for the Taft 7th floor input motion and $T = 0.19$ secs, $\xi = 0.3$ for the Pacoima input. Damping is as large as desired for control of the response. The fact that the performance of the wire rope supported cabinet was not significantly improved in comparison to the fixed cabinet is merely a result of the very high stiffness of the tested cabinet (frequency of 10.3 Hz under fixed conditions). Had the fixed cabinet had a lower frequency (say 5 Hz), its acceleration response would have been much larger because of its inability to dissipate energy ($\xi = 0.006$).

It may be concluded that overall, the seismic behavior of equipment may be substantially improved by supporting them on stiff wire rope isolators. Under such conditions, the isolators undergo small displacements, exhibit large damping capacity and prevent the occurrence of resonances.

Table 3-I - Characteristics of Earthquake Excitation in Testing Program (1 in.= 25.4 mm).

Record	TAFT	EL CENTRO	PACOIMA
	Kern County,CA July 21, 1952 Taft Lincoln School Tunnel	Imperial Valley,CA May 18, 1940 El Centro	San Fernando,CA February 9,1971 Pacoima Dam
Site	Rock	Stiff Soil	Rock
Magnitude	7.6	6.6	6.6
Local MMI	VII	VIII	IX
Distance from Source (Km)	56	8	3
Horizontal Component	N21E	S00E	S74W
Pk. Horizontal Displacement (in.)	2.64	4.28	4.26
Pk. Horizontal Velocity (in/s)	6.19	13.17	22.73
Pk. Horizontal Acceleration (g)	0.16	0.35	1.08
Pk. Vertical Displacement (in.)	1.98	2.19	7.60
Pk. Vertical Velocity (in/s)	2.63	4.27	22.95
Pk. Vertical Acceleration (g)	0.11	0.21	0.71

Table 3-II - Recorded Peak Response of Isolated Equipment for Taft Ground Motion. Value in Parenthesis is for Combined Horizontal and Vertical Input Motion (1 in.= 25.4 mm).

TAFT N21E GROUND				
	ISOLATED SYSTEM 1	ISOLATED SYSTEM 2	ISOLATED SYSTEM 3	FIXED
ACCELERATION (g)				
Table Horizontal	0.155 (0.155)	0.155 (0.153)	0.154 (0.154)	0.154 (0.152)
Isolator Horizontal	0.166 (0.165)	0.168 (0.158)	0.150 (0.154)	0.156 (0.157)
Level 1 Horizontal	0.100 (0.110)	0.163 (0.179)	0.186 (0.171)	0.187 (0.193)
Top Horizontal	0.220 (0.215)	0.262 (0.297)	0.305 (0.292)	0.250 (0.255)
Table Vertical	0.002 (0.121)	0.005 (0.117)	0.006 (0.123)	- (0.112)
Isolator S Vertical	0.055 (0.156)	0.031 (0.120)	0.045 (0.127)	- -
Isolator N Vertical	0.059 (0.222)	0.030 (0.138)	0.055 (0.162)	- -
Top Vertical	0.050 (0.216)	0.031 (0.135)	0.047 (0.157)	0.008 (0.118)
DISPLACEMENT (in)				
Table Horizontal	1.242 (1.224)	1.243 (1.223)	1.244 (1.222)	1.268 (1.354)
Isolator Horizontal	0.122 (0.103)	0.018 (0.022)	0.067 (0.070)	- -
Level 1 Horizontal	0.665 (0.657)	0.254 (0.238)	0.366 (0.463)	0.039 (0.039)
Top Horizontal	1.211 (1.221)	0.431 (0.395)	0.676 (0.860)	0.063 (0.063)
Table Vertical	0.013 (0.479)	0.012 (0.480)	0.012 (0.479)	- (0.433)
Isolator S Vertical	0.247 (0.258)	0.058 (0.052)	0.126 (0.173)	- -
Isolator N Vertical	0.198 (0.221)	0.074 (0.068)	0.119 (0.153)	- -

Table 3-III - Recorded Peak Response of Isolated Equipment for Taft 5th Floor Motion. Value in Parenthesis is for Combined Horizontal and Vertical Input Motion (1 in.= 25.4 mm).

TAFT N21E 5th FLOOR				
	ISOLATED SYSTEM 1	ISOLATED SYSTEM 2	ISOLATED SYSTEM 3	FIXED
ACCELERATION (g)				
Table Horizontal	0.266 (0.261)	0.262 (0.259)	0.262 (0.261)	0.272 (0.268)
Isolator Horizontal	0.289 (0.338)	0.299 (0.304)	0.290 (0.288)	0.276 (0.273)
Level 1 Horizontal	0.166 (0.173)	0.370 (0.322)	0.576 (0.552)	0.372 (0.378)
Top Horizontal	0.447 (0.449)	0.633 (0.540)	1.099 (1.065)	0.529 (0.378)
Table Vertical	0.002 (0.122)	0.005 (0.121)	0.007 (0.120)	- (0.119)
Isolator S Vertical	0.189 (0.325)	0.056 (0.127)	0.243 (0.256)	- -
Isolator N Vertical	0.131 (0.254)	0.111 (0.148)	0.281 (0.320)	- -
Top Vertical	0.118 (0.264)	0.093 (0.142)	0.332 (0.363)	0.021 (0.113)
DISPLACEMENT (in)				
Table Horizontal	1.672 (1.644)	1.670 (1.646)	1.674 (1.644)	1.654 (1.673)
Isolator Horizontal	0.256 (0.173)	0.327 (0.239)	0.444 (0.438)	- -
Level 1 Horizontal	1.731 (1.698)	1.070 (0.715)	3.105 (2.943)	0.043 (0.063)
Top Horizontal	3.214 (3.182)	1.805 (1.209)	5.882 (5.570)	0.083 (0.094)
Table Vertical	0.021 (0.479)	0.021 (0.479)	0.021 (0.479)	- (0.457)
Isolator S Vertical	0.768 (0.798)	0.235 (0.155)	1.388 (1.306)	- -
Isolator N Vertical	0.616 (0.583)	0.345 (0.227)	1.373 (1.311)	- -

Table 3-IV - Recorded Peak Response of Isolated Equipment for Taft 7th Floor Motion. Value in Parenthesis is for Combined Horizontal and Vertical Input Motion (1 in.= 25.4 mm).

TAFT N21E 7th FLOOR				
	ISOLATED SYSTEM 1	ISOLATED SYSTEM 2	ISOLATED SYSTEM 3	FIXED
ACCELERATION (g)				
Table Horizontal	0.469 (0.474)	0.473 (0.471)	0.475 (0.470)	0.475 (0.479)
Isolator Horizontal	0.673 (0.677)	0.537 (0.499)	0.484 (0.516)	0.482 (0.490)
Level 1 Horizontal	0.260 (0.250)	0.608 (0.580)	0.679 (0.674)	0.700 (0.726)
Top Horizontal	0.625 (0.639)	1.130 (0.979)	1.304 (1.293)	1.167 (1.199)
Table Vertical	0.006 (0.124)	0.008 (0.126)	0.009 (0.125)	- (0.114)
Isolator S Vertical	0.262 (0.302)	0.248 (0.279)	0.609 (0.550)	- -
Isolator N Vertical	0.255 (0.297)	0.261 (0.272)	0.573 (0.529)	- -
Top Vertical	0.230 (0.299)	0.230 (0.248)	0.769 (0.711)	0.044 (0.118)
DISPLACEMENT (in)				
Table Horizontal	2.105 (2.064)	2.105 (2.064)	2.105 (2.062)	2.075 (2.102)
Isolator Horizontal	0.302 (0.214)	0.687 (0.581)	0.615 (0.584)	- -
Level 1 Horizontal	2.234 (2.209)	2.404 (1.952)	4.535 (4.440)	0.094 (0.106)
Top Horizontal	4.163 (4.167)	4.099 (3.305)	8.998 (8.785)	0.185 (0.213)
Table Vertical	0.032 (0.478)	0.033 (0.478)	0.032 (0.478)	- (0.445)
Isolator S Vertical	1.031 (1.054)	0.702 (0.494)	2.069 (1.948)	- -
Isolator N Vertical	0.806 (0.753)	0.758 (0.667)	2.516 (2.443)	- -

Table 3-V - Recorded Peak Response of Isolated Equipment for El Centro Ground Motion. Value in Parenthesis is for Combined Horizontal and Vertical Input Motion (1 in.= 25.4 mm).

EL CENTRO S00E GROUND				
	ISOLATED SYSTEM 1	ISOLATED SYSTEM 2	ISOLATED SYSTEM 3	FIXED
ACCELERATION (g)				
Table Horizontal	0.373 (0.383)	0.377 (0.382)	0.367 (0.381)	0.361 (0.368)
Isolator Horizontal	0.600 (0.609)	0.463 (0.412)	0.469 (0.519)	0.368 (0.374)
Level 1 Horizontal	0.277 (0.300)	0.405 (0.360)	0.490 (0.466)	0.536 (0.556)
Top Horizontal	0.546 (0.586)	0.795 (0.673)	0.903 (0.991)	0.877 (0.898)
Table Vertical	0.004 (0.154)	0.008 (0.191)	0.008 (0.193)	- (0.204)
Isolator S Vertical	0.190 (0.233)	0.218 (0.228)	0.252 (0.431)	- -
Isolator N Vertical	0.196 (0.241)	0.101 (0.216)	0.149 (0.323)	- -
Top Vertical	0.201 (0.241)	0.085 (0.219)	0.169 (0.315)	0.028 (0.209)
DISPLACEMENT (in)				
Table Horizontal	2.213 (2.252)	2.213 (2.252)	2.214 (2.247)	2.240 (2.240)
Isolator Horizontal	0.401 (0.428)	0.392 (0.282)	0.248 (0.309)	- -
Level 1 Horizontal	2.626 (2.879)	1.324 (0.947)	1.307 (2.023)	0.083 (0.079)
Top Horizontal	4.753 (5.256)	2.247 (1.626)	2.489 (3.864)	0.157 (0.185)
Table Vertical	0.035 (0.539)	0.036 (0.537)	0.038 (0.540)	- (0.504)
Isolator S Vertical	1.145 (1.295)	0.379 (0.252)	0.521 (0.867)	- -
Isolator N Vertical	0.844 (0.899)	0.363 (0.278)	0.492 (0.793)	- -

Table 3-VI - Recorded Peak Response of Isolated Equipment for El Centro 5th Floor Motion. Value in Parenthesis is for Combined Horizontal and Vertical Input Motion (1 in.= 25.4 mm).

EL CENTRO S00E 5th FLOOR				
	ISOLATED SYSTEM 1	ISOLATED SYSTEM 2	ISOLATED SYSTEM 3	FIXED
ACCELERATION (g)				
Table Horizontal	0.424 (0.424)	0.428 (0.427)	0.429 (0.428)	0.417 (0.422)
Isolator Horizontal	0.408 (0.448)	0.529 (0.584)	0.684 (0.860)	0.424 (0.429)
Level 1 Horizontal	0.379 (0.377)	0.792 (0.703)	0.925 (1.603)	0.529 (0.762)
Top Horizontal	0.771 (0.765)	1.117 (1.020)	1.355 (2.048)*	0.729 (0.761)
Table Vertical	0.006 (0.196)	0.012 (0.192)	0.012 (0.194)	- (0.210)
Isolator S Vertical	0.376 (0.446)	0.098 (0.228)	0.382 (1.452)	- -
Isolator N Vertical	0.367 (0.352)	0.115 (0.309)	0.320 (1.069)	- -
Top Vertical	0.463 (0.454)	0.101 (0.277)	0.386 (1.242)	0.038 (0.214)
DISPLACEMENT (in)				
Table Horizontal	4.241 (4.237)	4.243 (4.238)	4.250 (4.233)	4.213 (4.252)
Isolator Horizontal	0.698 (0.671)	0.920 (0.747)	0.533 (4.820)	- -
Level 1 Horizontal	5.760 (5.497)	2.910 (2.290)	3.239 (10.240)*	0.094 (0.098)
Top Horizontal	10.652 (10.157)	4.859 (3.804)	6.225 (15.360)*	0.177 (0.173)
Table Vertical	0.132 (0.518)	0.131 (0.518)	0.132 (0.518)	- (0.472)
Isolator S Vertical	2.921 (2.763)	0.725 (0.567)	1.196 (4.084)	- -
Isolator N Vertical	2.618 (2.428)	0.967 (0.759)	1.622 (3.550)	- -

* : Value exceeded the limit of instrument.

Table 3-VII - Recorded Peak Response of Isolated Equipment for El Centro 7th Floor Motion. Value in Parenthesis is for Combined Horizontal and Vertical Input Motion (1 in.= 25.4 mm).

EL CENTRO S00E 7th FLOOR				
	ISOLATED SYSTEM 1	ISOLATED SYSTEM 2	ISOLATED SYSTEM 3	FIXED
ACCELERATION (g)				
Table Horizontal	0.905 (0.736)	0.720 (0.747)	0.725 -	0.728 (0.693)
Isolator Horizontal	1.361 (1.219)	1.050 (0.975)	1.856 -	0.745 (0.711)
Level 1 Horizontal	0.594 (0.550)	1.408 (1.272)	1.773 -	0.985 (0.968)
Top Horizontal	1.057 (0.987)	2.048* (1.960)	2.048* -	1.780 (1.777)
Table Vertical	0.017 (0.192)	0.024 (0.190)	0.019 -	- (0.205)
Isolator S Vertical	0.434 (0.485)	0.474 (0.509)	1.458 -	- -
Isolator N Vertical	0.733 (0.764)	0.369 (0.484)	1.412 -	- -
Top Vertical	0.825 (0.853)	0.473 (0.444)	1.526 -	0.073 (0.213)
DISPLACEMENT (in)				
Table Horizontal	5.190 (5.191)	5.192 (5.202)	5.200 -	5.157 (5.157)
Isolator Horizontal	0.749 (0.656)	1.715 (1.558)	1.284 -	- -
Level 1 Horizontal	6.444 (6.344)	5.860 (5.246)	10.240* -	0.177 (0.177)
Top Horizontal	11.860 (11.752)	9.903 (8.868)	15.360* -	0.350 (0.343)
Table Vertical	0.197 (0.514)	0.196 (0.514)	0.198 -	- (0.487)
Isolator S Vertical	3.279 (3.262)	1.588 (1.424)	4.186* -	- -
Isolator N Vertical	2.705 (2.553)	2.187 (1.939)	3.728 -	- -

* : Value exceeded the limit of instrument.

Table 3-VIII - Recorded Peak Response of Isolated Equipment for Pacoima Dam Ground Motion. Value in Parenthesis is for Combined Horizontal and Vertical Input Motion (1 in.= 25.4 mm).

PACOIMA DAM S74W GROUND				
	ISOLATED SYSTEM 1	ISOLATED SYSTEM 2	ISOLATED SYSTEM 3	FIXED
ACCELERATION (g)				
Table Horizontal	0.800 (0.829)	0.816 (0.826)	0.815 (0.830)	0.867 (0.867)
Isolator Horizontal	1.545 (1.951)	1.074 (1.009)	1.012 (1.250)	0.876 (0.896)
Level 1 Horizontal	0.572 (0.767)	0.775 (0.759)	0.783 (0.600)	1.136 (1.181)
Top Horizontal	0.985 (1.300)	1.716 (1.804)	1.548 (1.450)	2.610 (2.650)
Table Vertical	0.010 (0.801)	0.017 (0.788)	0.017 (0.791)	- (0.778)
Isolator S Vertical	0.529 (1.776)	0.490 (1.012)	0.751 (1.198)	- -
Isolator N Vertical	0.495 (2.048)*	0.419 (1.042)	0.571 (0.916)	- -
Top Vertical	0.532 (2.026)*	0.370 (1.095)	0.612 (0.942)	0.093 (0.811)
DISPLACEMENT (in)				
Table Horizontal	4.053 (3.984)	4.054 (3.985)	4.058 (3.982)	4.055 (4.094)
Isolator Horizontal	1.042 (1.187)	0.833 (0.774)	0.491 (0.513)	- -
Level 1 Horizontal	7.038 (7.368)	2.976 (2.820)	3.305 (2.845)	0.157 (0.283)
Top Horizontal	12.857 (13.517)	5.077 (4.854)	6.284 (5.492)	0.343 (0.433)
Table Vertical	0.120 (2.778)	0.120 (2.778)	0.121 (2.776)	- (2.890)
Isolator S Vertical	3.519 (3.600)	0.883 (0.843)	1.500 (1.252)	- -
Isolator N Vertical	2.696 (3.169)	0.765 (0.759)	1.090 (1.024)	- -

* : Value exceeded the limit of instrument.

Table 3-IX - Relation Between Quantities in Tables of Response and Recording Instruments.

Response	Quantity in Tables 3-II to 3-VIII	Instrument in Fig. 3-3
Acceleration	Table Horizontal	AFCH
	Isolator Horizontal	AHBC
	Level 1 Horizontal	AH1C
	Top Horizontal	AHTC
	Table Vertical	AFCV
	Isolator S Vertical	AVBS
	Isolator N Vertical	AVBN
	Top Vertical	AVTN
Displacement	Table Horizontal	DLAT
	Isolator Horizontal	DHBE-DLAT
	Level 1 Horizontal	DH1E-DLAT
	Top Horizontal	Max(DHTE-DLAT,DHTW-DLAT)
	Table Vertical	DVRT
	Isolator S Vertical	DVBS
	Isolator N Vertical	DVBN

Table 3-X - Dynamic Characteristics of Isolated Cabinet as Determined from Pull-Release Tests (1 in.=25.4 mm).

System	Range of Amplitude of Displacement of C.M. (inch)	Period of Free Vibration (sec)	Equivalent Viscous Damping Ratio
1	2.8 - 2	1.15	0.11
3	3.6 - 3	0.82	0.06

Table 3-XI - Analytical Peak Response of Equipment System 4 and Experimental Peak Response of Fixed Cabinet (1 in.= 25.4 mm).

	Taft 5th		Taft 7th		El Centro 5th		El Centro 7th		Pacoima Ground	
	System 4	Fixed	System 4	Fixed	System 4	Fixed	System 4	Fixed	System 4	Fixed
Top Horizontal Acceleration (g)	0.583	0.529	1.126	1.167	0.618	0.729	1.223	1.780	1.474	2.610
Top Horizontal Displacement (in)	0.107	0.083	0.305	0.185	0.143	0.177	0.358	0.350	0.613	0.343
Isolator Horizontal Displacement (in)	0.014	-	0.036	-	0.018	-	0.043	-	0.063	-
Isolator Vertical S Displacement (in)	0.018	-	0.053	-	0.021	-	0.052	-	0.088	-
Isolator Vertical N Displacement (in)	0.016	-	0.046	-	0.024	-	0.062	-	0.117	-

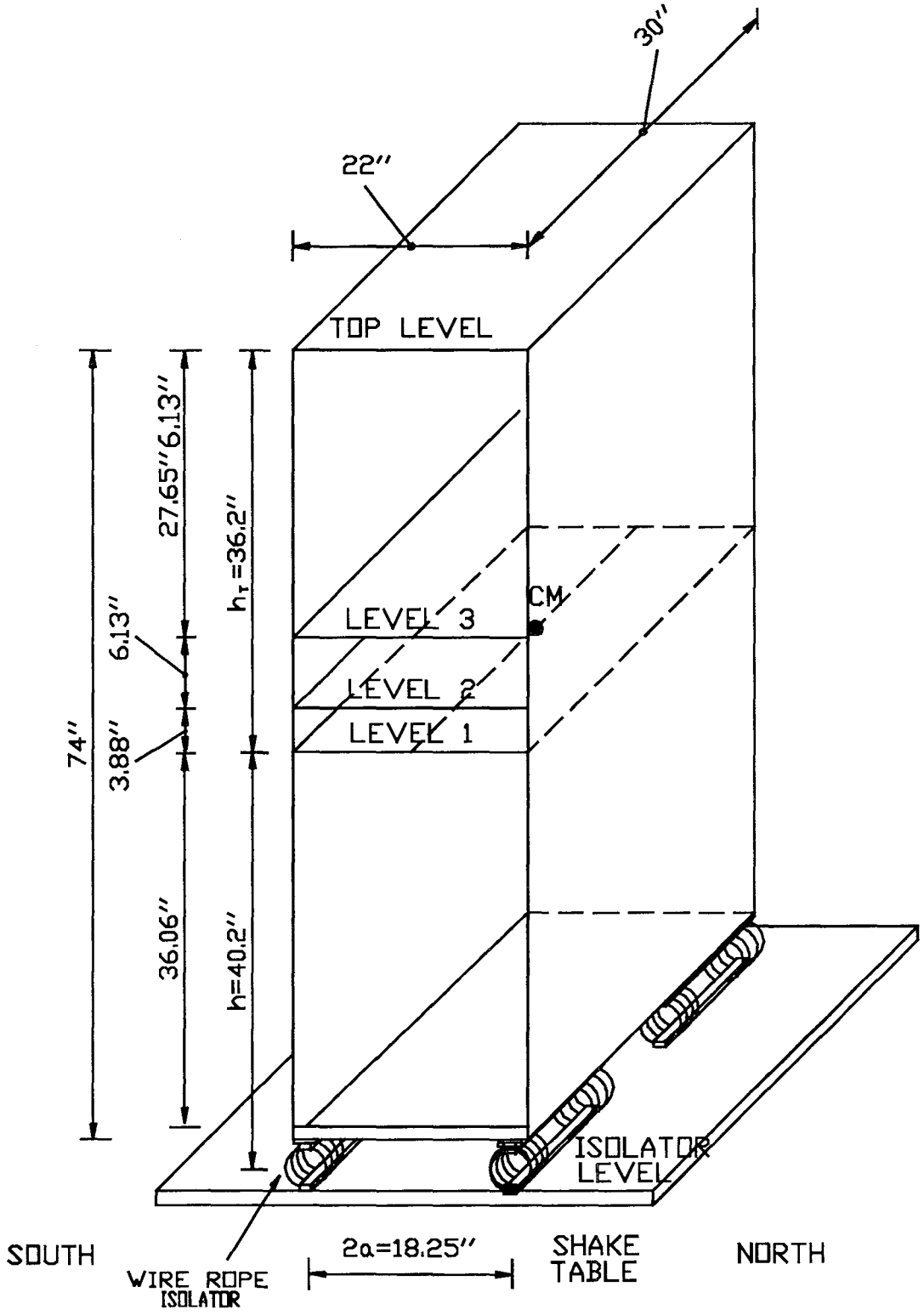

Figure 3-1 Tested Equipment Cabinet (1 in.= 25.4 mm).

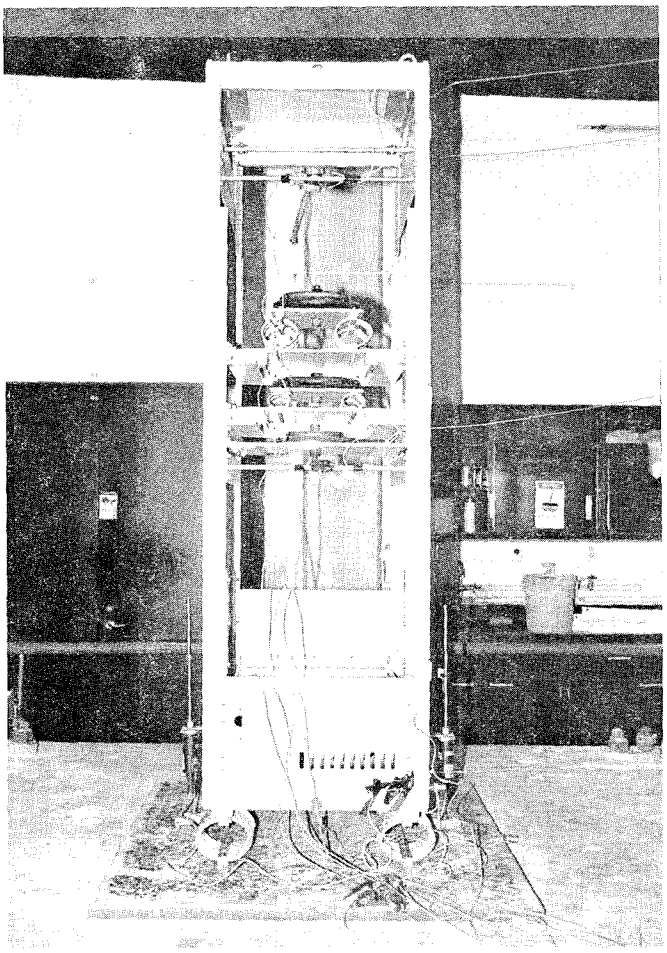

(a)

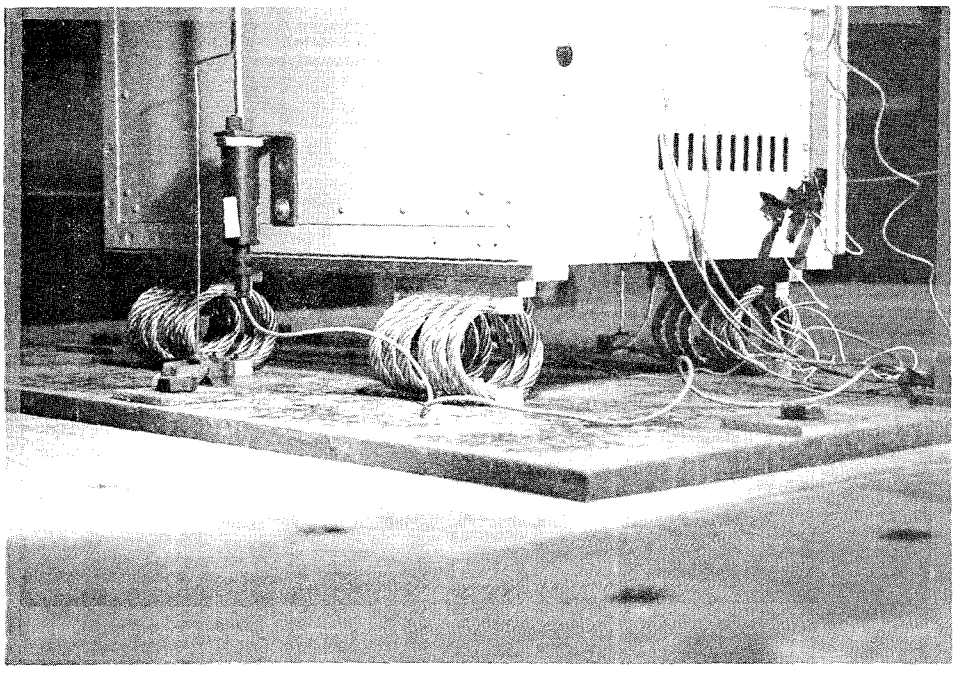

(b)

Figure 3-2 Views of Isolated Cabinet on Shake Table (a) Transverse View, (b) Isolation System (No.3).

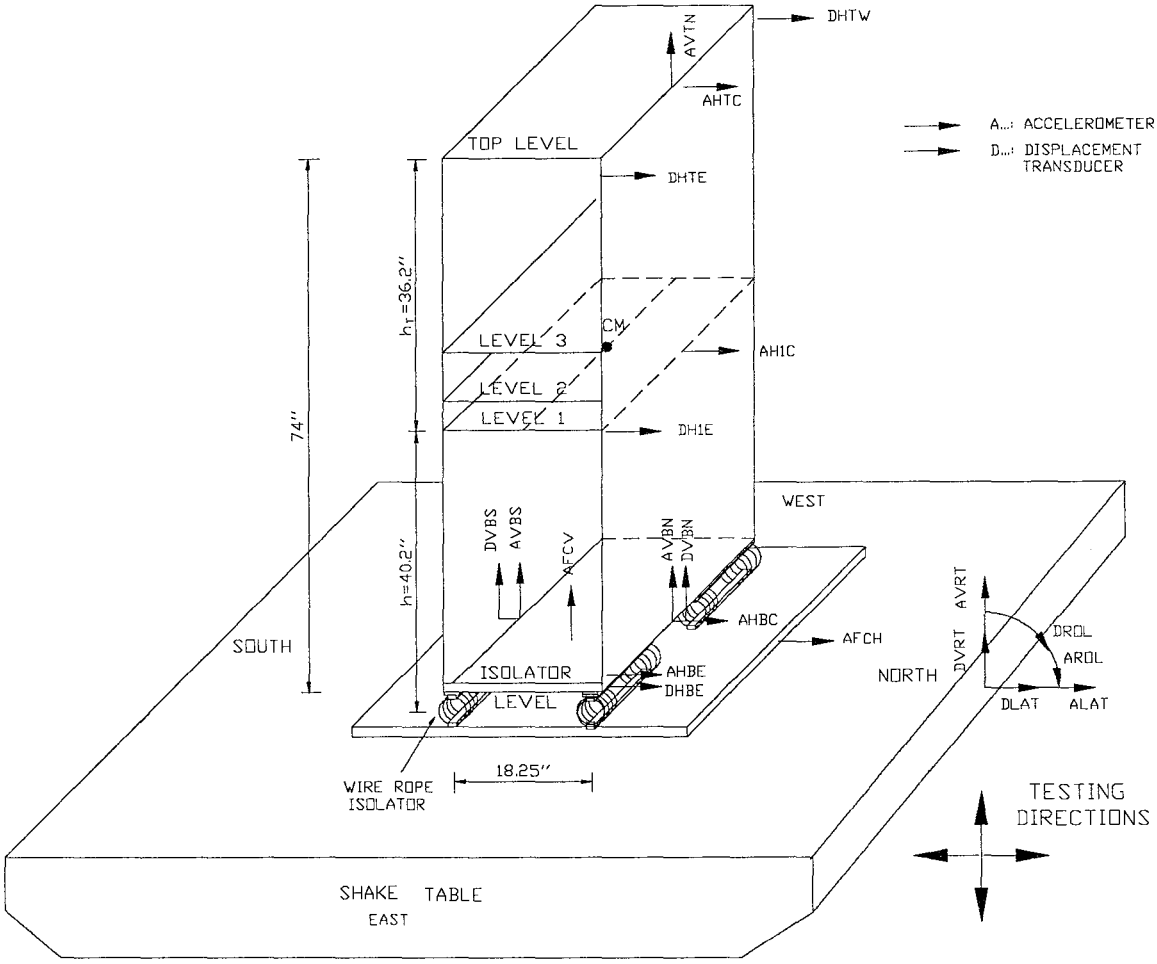

Figure 3-3 Instrumentation Diagram (1 in.= 25.4 mm).

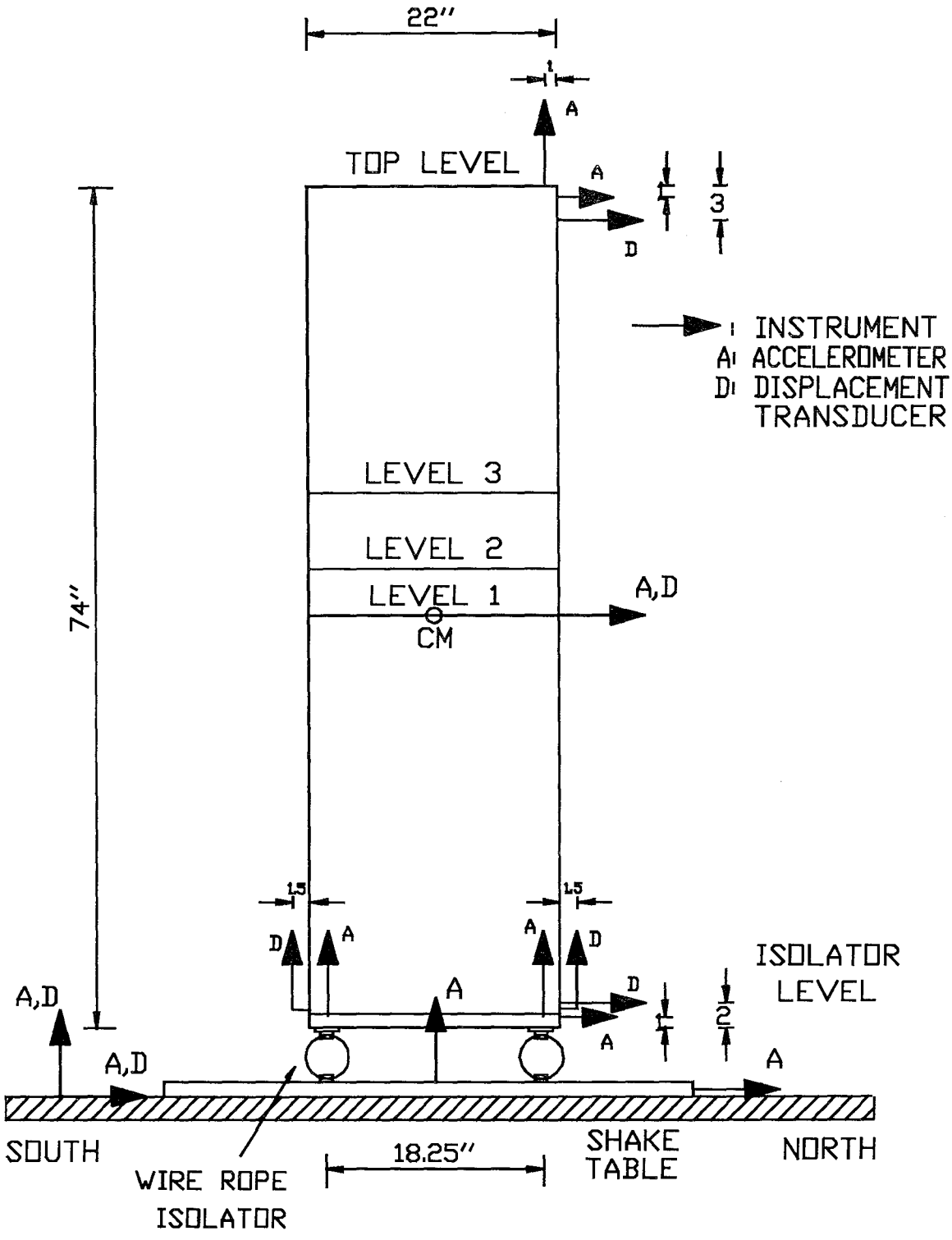

Figure 3-4 Location of Instruments (1 in.= 25.4 mm).

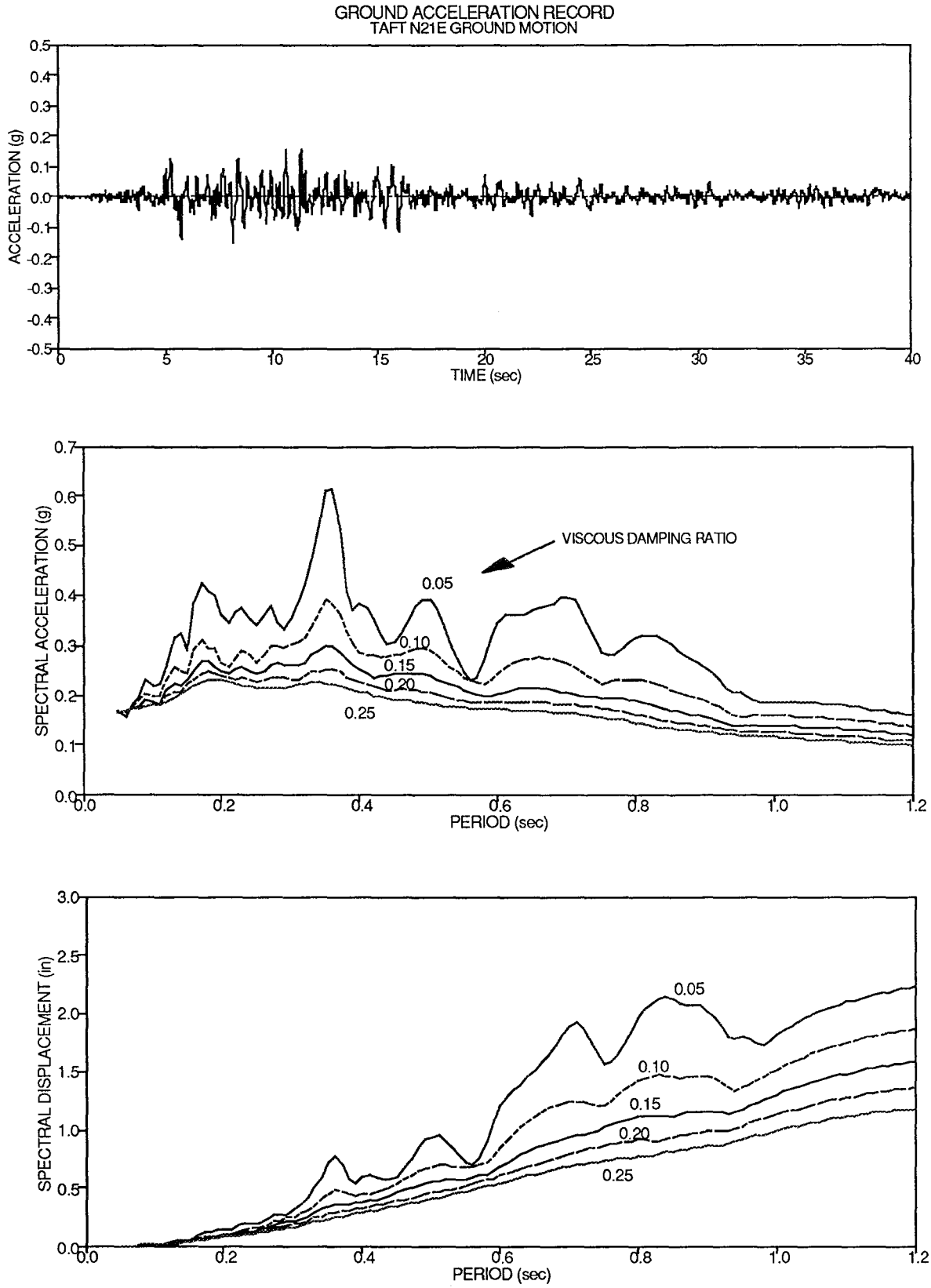

Figure 3-5 Time History of Ground Acceleration of Taft N21E Motion and its Acceleration and Displacement Response Spectra (1 in.= 25.4 mm).

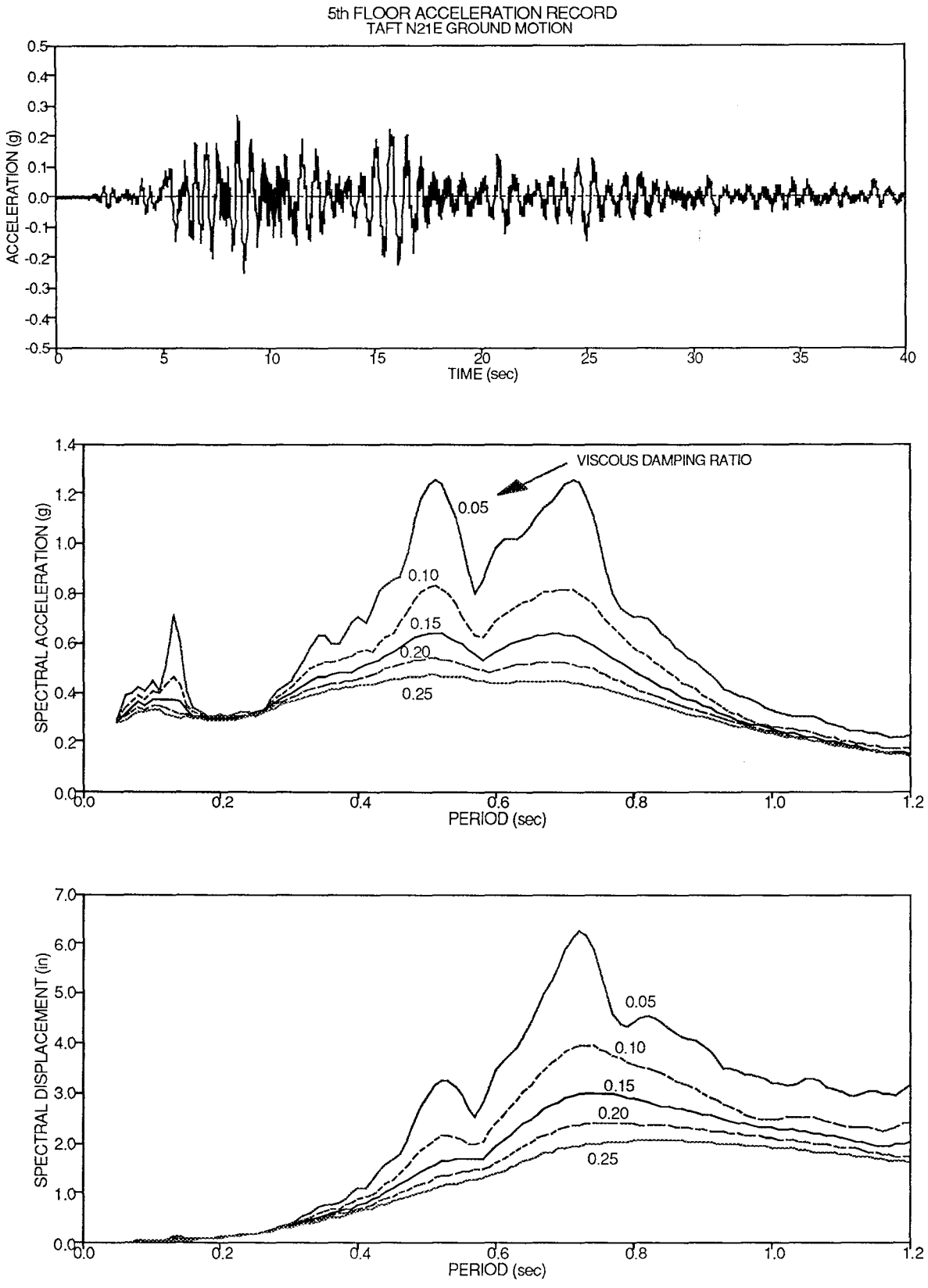

Figure 3-6 Time History of 5th Floor Acceleration of 7-story Building Excited by Taft N21E Motion and its Acceleration and Displacement Response Spectra (1 in.= 25.4 mm).

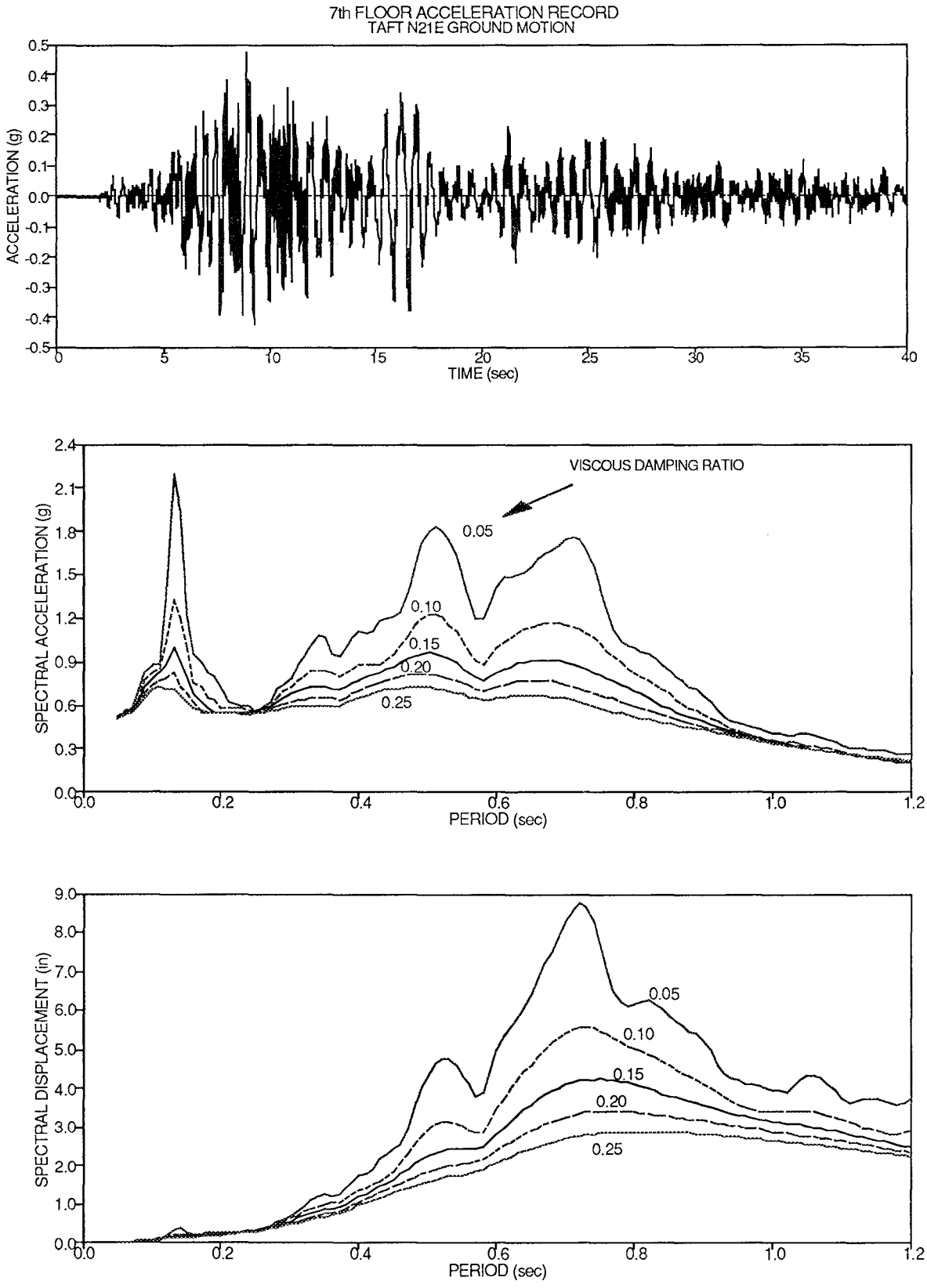

Figure 3-7 Time History of 7th Floor Acceleration of 7-story Building Excited by Taft N21E Motion and its Acceleration and Displacement Response Spectra (1 in.= 25.4 mm).

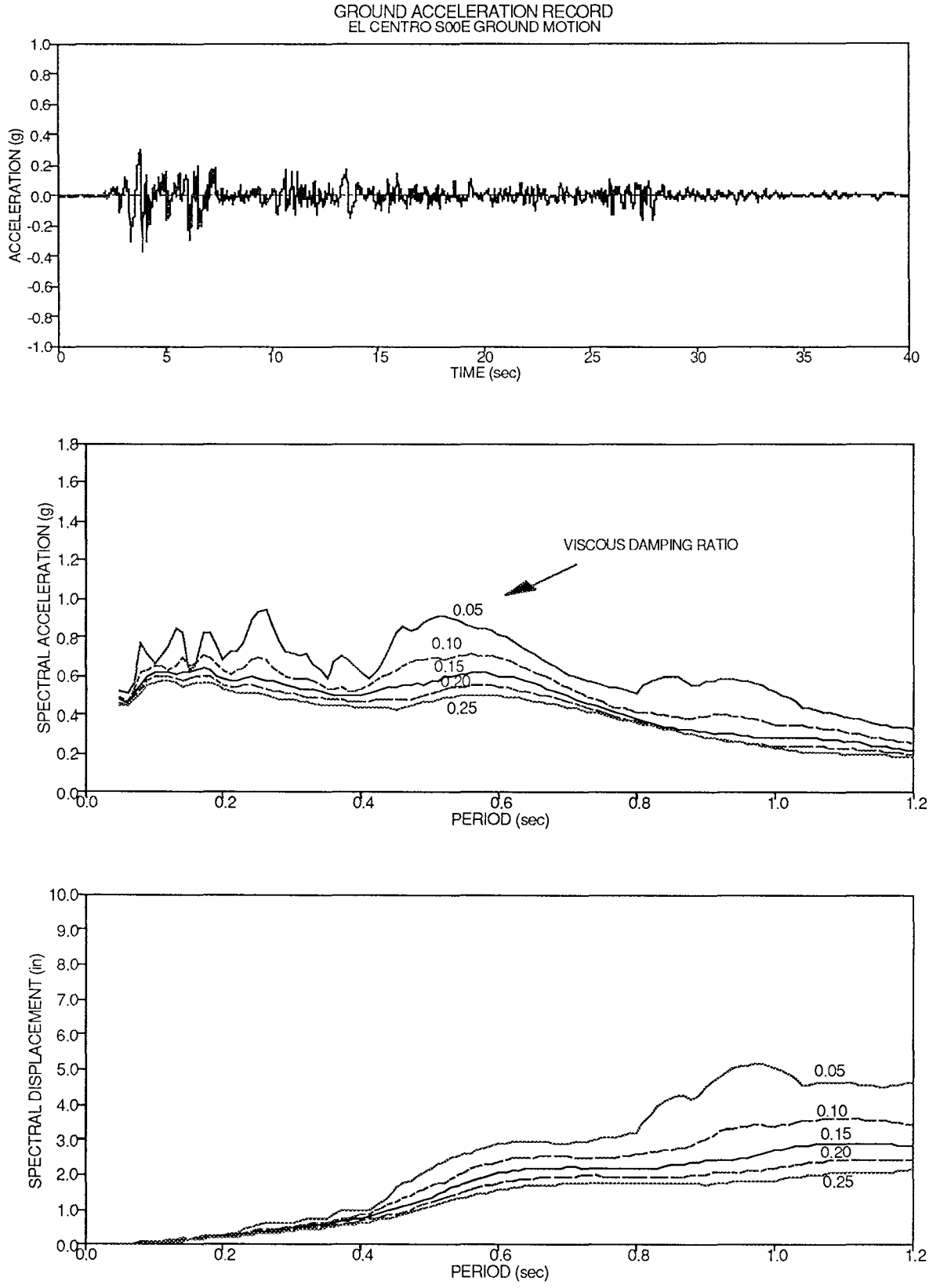

Figure 3-8 Time History of Ground Acceleration of El Centro S00E Motion and its Acceleration and Displacement Response Spectra (1 in.= 25.4 mm).

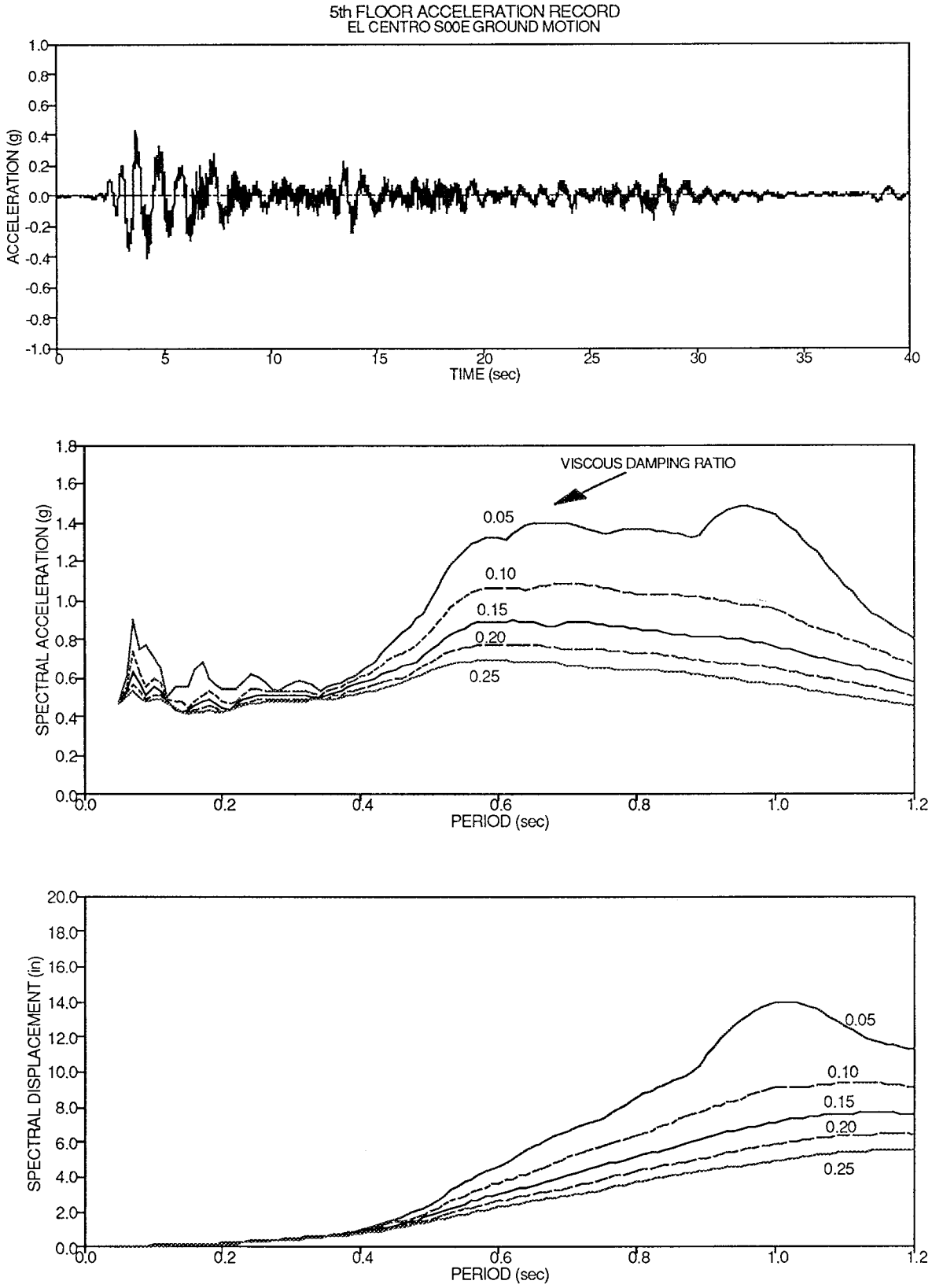

Figure 3-9 Time History of 5th Floor Acceleration of 7-story Building Excited by El Centro S00E Motion and its Acceleration and Displacement Response Spectra (1 in.= 25.4 mm).

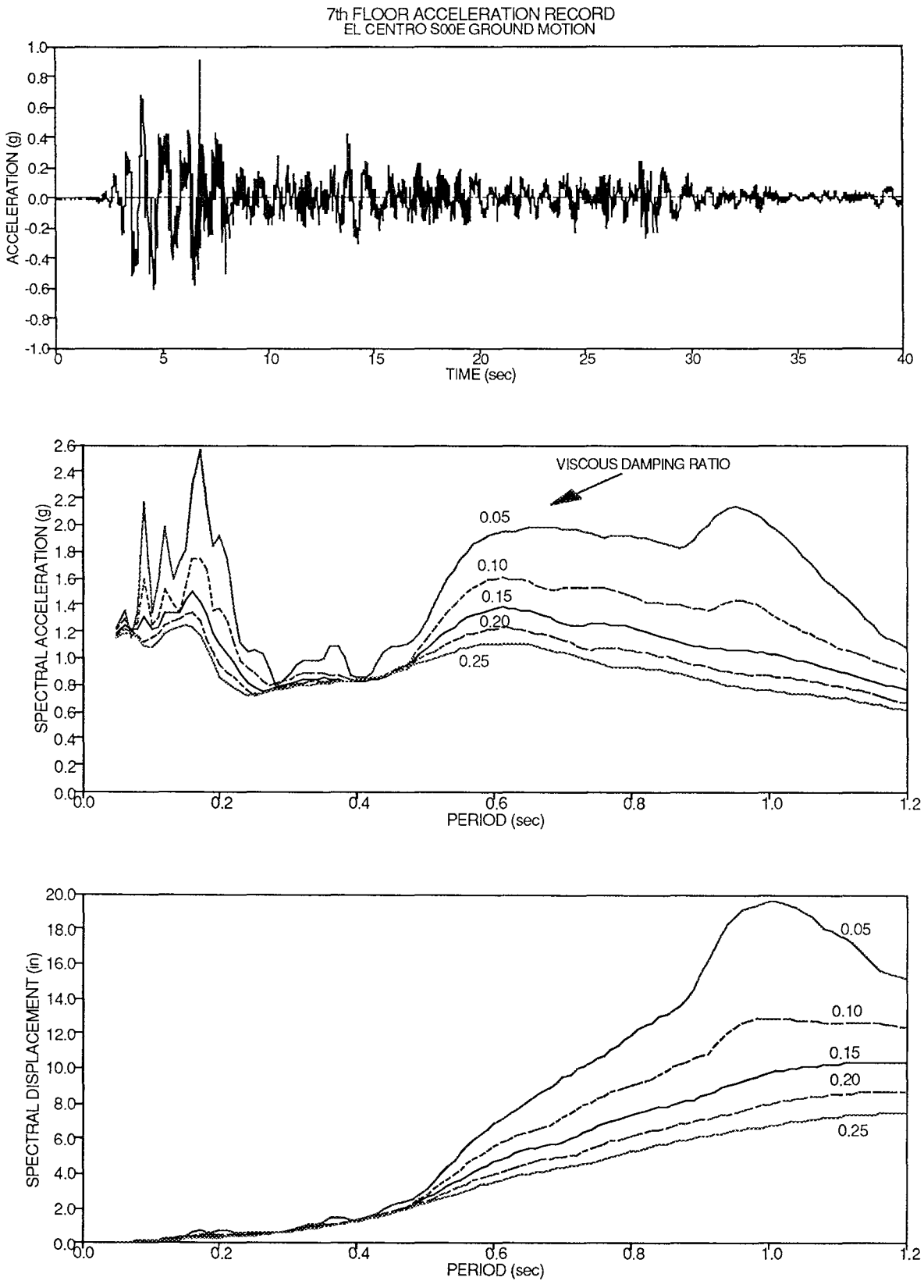

Figure 3-10 Time History of 7th Floor Acceleration of 7-story Building Excited by El Centro S00E Motion and its Acceleration and Displacement Response Spectra (1 in.= 25.4 mm).

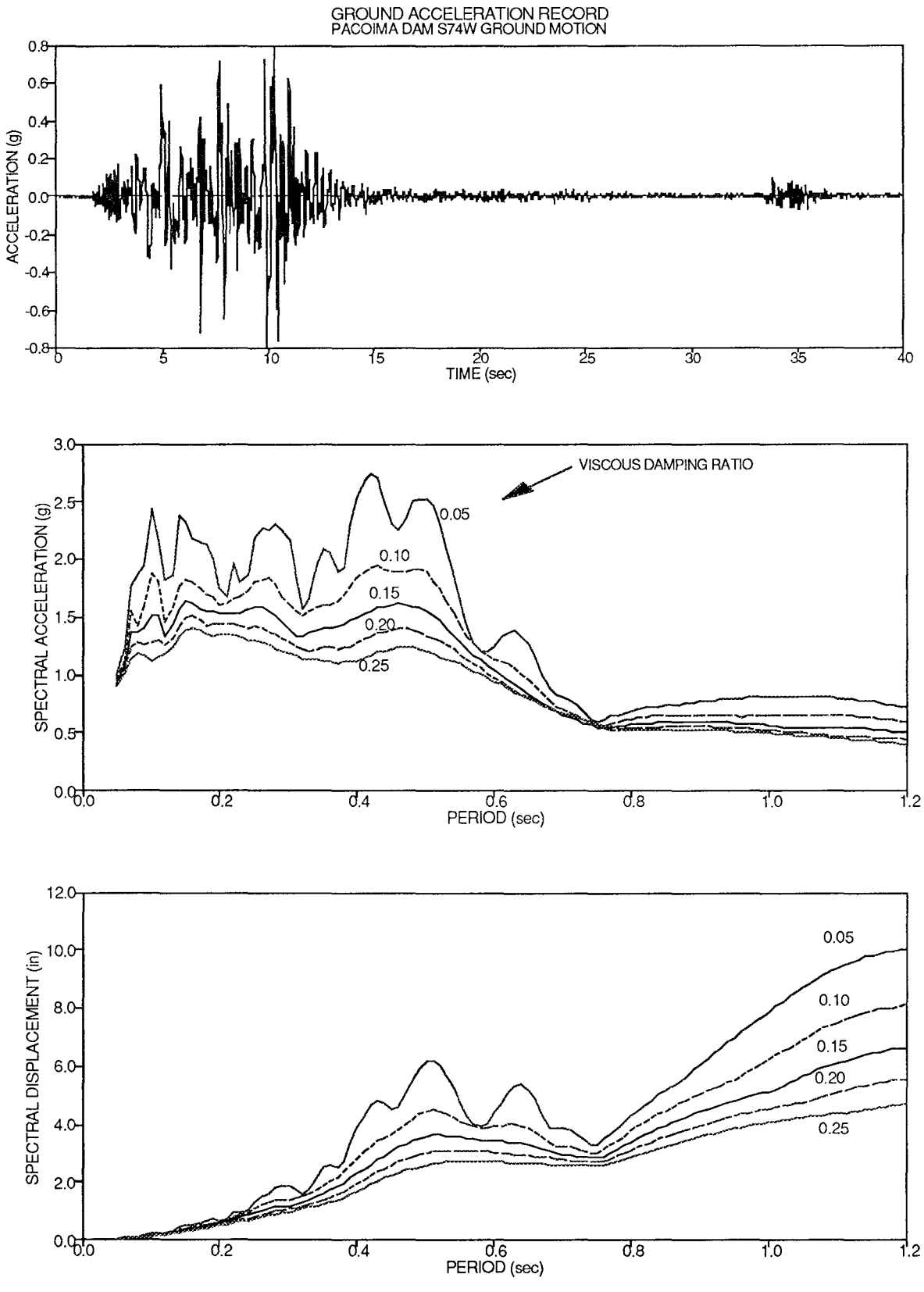

Figure 3-11 Time History of Ground Acceleration of Pacoima Dam S74W Motion and its Acceleration and Displacement Response Spectra (1 in.= 25.4 mm).

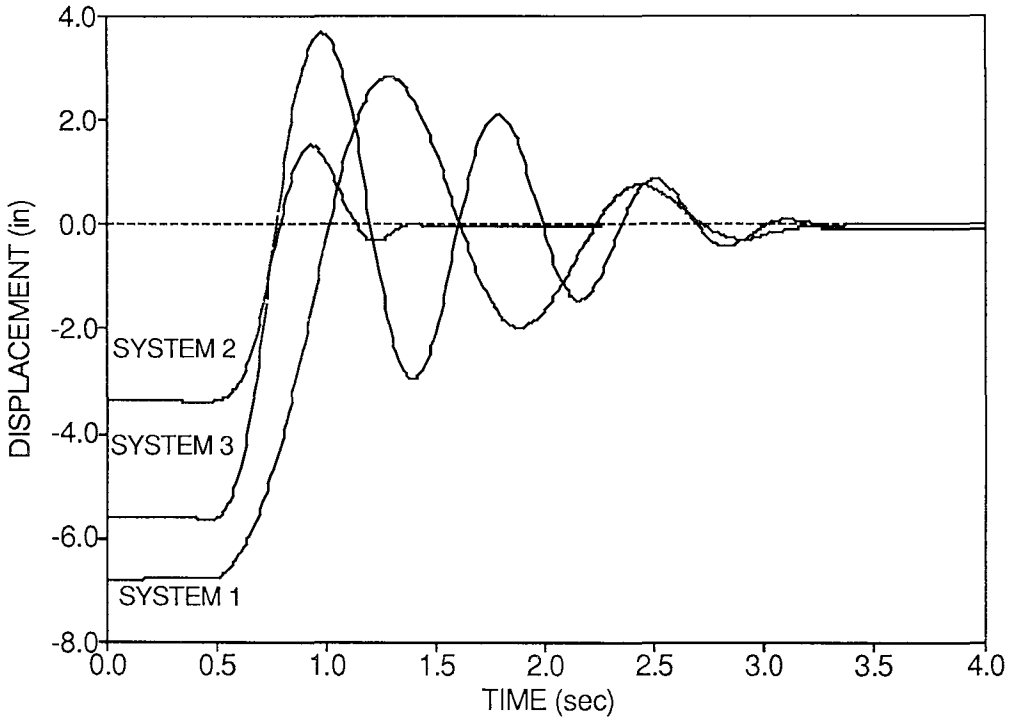

Figure 3-12 Displacement Histories of Center of Mass of Isolated Equipment in Pull-Release Tests (1 in.= 25.4 mm).

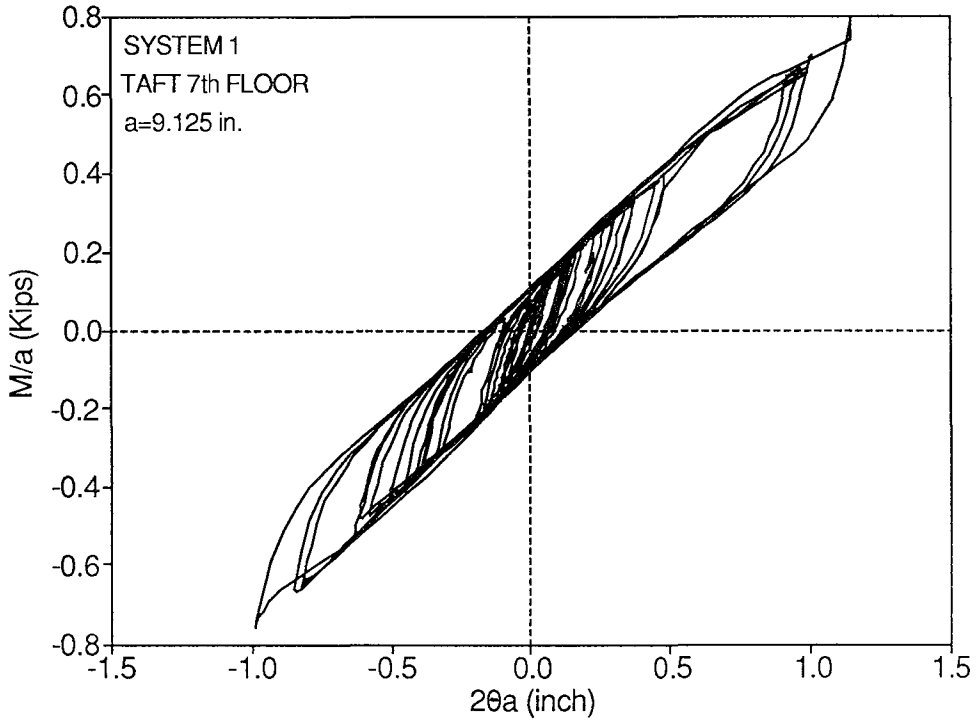

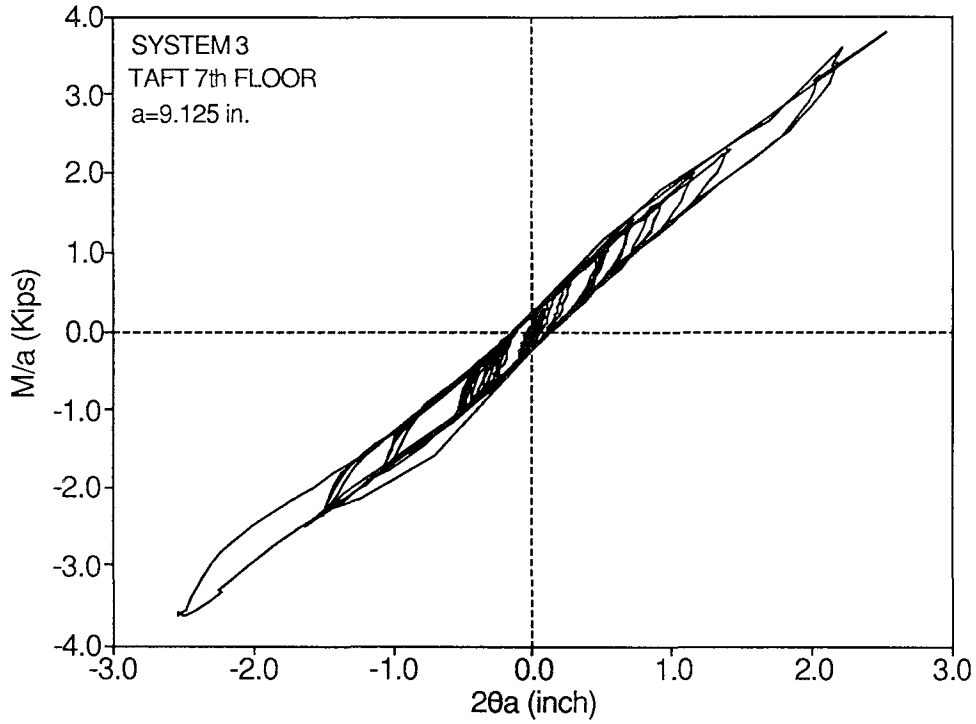

Figure 3-13 Moment-Rotation Loops of Isolated Cabinet in Test With Taft 7th Floor Excitation (1 in.= 25.4 mm, 1 Kip= 4.46 kN).

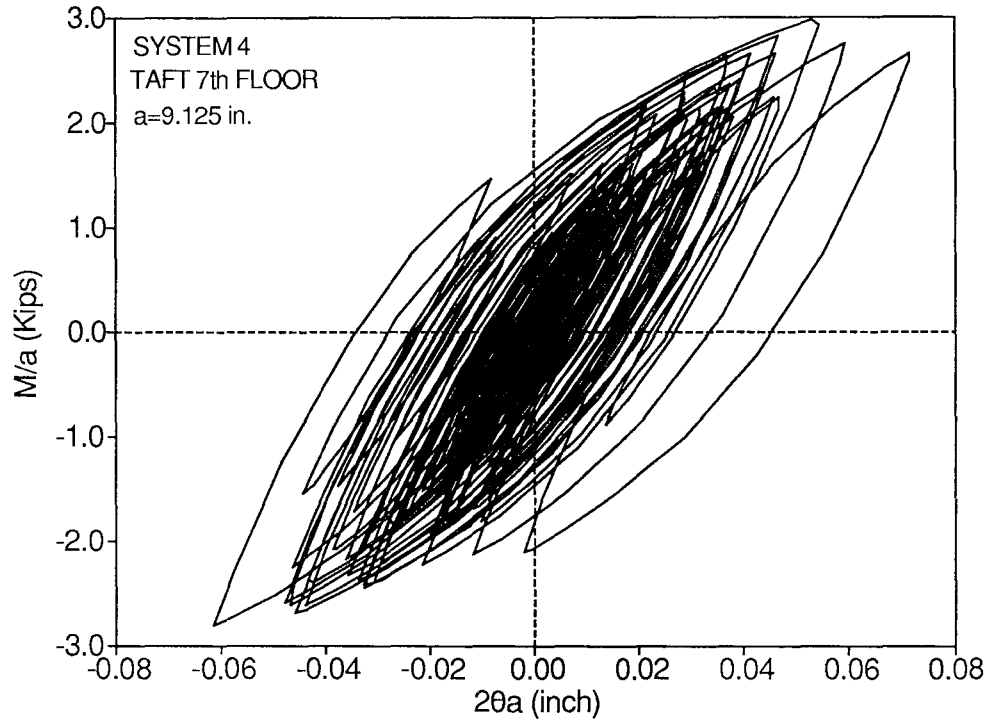

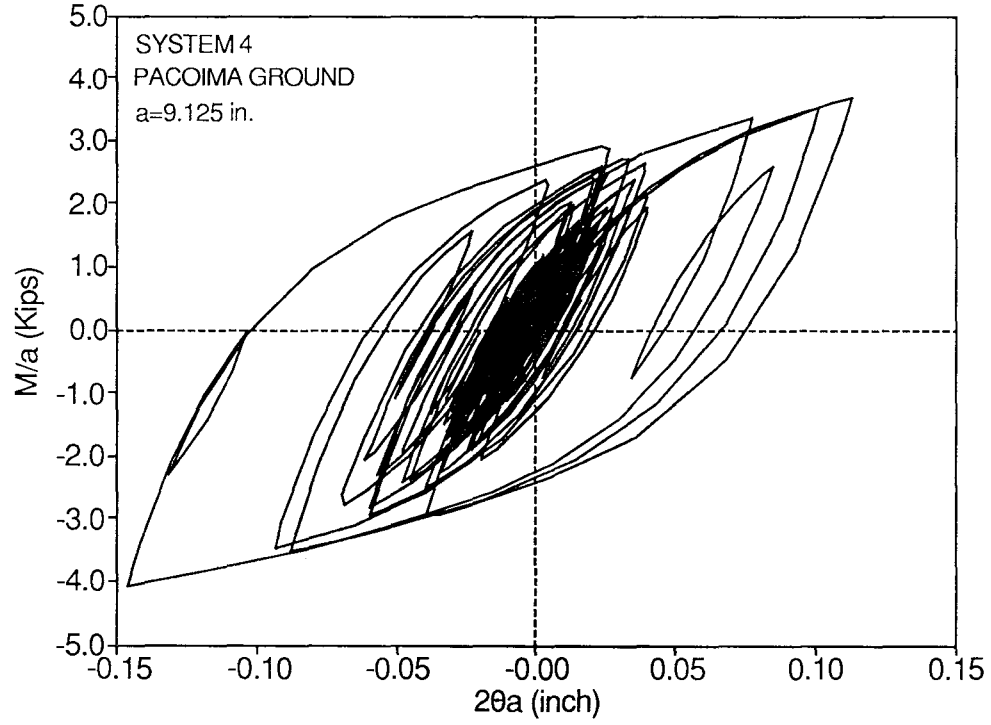

Figure 3-14 Moment-Rotation Loops of System 4 (1 in.= 25.4 mm, 1 Kip= 4.46 kN).

SECTION 4

ANALYTICAL PREDICTION OF RESPONSE

A mathematical model of equipment supported by wire rope isolators is developed for the analytical prediction of dynamic response. The model accounts only for in - plane response as if the excitation consists of only components in a vertical plane and the system exhibits no eccentricities. Furthermore, three assumptions are made:

1. The possible interaction between vertical and horizontal components of force developed at a wire rope isolator is negligible. Each isolator is modeled by two independent hysteretic elements (springs) which exhibit the characteristics identified in section 2. The two springs are placed in the vertical and horizontal directions at each location of wire rope isolator.
2. The rotational stiffness of wire rope isolators is negligible.
3. The equipment is rigid. This assumption can be easily relaxed.

Figure 4-1 shows the model of a rigid equipment supported by wire rope isolators. The springs representing wire rope isolators are symmetrically placed at distance a from the center of mass and at the same height h below the center of mass. The degrees of freedom are selected to be the horizontal, u_x, and vertical u_z, displacements and rotation, θ, of the center of mass.

4.1 Equations of Motion for Large Rotations

The equations of motion are first derived by considering large rotations and subsequently reduced to their geometrically linear form (small rotations).

Two orthogonal coordinate systems are defined. The first, XZ, is fixed in time and defined to have its origin at the initial position of static equilibrium (at time t=0) of the center of mass. The second, X´Z´, is moving with the center of mass as illustrated in Figure 4-1. The degrees of freedom are the translations, u_x and u_z of the center of mass with respect to the initial position (CM in Figure 4-1) and its clockwise rotation θ. It should be noted that in classical terminology, coordinates XZ are refer to as reference or material or configuration or Lagrangian coordinates and coordinates X´Z´ are refer to as present or spatial or Eulerian coordinates.

A point i having coordinates (X'_i, Z'_i) in the moving system can be defined in terms of coordinates in the fixed-initial system by the following transformation:

$$\begin{bmatrix} X_i \\ Z_i \end{bmatrix} = \begin{bmatrix} u_x \\ u_z \end{bmatrix} + \begin{bmatrix} \cos\theta & \sin\theta \\ -\sin\theta & \cos\theta \end{bmatrix} \cdot \begin{bmatrix} X'_i \\ Z'_i \end{bmatrix} \tag{4-1}$$

The displacements of point i with respect to its initial position are

$$\begin{bmatrix} u_{xi} \\ u_{zi} \end{bmatrix} = \begin{bmatrix} X_i \\ Z_i \end{bmatrix} - \begin{bmatrix} X'_i \\ Z'_i \end{bmatrix} \tag{4-2}$$

At time t=0 the two systems are identical and therefore $X_i = X'_i$ and $Z_i = Z'_i$.

The displacements of some points of interest are derived from equations 4-1 and 4-2 and given below. These points are B1 and B2 at the bearing level and T2 at the top level of the equipment (see Figure 4-2). These points have the following coordinates with respect to the moving system:

$X'_{B1} = -a$, $X'_{B2} = a$, $Z'_{B1} = Z'_{B1} = -h$, $X'_{T2} = b$, $Z'_{T2} = h_T$.

$$u_{xB1} = u_x - a(\cos\theta - 1) - h.\sin\theta \tag{4-3}$$

$$u_{zB1} = u_z + h(1 - \cos\theta) + a.\sin\theta \tag{4-4}$$

$$u_{xB2} = u_x + a(\cos\theta - 1) - h.\sin\theta \tag{4-5}$$

$$u_{zB2} = u_z + h(1 - \cos\theta) - a.\sin\theta \tag{4-6}$$

$$u_{xT2} = u_x + b(\cos\theta - 1) + h_T.\sin\theta \tag{4-7}$$

$$u_{zT2} = u_z - h_T(1 - \cos\theta) - b.\sin\theta \tag{4-8}$$

The equations of motion of the equipment are derived from dynamic equilibrium using the free body diagram of Figure 4-2:

$$m\ddot{u}_x + 2F_{x1} + 2F_{x2} = -m\ddot{u}_{gx} \tag{4-9}$$

$$m\ddot{u}_z + 2F_{z1} + 2F_{z2} + W = -m\ddot{u}_{gz} \tag{4-10}$$

$$I_o\ddot{\theta} - 2F_{x1}D_{z1} - 2F_{x2}D_{z2} + 2F_{z1}D_{x1} - 2F_{z2}D_{x2} = 0 \tag{4-11}$$

in which $I_o = mr^2$ is the moment of inertia of the equipment about the horizontal axis passing through the center of mass, r = radius of gyration, m = mass, W = weight and $\ddot{u}_{gx}$ and $\ddot{u}_{gz}$ are the horizontal and vertical components of the input motion, respectively. Furthermore, F_{x1} and F_{x2} are the spring forces in the horizontal direction at points B1 and B2 which are given by equations 2-1 and 2-2 for displacement $U = u_{xB1}$ and $U = u_{xB2}$, respectively. Moreover F_{z1} and F_{z2} are the spring forces in the vertical direction at points B1 and B2 which are given by equations 2-5 to 2-7 and 2-2 for vertical displacement $U = u_{zB1}$ and $U = u_{zB2}$, respectively. Distances D_{x1}, D_{x2}, D_{z1} and D_{z2} represent the horizontal and vertical arms of isolator forces with respect to the center of mass and are given by the following expressions:

$$D_{x1} = a.\cos\theta + h.\sin\theta \tag{4-12}$$

$$D_{x2} = a.\cos\theta - h.\sin\theta \tag{4-13}$$

$$D_{z1} = -a.\sin\theta + h.\cos\theta \tag{4-14}$$

$$D_{z2} = a.\sin\theta + h.\cos\theta \tag{4-15}$$

Equations 2-1, 2-2, 2-5 to 2-7, 4-3 to 4-6 and 4-9 to 4-15 form a system of ten first order differential equations. Initial conditions are zero except for displacement u_z which is equal to the static vertical displacement of the isolators due to the weight of the equipment. Numerical solutions were derived by use of Gear's implicit multistep integration scheme with adaptive time step (Gear 1971, IMSL 1987).

4.2 Equations of Motion for Small Rotations

For small rotations, $\sin\theta$ and $\cos\theta$ may be expanded in binomial series. Correct to $O(\theta^2)$, $\cos\theta$ and $\sin\theta$ may be replaced by 1 and θ, respectively. The error involved in such an approximation does not exceed 2% of exact for values of θ up to 0.2 rad (11.4 degrees). In all of the tests presented in section 3 the angle of rotation did not exceed this limit. Accordingly, the geometrically linear equations of motion introduce errors which are insignificant for practical purposes.

The geometrically linear form of equations 4-3 to 4-15 is:

$$u_{xB1} = u_{xB2} = u_{xb} = u_x - h.\theta \tag{4-16}$$

$$u_{zB1} = u_z + a.\theta \tag{4-17}$$

$$u_{zB2} = u_z - a.\theta \tag{4-18}$$

$$D_{x1} = a + h.\theta \tag{4-19}$$

$$D_{x2} = a - h.\theta \tag{4-20}$$

$$D_{z1} = -a.\theta + h \tag{4-21}$$

$$D_{z2} = a.\theta + h \tag{4-22}$$

As a result of equation 4-16,

$$F_{x1} = F_{x2} = F_x \tag{4-23}$$

and the equations of motion modify to

$$m\ddot{u}_x + 4F_x = -m\ddot{u}_{gx} \tag{4-23}$$

$$m\ddot{u}_z + 2F_{z1} + 2F_{z2} + W = -m\ddot{u}_{gz} \tag{4-25}$$

$$I_o\ddot{\theta} - 4F_x h + 2F_{z1}(a + h\theta) - 2F_{z2}(a - h\theta) = 0 \tag{4-26}$$

In these equations, F_x is given by equations 2-1 and 2-2 with $U = U_{xb}$ and F_{z1} and F_{z2} are given by equations 2-1, 2-5 to 2-7 with $U = u_{zB1}$ (eq. 4-17) and $U = u_{zB2}$ (eq. 4-18), respectively.

Integration of the geometrically linear equations of motion resulted in responses which were almost identical to those obtained from the geometrically nonlinear equations. This was the case for all analyzed systems, some of which underwent rotations of up to 0.2 rad.

The geometrically linear equations of motion are useful in the development of a simplified analysis procedure which can be used together with floor response spectra to obtain estimates of the peak response.

4.3 Simplified Analysis Procedure

A simplified analysis procedure is developed by assuming that each wire rope isolator may be represented by two linear springs of stiffness K_x in the horizontal direction and stiffness K_z in the vertical direction. Furthermore, the energy dissipation is accounted for by the use of equivalent viscous damping ratios in modal analysis. Forces F_x, F_{z1} and F_{z2} are expressed as

$$F_x = K_x(u_x - h\theta) \tag{4-27}$$

$$F_{z1} = K_z(u_z + a\theta) \tag{4-28}$$

$$F_{z2} = K_z(u_z - a\theta) \tag{4-29}$$

Substituting equations 4-27 to 4-29 into 4-24 to 4-26, the linear equations of motion are derived after droping higher order terms:

$$m\ddot{u}_x + 4K_x u_x - 4K_x h\theta = -m\ddot{u}_{gx} \tag{4-30}$$

$$m\ddot{u}_z + 4K_z u_z + W = -m\ddot{u}_{gz} \tag{4-31}$$

$$I_o\ddot{\theta} - 4K_x h u_x + (4K_z a^2 + 4K_x h^2)\theta = 0 \tag{4-32}$$

In these equations u_z is decoupled from the other degrees of freedom because the system has no eccentricities. Accordingly, the analysis for vertical excitation may be performed independently of that for horizontal excitation.

Concentrating on the coupled horizontal - rocking response, equations 4-30 and 4-32 are expressed in the following matrix form upon division by mass m:

$$[I]\{\ddot{U}\} + [K]\{U\} = -\{R\}\ddot{u}_{gx} \tag{4-33}$$

where [I] is the identity matrix,

$$\{U\} = \begin{Bmatrix} u_x \\ r\theta \end{Bmatrix}, \quad \{R\} = \begin{Bmatrix} 1 \\ 0 \end{Bmatrix} \tag{4-34}$$

and

$$[K] = \begin{bmatrix} \omega_x^2 & -\omega_x^2\left(\frac{h}{r}\right) \\ -\omega_x^2\left(\frac{h}{r}\right) & \omega_x^2\left(\frac{h}{r}\right)^2 + \omega_z^2\left(\frac{a}{r}\right)^2 \end{bmatrix} \tag{4-35}$$

In the above equation

$$\omega_x = \left(\frac{4K_x}{m}\right)^{1/2}, \quad \omega_z = \left(\frac{4K_z}{m}\right)^{1/2} \tag{4-36}$$

are the roll and vertical frequencies of the isolated equipment, respectively.

Equations 4-33 may be solved for the modal properties of the linearized system which together with representative damping ratios may be used to obtain estimates of the peak response of the system to horizontal excitation. In free vibration, $\ddot{u}_{gx} = 0$ and

$$\{U\} = \{\phi_n\} e^{i\omega_n t} \tag{4-37}$$

in which ω_n = frequency of free vibration and ϕ_{xn} and $\phi_{\theta n}$ are elements of mode shape $\{\phi_n\}$ corresponding to u_x and $r\theta$, respectively. Equation 4-33 takes the form:

$$\begin{bmatrix} \omega_x^2 - \omega_n^2 & -\omega_x^2\left(\frac{h}{r}\right) \\ -\omega_x^2\left(\frac{h}{r}\right) & \omega_x^2\left(\frac{h}{r}\right)^2 + \omega_z^2\left(\frac{a}{r}\right)^2 - \omega_n^2 \end{bmatrix} \begin{Bmatrix} \phi_{xn} \\ \phi_{\theta n} \end{Bmatrix} = \begin{Bmatrix} 0 \\ 0 \end{Bmatrix} \tag{4-38}$$

The requirement for nontrivial solution gives the characteristic equation from where the frequencies of the coupled system, ω_1 and ω_2, may be calculated:

$$\omega_n^4 - \left[\omega_x^2\left(1 + \left(\frac{h}{r}\right)^2\right) + \omega_z^2\left(\frac{a}{r}\right)^2\right]\omega_n^2 + \omega_x^2\omega_z^2\left(\frac{a}{r}\right)^2 = 0\ ,\quad n = 1,2 \tag{4-39}$$

With the frequencies calculated from equation 4-39, equation 4-38 is used to obtain the mode shapes.

The calculation of peak response values may be performed by the modal analysis approach (Clough 1975). Applying the transformation

$$\{U\} = [\Phi]\{y\} \tag{4-40}$$

to equation 4-33, using the orthogonality conditions and introducing modal damping one obtains

$$\ddot{y}_n + 2\xi_n\omega_n\dot{y}_n + \omega_n^2 y_n = -\frac{[\Phi]^T\{R\}\ddot{u}_{gx}}{[\Phi]^T[\Phi]}\ ,\ n = 1,2 \tag{4-41}$$

In the above equations $[\Phi]$ is a matrix containing in its columns the two mode shapes and ξ_n is the damping ratio in

mode n. Peak modal responses are calculated from response spectra of the floor motion:

$$\max y_n = \frac{[\Phi]^T\{R\}}{[\Phi]^T[\Phi]} S_d(\omega_n,\xi_n) \tag{4-42}$$

$$\max \ddot{y}_{n\,TOTAL} = \frac{[\Phi]^T\{R\}}{[\Phi]^T[\Phi]} S_a(\omega_n,\xi_n) \tag{4-43}$$

where S_d and S_a are, respectively, the spectral displacement and spectral acceleration of the floor motion for frequency ω_n and damping ratio ξ_n. Peak responses for each mode are calculated by use of equation 4-40 and then combined by the square-root-sum-squares (SRSS) combination rule.

The simplified procedure is very useful in obtaining quick estimates of the peak response. It requires, however the effective stiffnesses of the wire rope isolators and the effective damping ratio of the system. The effective stiffness may be obtained from experimental force - displacement loops of the isolators. This requires the employment of an iterative procedure to first calculate displacements and subsequently estimate stiffnesses and refine calculations. The effective damping ratio, however, can not be a-priori selected. A nonlinear dynamic analysis for harmonic excitation may be performed and calculated moment - rotation loops may be used to obtain values of effective damping ratio (see section 3.3). Otherwise, damping must be selected with conservatism and based on experience.

4.4 Comparison of Experimental and Analytical Results

Comparisons of experimental and analytical time histories of response of system 1 are presented in Figures 4-3 to 4-21. All analyses were based on the geometrically nonlinear formulation of section 4.1. Analyses with the geometrically linear equations of section 4.2 gave almost identical results. The parameters in the analytical model were W = 400 lbs (1784 N), r = 22.83 in. (580 mm), a = 9.125 in. (231.8 mm), h = 40.2 in. (1021 mm) and h_T = 36.2 in. (919.5 mm).

The analytical time history results are in good agreement with the experimental results. The content in frequency is reproduced very well, however the displacements are in many cases overpredicted. A number of factors may be contributing to this, with the two dominating ones being the neglect of interaction and lesser energy dissipation in the mathematical model of the isolators.

Peak response values of system 1 as computed by time history analysis and by the simplified method are compared to experimental results in Table 4-I. The simplified method required estimates of isolator stiffnesses and damping ratio. They were determined by the following procedure. The system was numerically analyzed for harmonic excitation and loops of moment - rotation were determined (see section 3.3, equations 3-1 and 3-2). From these loops, which are shown in Figure 4-22, values of effective period and equivalent viscous damping ratio (equations 3-3 and 3-4) were calculated. Furthermore,

representative values of the vertical isolators stiffness, K_z, were determined from

$$K_r = \frac{M}{\theta} = 4K_z a^2 \qquad (4\text{-}44)$$

These quantities are listed in Table 4-II as function of the amplitude of rotation ($2\theta a$). Moreover, representative values of the isolator horizontal stiffness, K_x, were determined from experimental lateral force - displacement loops (see section 2, Fig. 2-4).

The analysis was performed by assuming a representative value of rotation, θ, then selecting appropriate values of vertical stiffness, K_z, and damping ratio, ξ, and performing response spectrum analysis (section 4.3). Subsequently, the calculated value of rotation was used to improve the estimates of K_z and ξ using the data of Table 4-II and the analysis was repeated. This iterative process was applied for four of the floor excitations using the spectra of Figures 3-5 to 3-10. The calculated system characteristics are presented in Table 4-III, while the response is presented in Table 4-I. It should be noted that the damping factor in the second mode was not known and was assumed to be equal to that in the first mode.

The results of Table 4-I demonstrate good agreement between analytical and experimental peak response values. It may be stated that the simplified method is sufficiently accurate to represent a useful design tool.

Table 4-I - Comparison of Experimental and Analytical Peak Response Values (1 in.= 25.4 mm).

	TAFT N21E GROUND MOTION			TAFT N21E 7th FLOOR		
	Experiment	Time History	Simplified Method	Experiment	Time History	Simplified Method
Top Horizontal Acceleration (g)	0.220	0.233	0.248	0.625	0.648	0.706
Top Horizontal Displacement (in)	1.211	1.214	1.620	4.163	4.449	4.906
Isolator Horizontal Displacement (in)	0.122	0.100	0.182	0.302	0.412	0.529
Isolator S Vertical Displacement (in)	0.247	0.247	0.262	1.031	1.001	0.799
Isolator N Vertical Displacement (in)	0.198	0.186	0.262	0.806	0.977	0.799

Table 4-I - Continued.

	EL CENTRO S00E GROUND MOTION			EL CENTRO S00E 7th FLOOR		
	Experiment	Time History	Simplified Method	Experiment	Time History	Simplified Method
Top Horizontal Acceleration (g)	0.546	0.516	0.616	1.057	0.872	0.984
Top Horizontal Displacement (in)	4.753	4.868	4.736	11.860	11.762	15.220
Isolator Horizontal Displacement (in)	0.401	0.467	0.505	0.749	1.182	1.300
Isolator S Vertical Displacement (in)	1.145	1.137	0.770	3.279	3.070	2.534
Isolator N Vertical Displacement (in)	0.844	0.914	0.770	2.705	3.133	2.534

Table 4-II - Properties of System 1 Extracted from Moment-Rotation Loops of Fig.4-22 (1 in.= 25.4 mm, 1 Kip= 4.46 kN).

M/a (Kips)	2θa (in.)	K_z (Kip/in)	Effective Period (sec)	Equivalent Viscous Damping Ratio
0.423	0.590	0.360	0.86	0.132
0.600	1.000	0.300	0.94	0.098
0.730	1.513	0.241	1.04	0.074

Table 4-III - Characteristics of System 1 used in Simplified Analysis (1 in.= 25.4 mm, 1 Kip= 4.46 kN).

EXCITATION	K_x (Kip/in)	K_z (Kip/in)	ω_x (r/s)	ω_z (r/s)	T_1 (sec)	T_2 (sec)	ξ_1	ξ_2
Taft Ground	0.179	0.360	26.29	37.29	0.88	0.12	0.15	0.15
Taft 7th Floor	0.179	0.300	26.29	34.04	0.96	0.12	0.10	0.10
El Centro Ground	0.179	0.300	26.29	34.04	0.96	0.12	0.10	0.10
El Centro 7th Floor	0.179	0.100	26.29	19.65	0.64	0.12	0.05	0.05

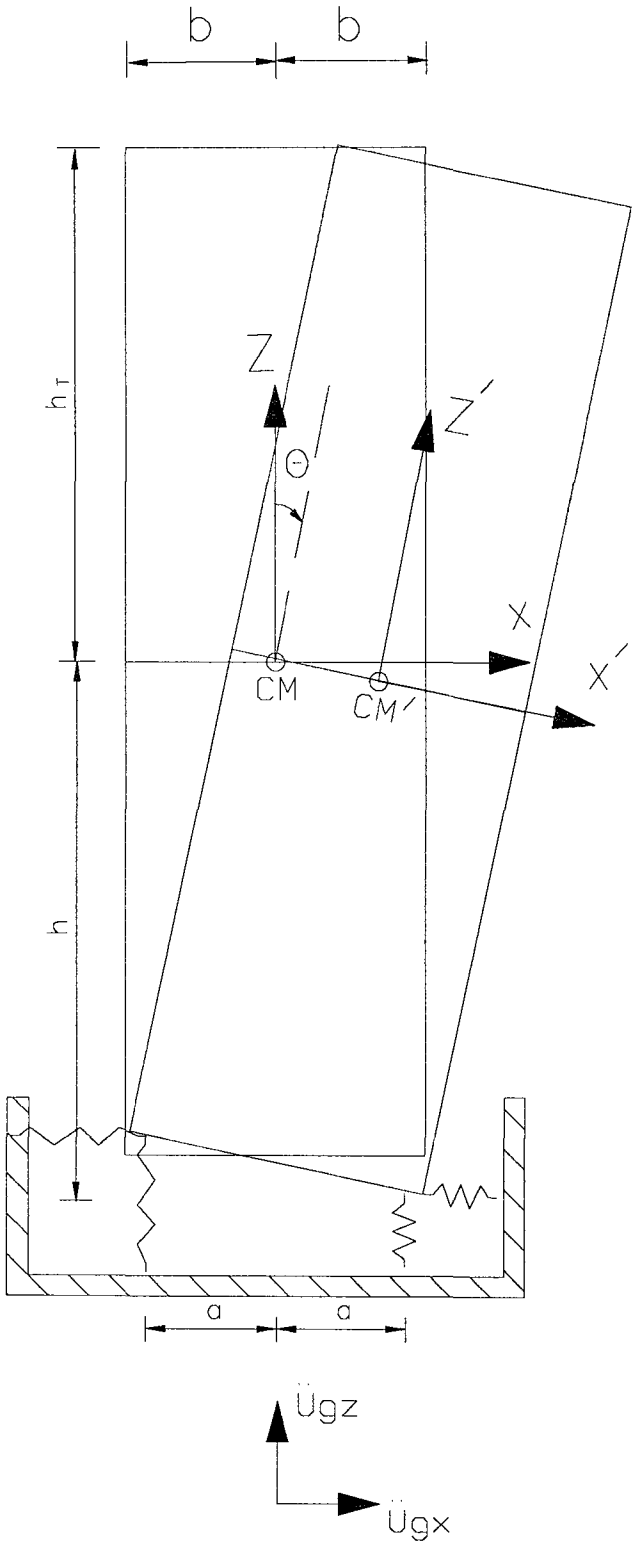

Figure 4-1 Model of Equipment Supported by Wire Rope Isolators.

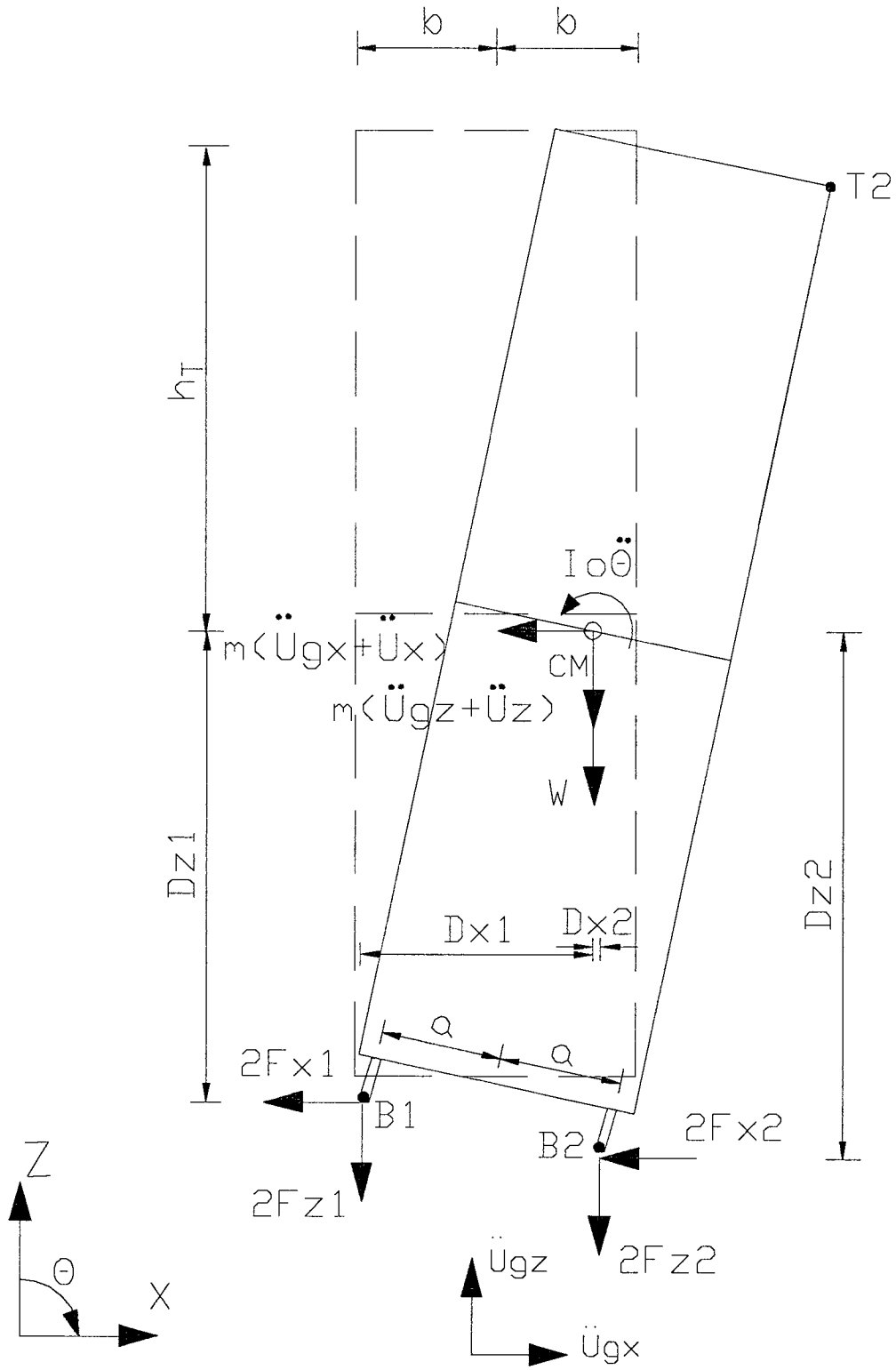

Figure 4-2 Free Body Diagram of Equipment.

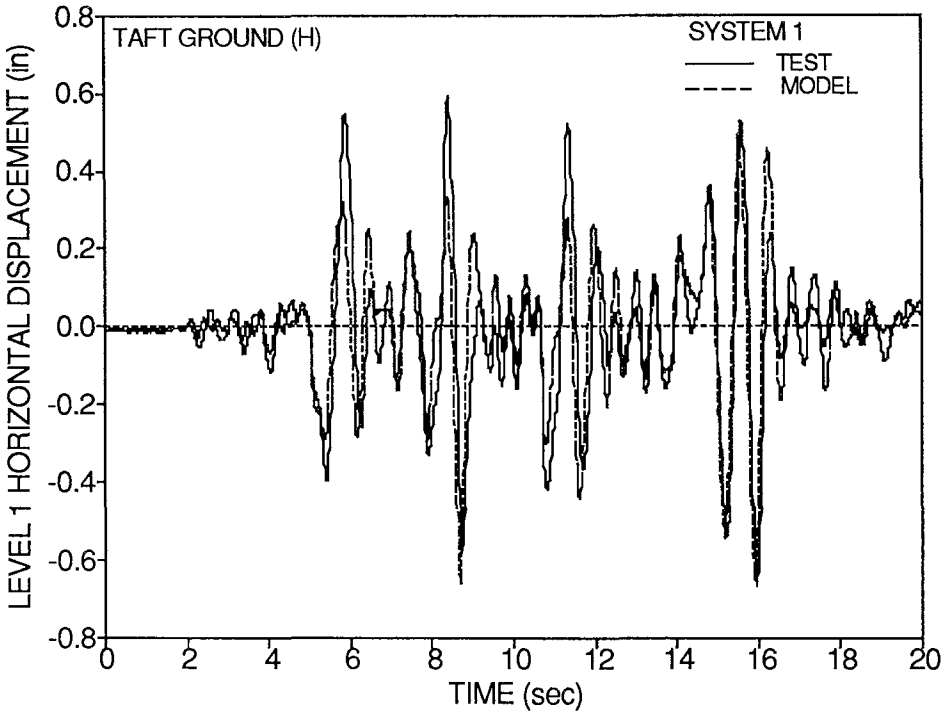

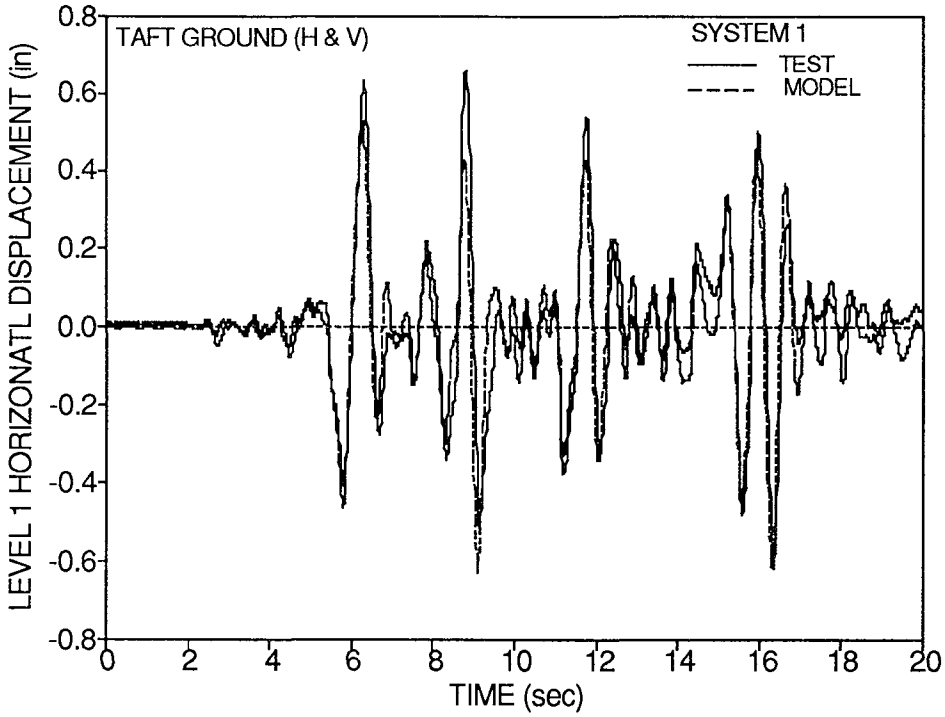

Figure 4-3 Comparison of Experimental and Analytical Time Histories of Horizontal Displacement of Level 1 for Taft Ground Motion (1 in.= 25.4 mm).

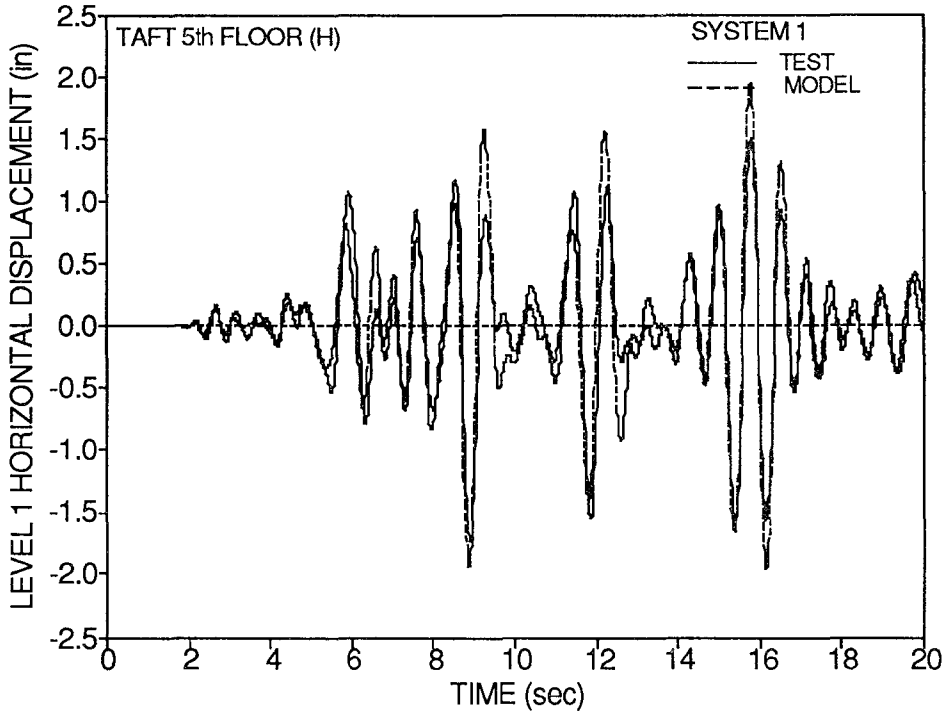

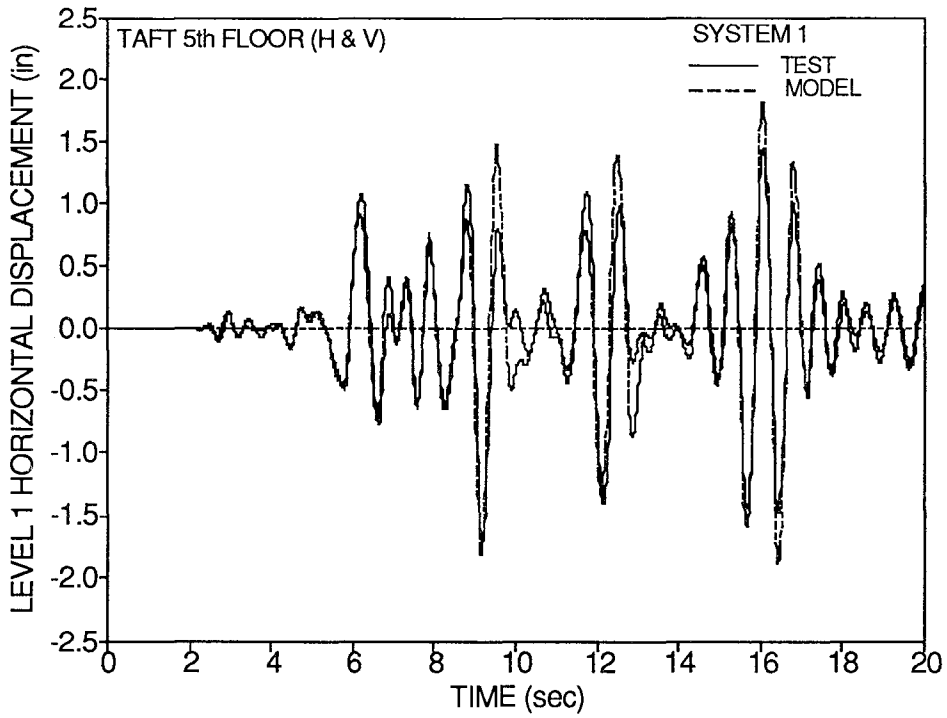

Figure 4-4 Comparison of Experimental and Analytical Time Histories of Horizontal Displacement of Level 1 for Taft 5th Floor Motion (1 in.= 25.4 mm).

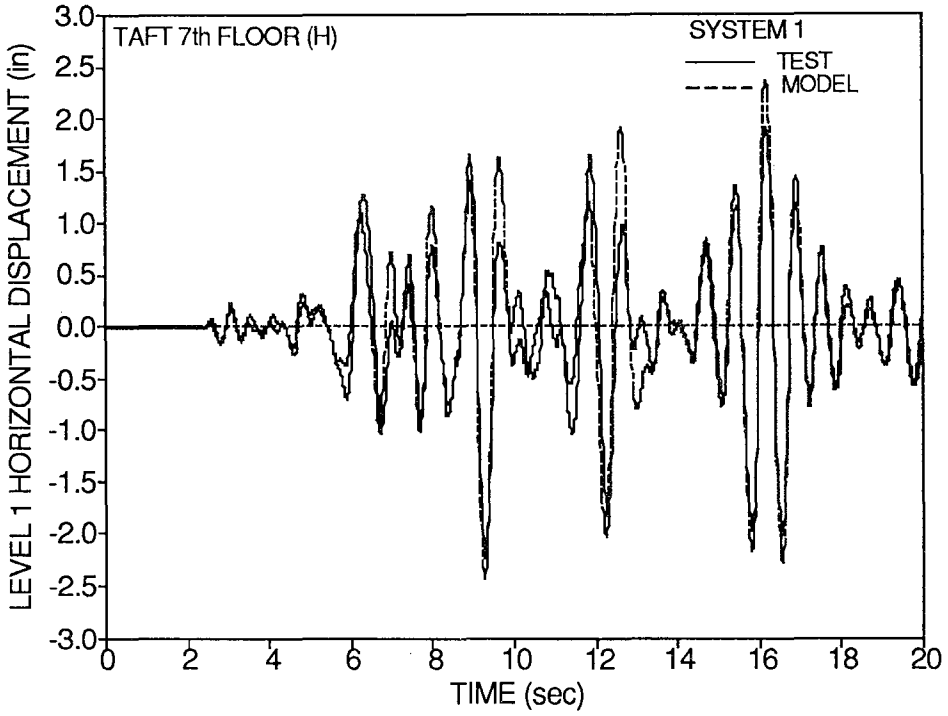

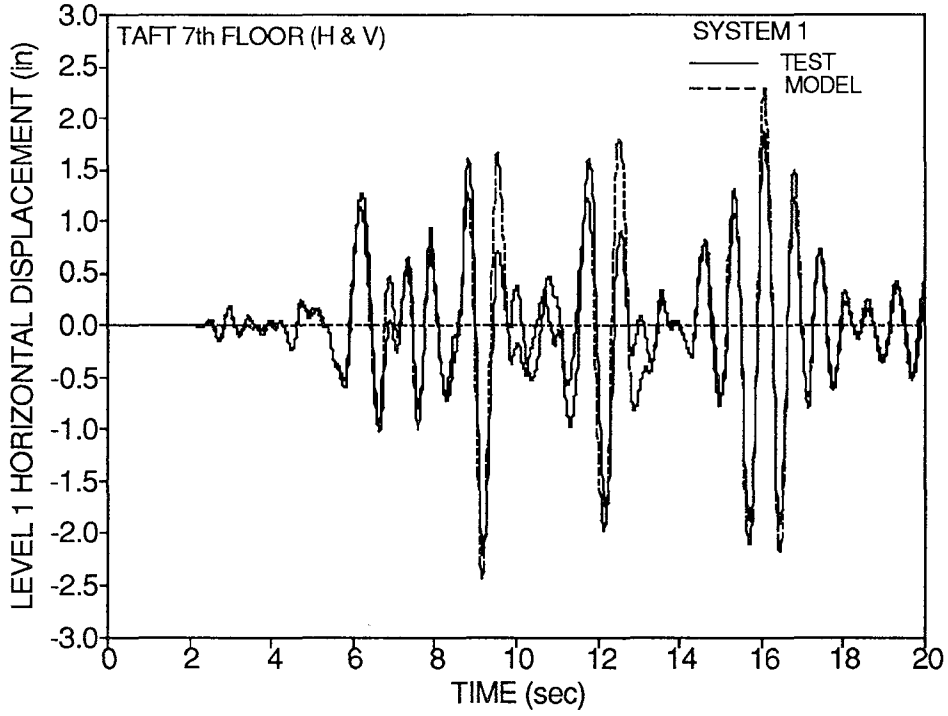

Figure 4-5 Comparison of Experimental and Analytical Time Histories of Horizontal Displacement of Level 1 for Taft 7th Floor Motion (1 in.= 25.4 mm).

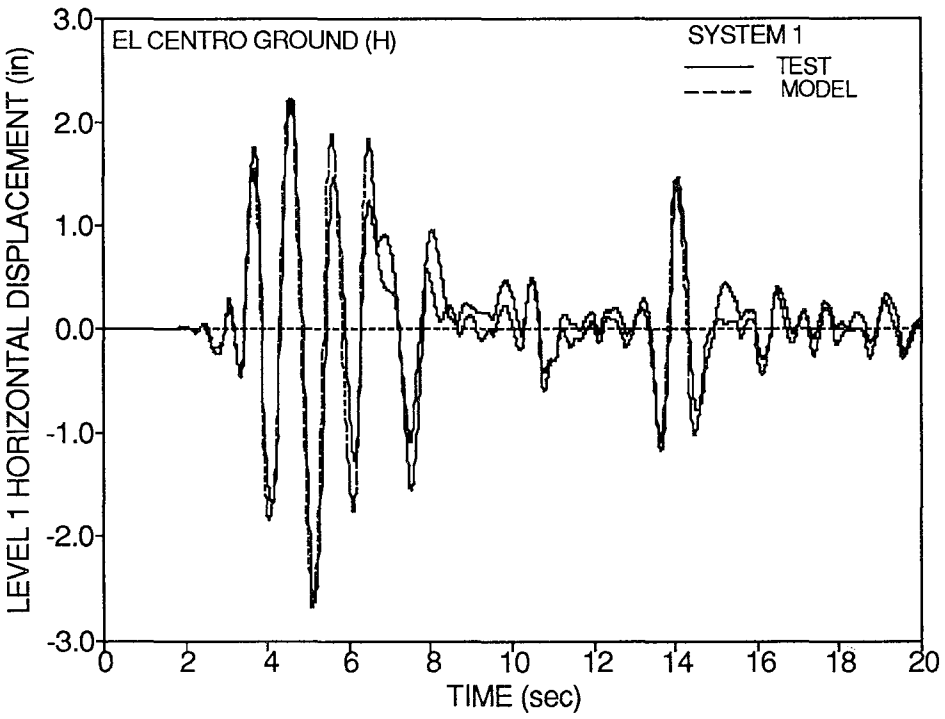

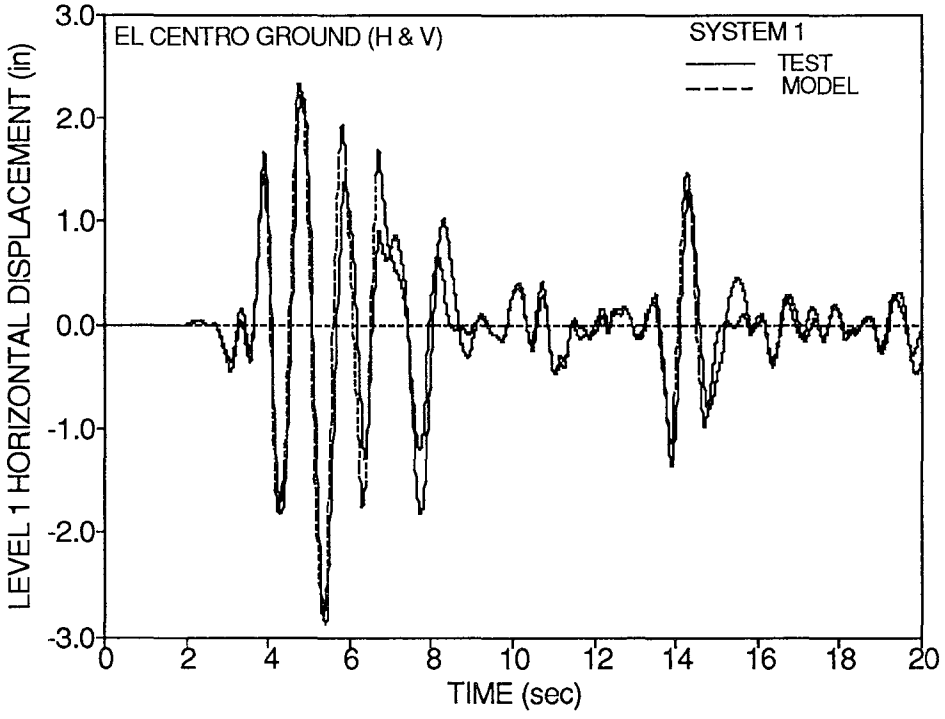

Figure 4-6 Comparison of Experimental and Analytical Time Histories of Horizontal Displacement of Level 1 for El Centro Ground Motion (1 in.= 25.4 mm).

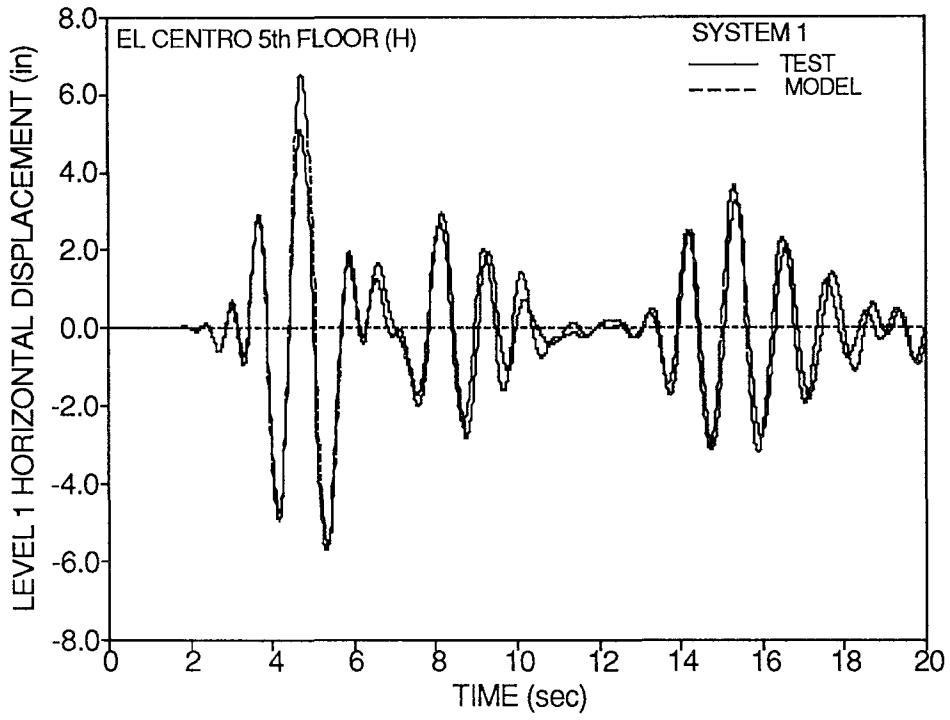

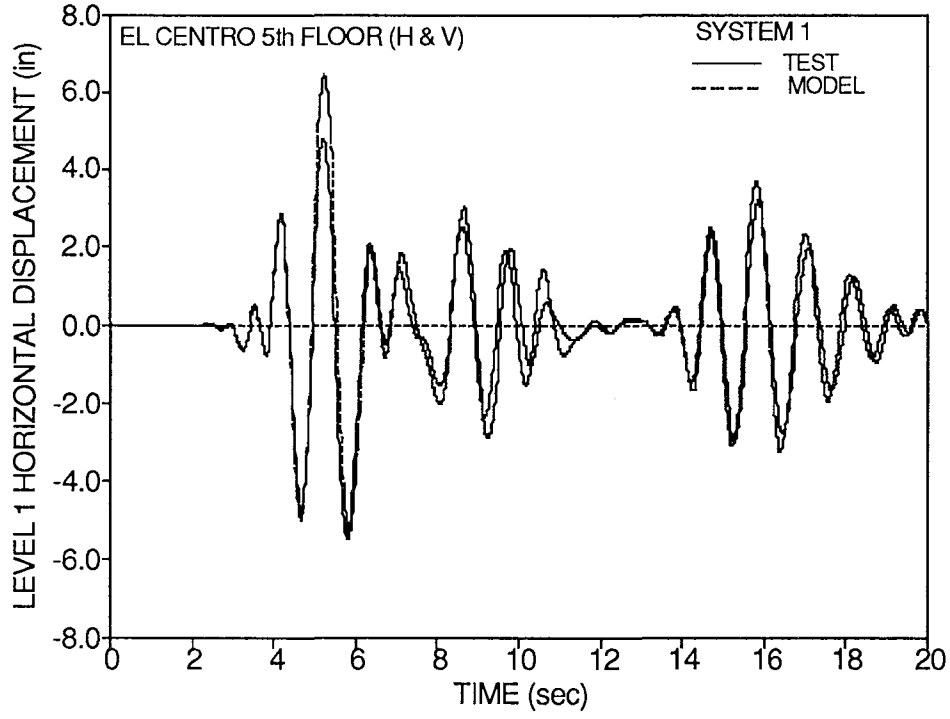

Figure 4-7 Comparison of Experimental and Analytical Time Histories of Horizontal Displacement of Level 1 for El Centro 5th Floor Motion (1 in.= 25.4 mm).

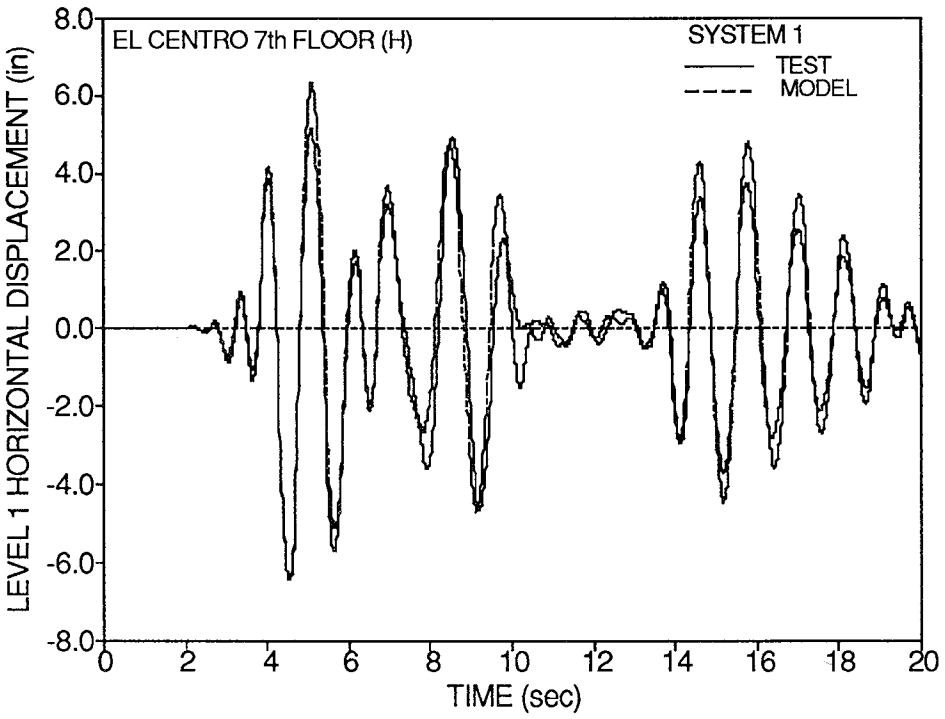

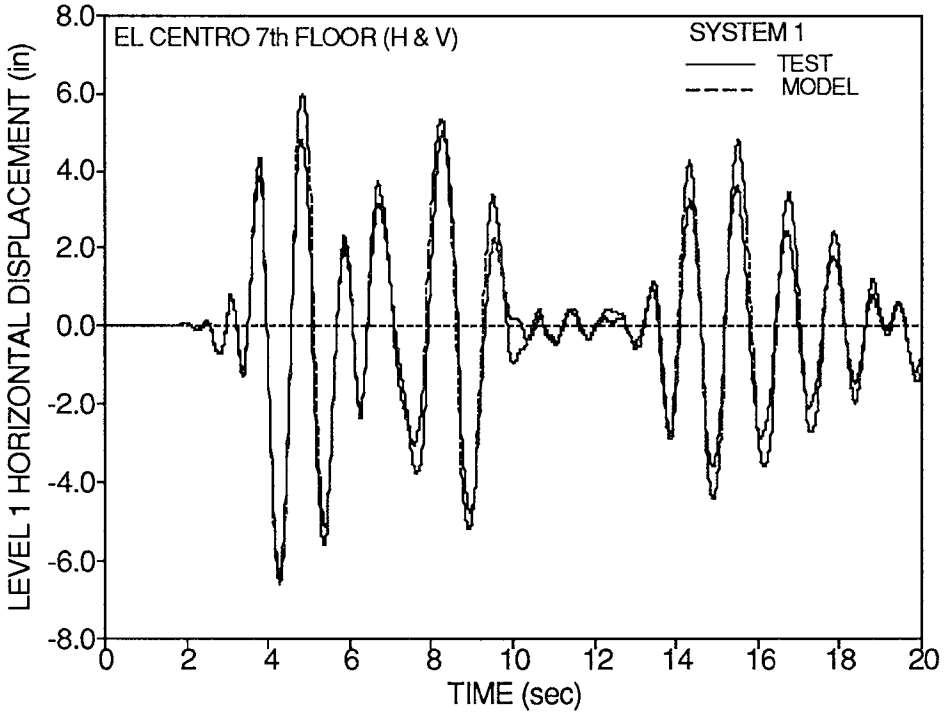

Figure 4-8 Comparison of Experimental and Analytical Time Histories of Horizontal Displacement of Level 1 for El Centro 7th Floor Motion (1 in.= 25.4 mm).

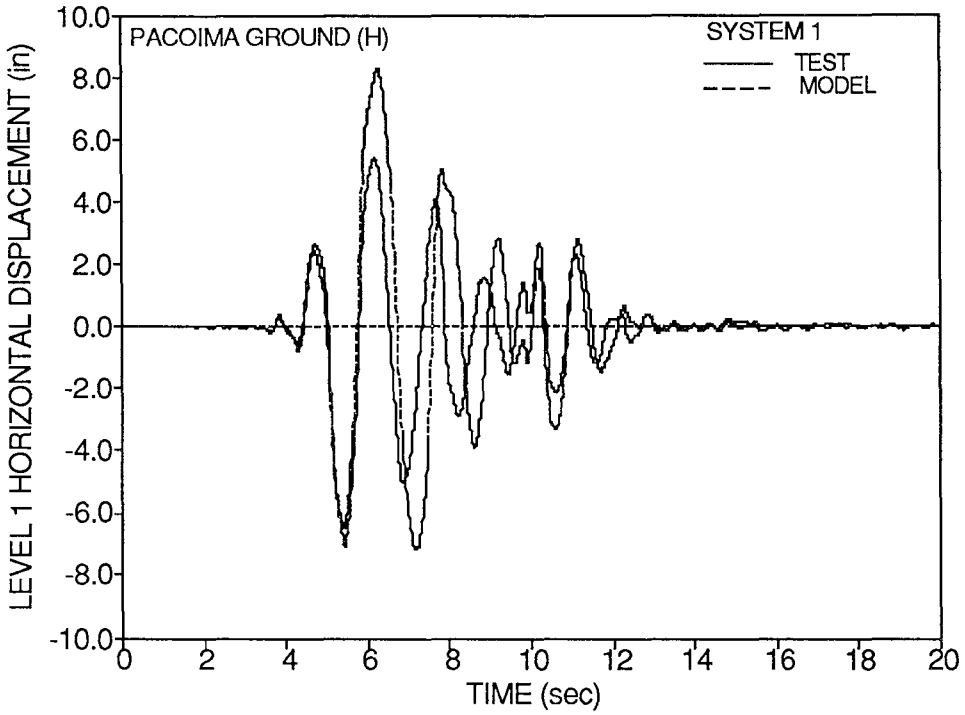

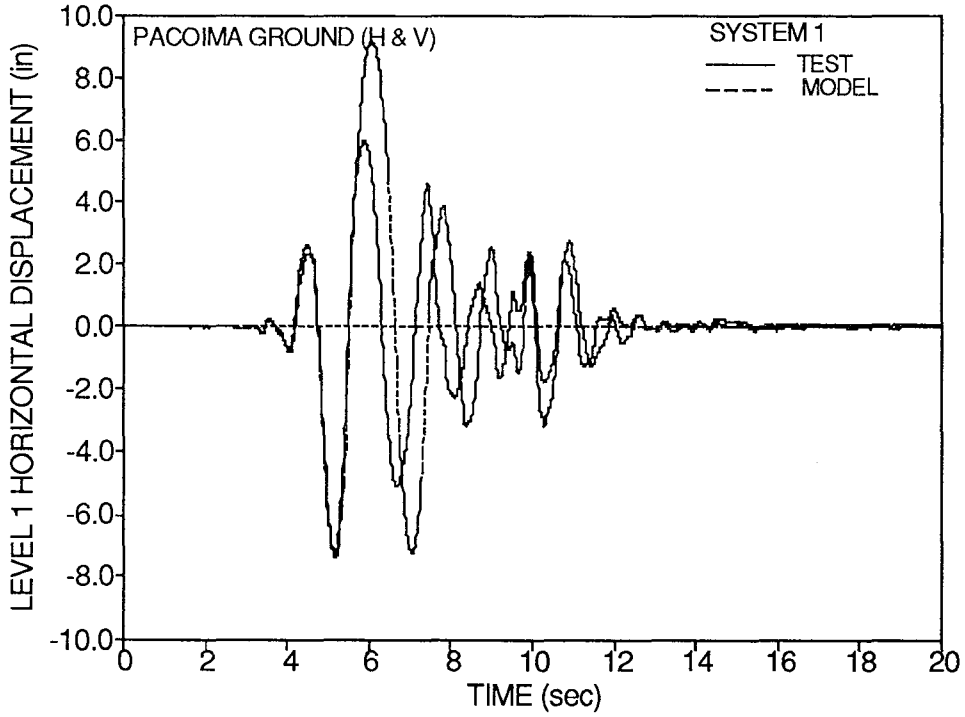

Figure 4-9 Comparison of Experimental and Analytical Time Histories of Horizontal Displacement of Level 1 for Pacoima Ground Motion (1 in.= 25.4 mm).

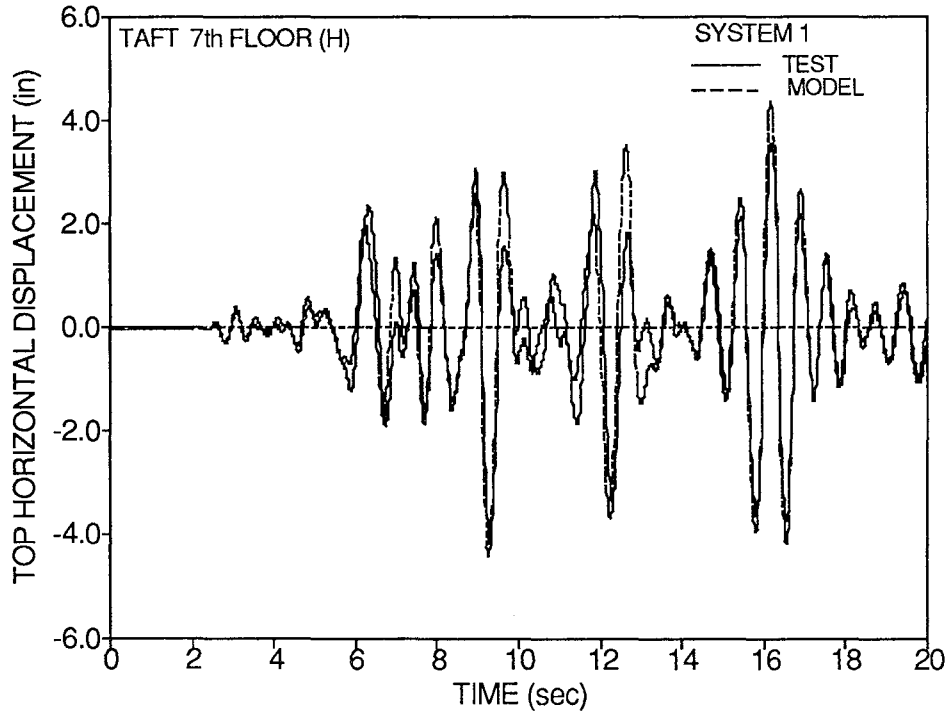

Figure 4-10 Comparison of Experimental and Analytical Time Histories of Horizontal Displacement of Top for Taft 7th Floor Motion (1 in.= 25.4 mm).

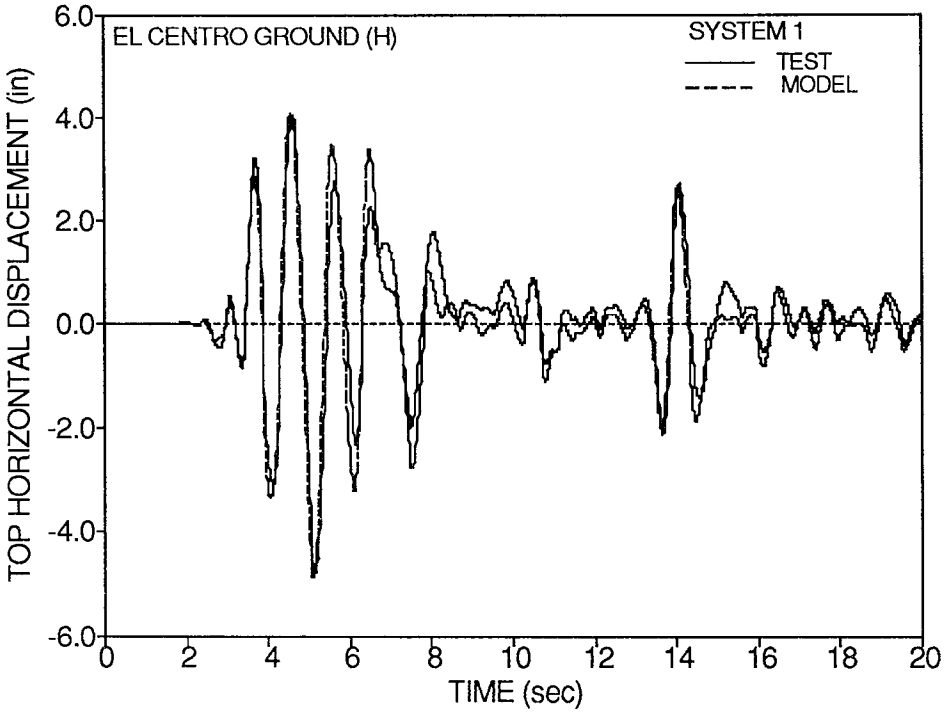

Figure 4-11 Comparison of Experimental and Analytical Time Histories of Horizontal Displacement of Top for El Centro Ground Motion (1 in.= 25.4 mm).

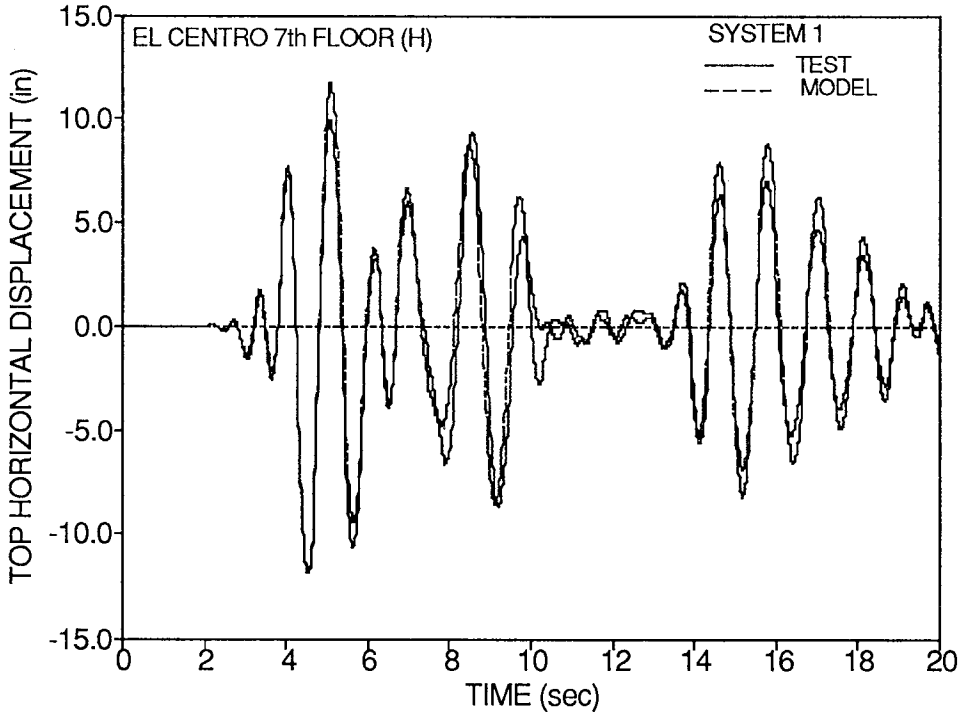

Figure 4-12 Comparison of Experimental and Analytical Time Histories of Horizontal Displacement of Top for El Centro 7th Floor Motion (1 in.= 25.4 mm).

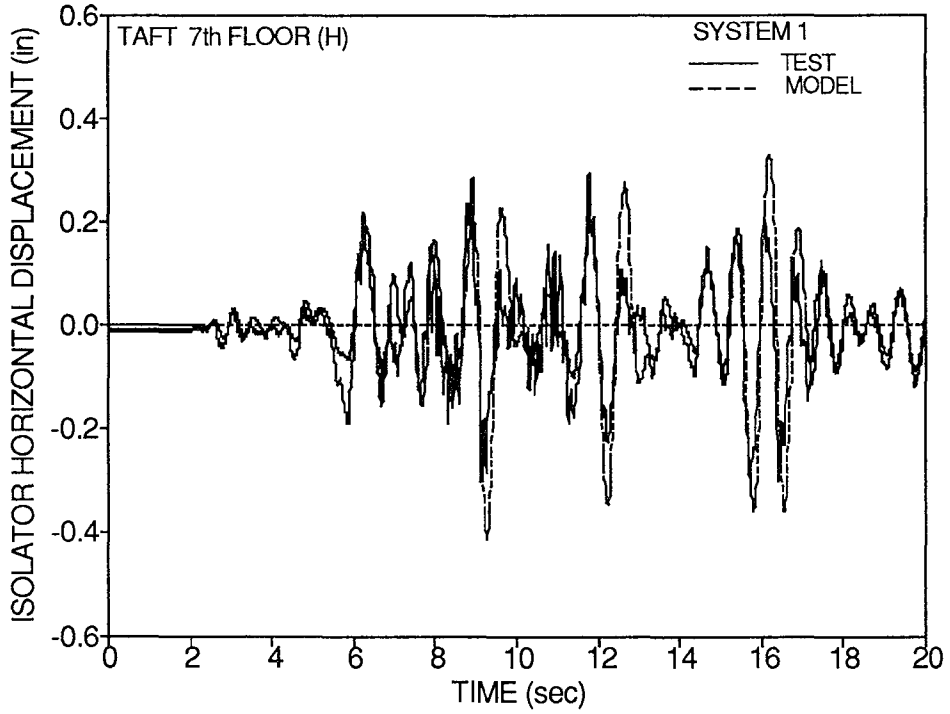

Figure 4-13 Comparison of Experimental and Analytical Time Histories of Horizontal Isolator Displacement for Taft 7th Floor Motion (1 in.= 25.4 mm).

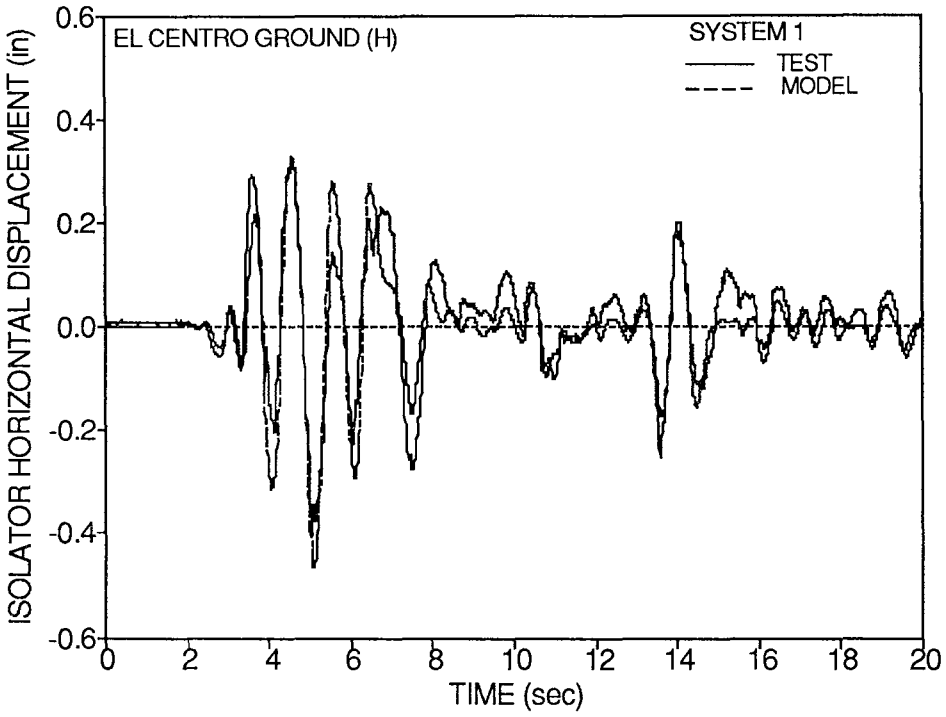

Figure 4-14 Comparison of Experimental and Analytical Time Histories of Horizontal Isolator Displacement for El Centro Ground Motion (1 in.= 25.4 mm).

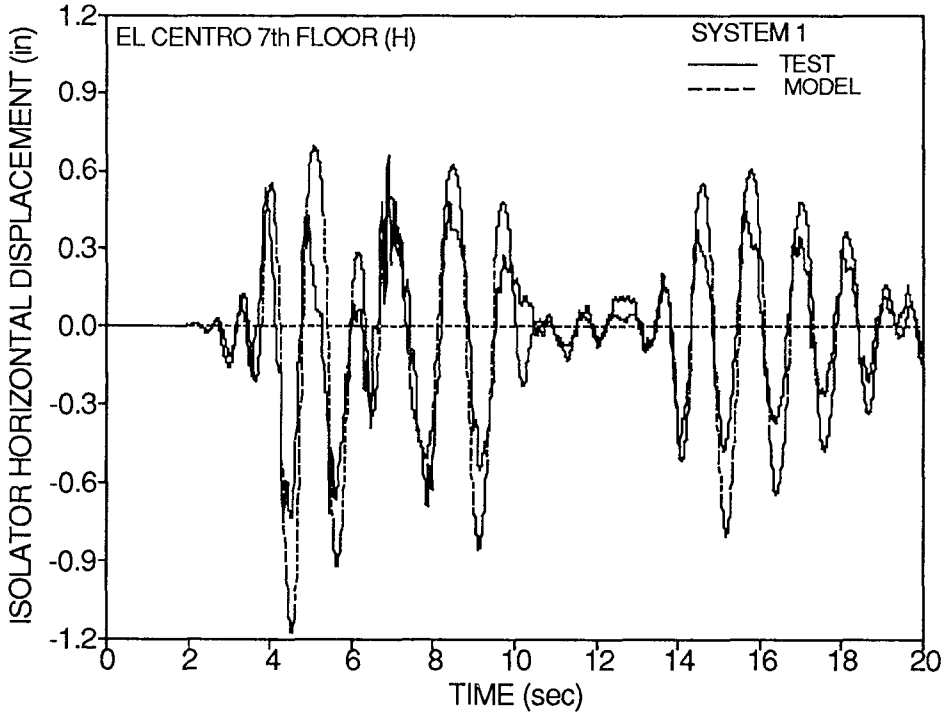

Figure 4-15 Comparison of Experimental and Analytical Time Histories of Horizontal Isolator Displacement for El Centro 7th Floor Motion (1 in.= 25.4 mm).

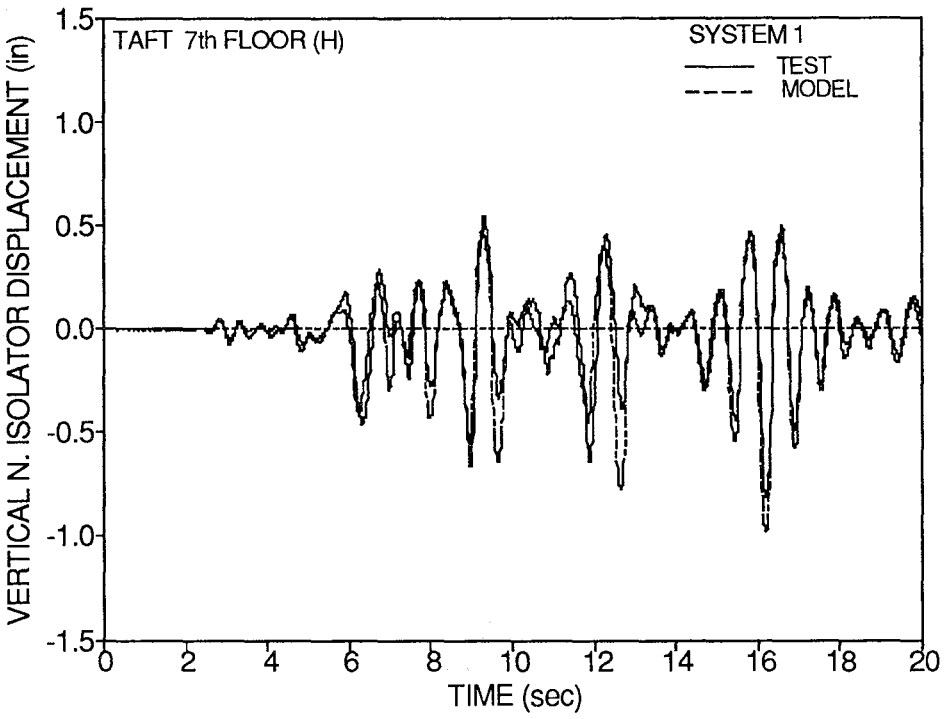

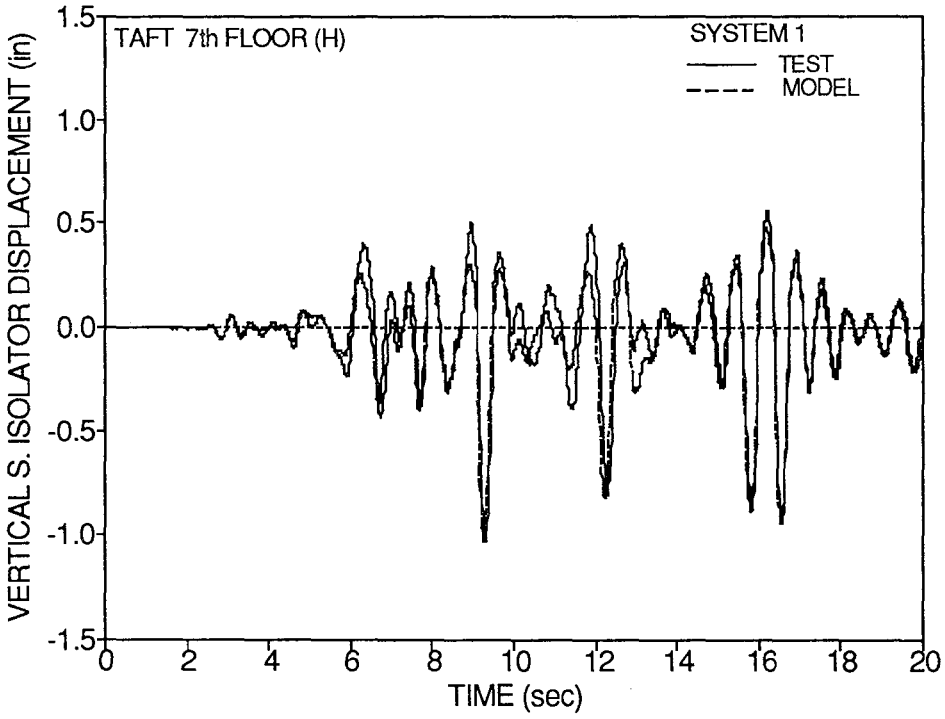

Figure 4-16 Comparison of Experimental and Analytical Time Histories of Vertical Isolator Displacement for Taft 7th Floor Motion (1 in.= 25.4 mm).

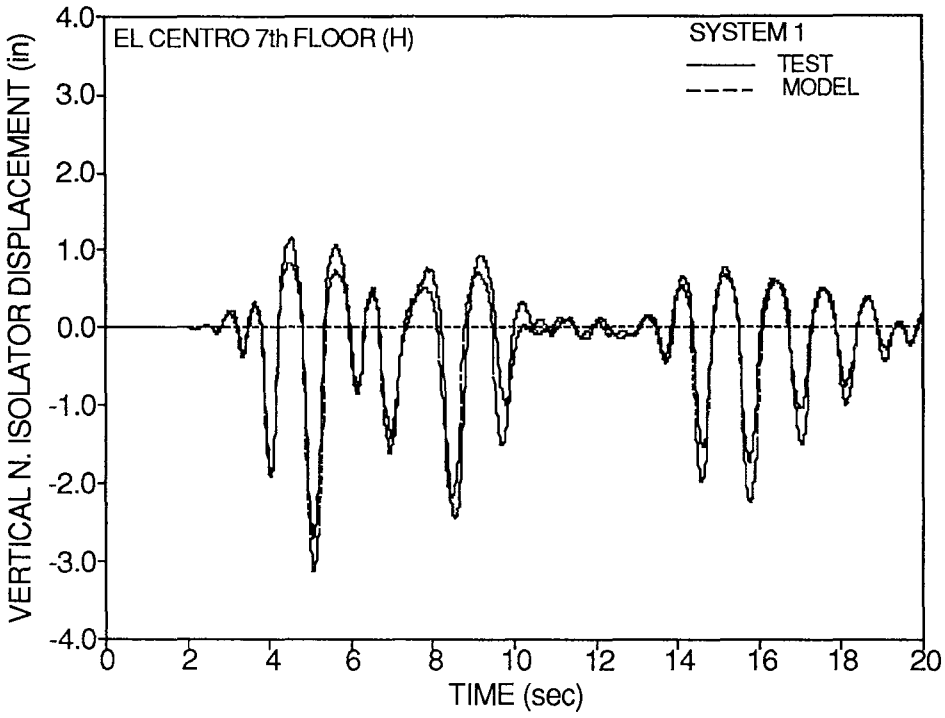

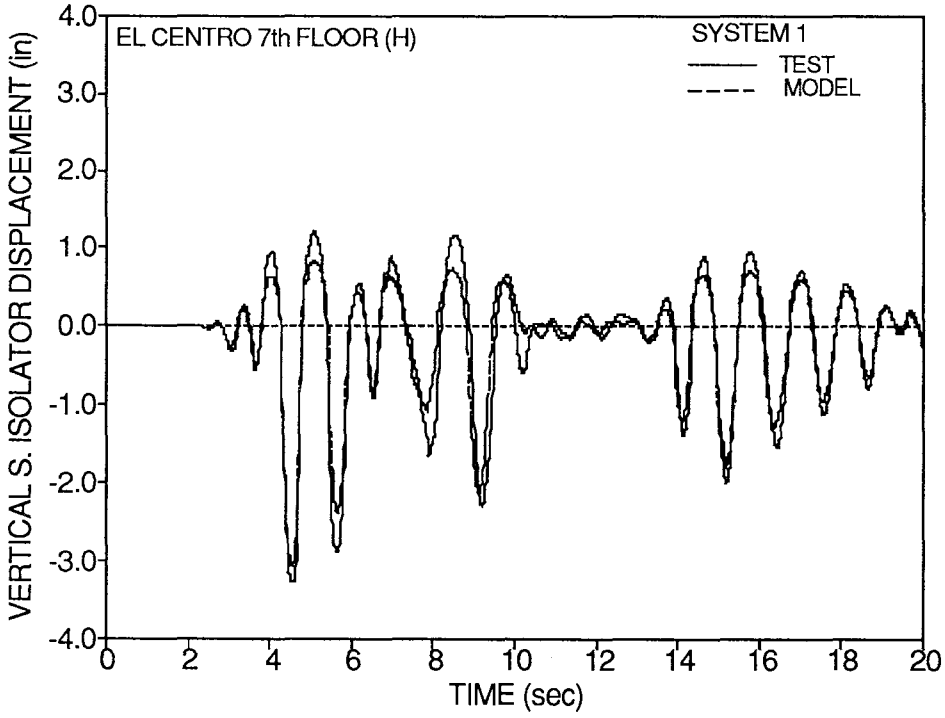

Figure 4-17 Comparison of Experimental and Analytical Time Histories of Vertical Isolator Displacement for El Centro 7th Floor Motion (1 in.= 25.4 mm).

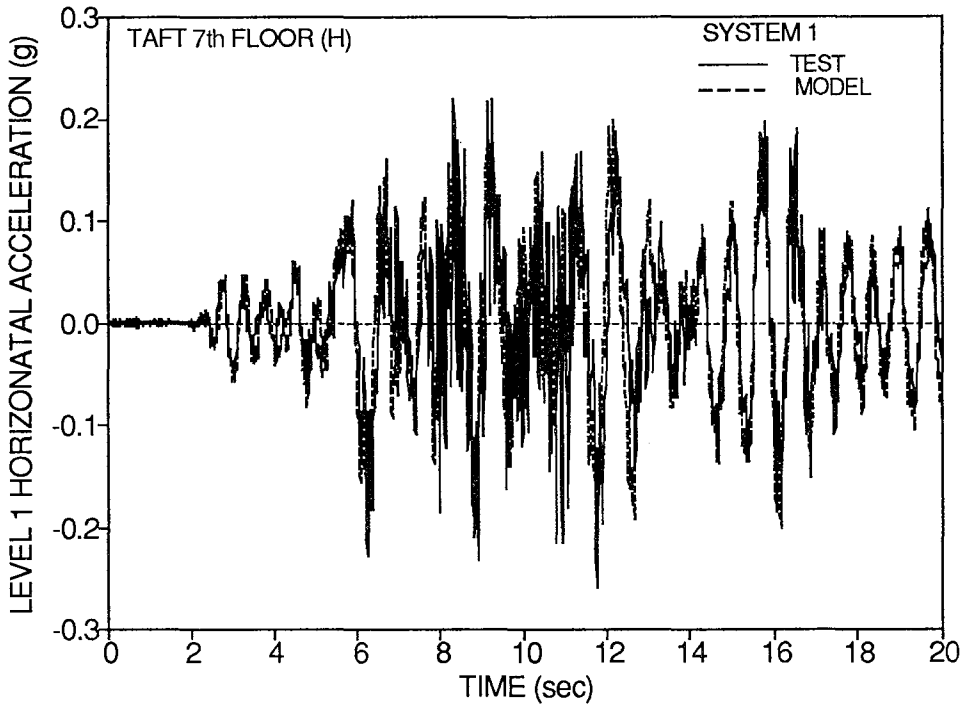

Figure 4-18 Comparison of Experimental and Analytical Time Histories of Horizontal Acceleration of Level 1 for Taft 7th Floor Motion (1 in.= 25.4 mm).

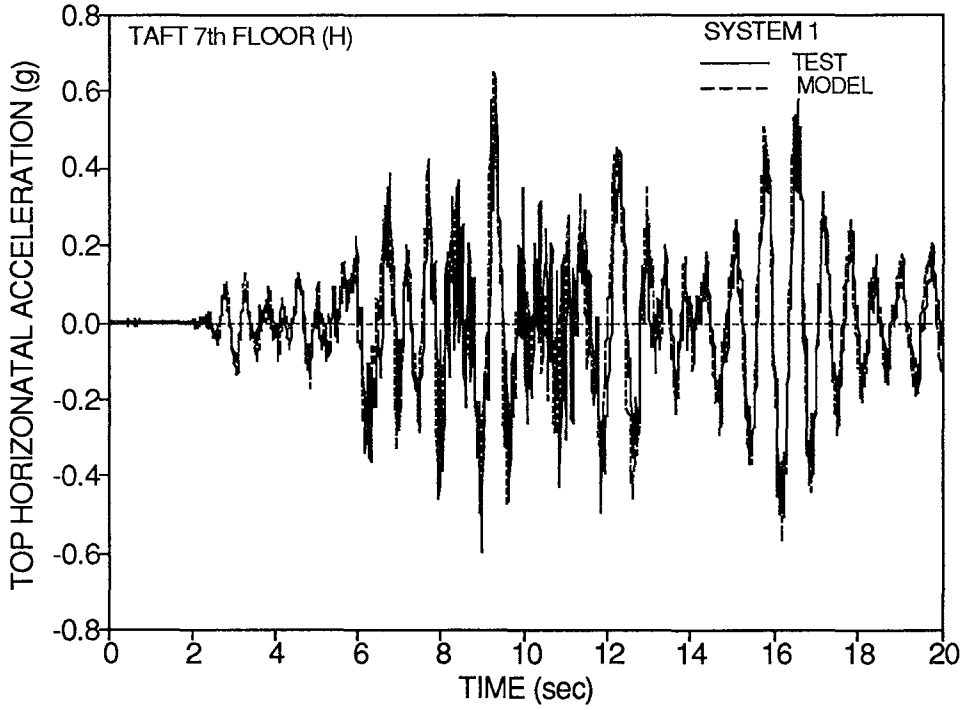

Figure 4-19 Comparison of Experimental and Analytical Time Histories of Top Horizontal Acceleration for Taft 7th Floor Motion (1 in.= 25.4 mm).

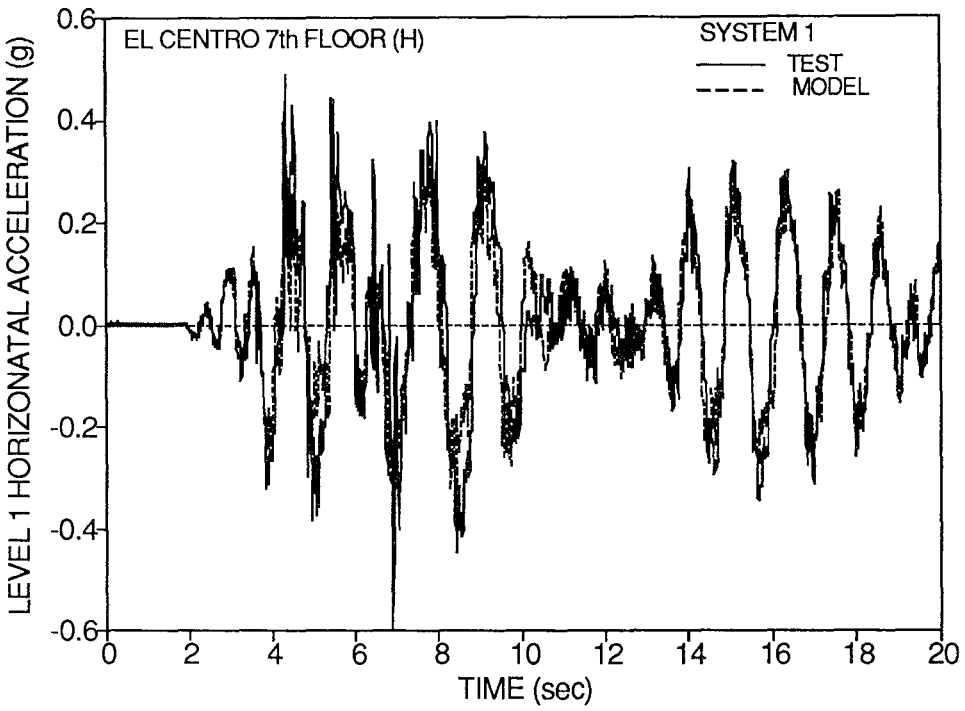

Figure 4-20 Comparison of Experimental and Analytical Time Histories of Horizontal Acceleration of Level 1 for El Centro 7th Floor Motion (1 in.= 25.4 mm).

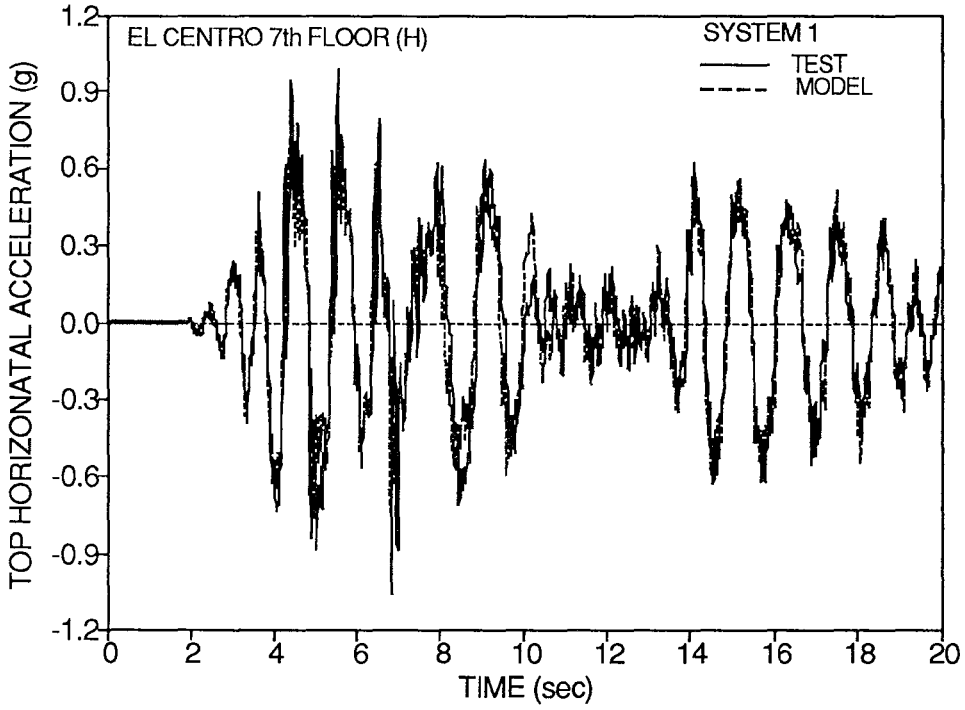

Figure 4-21 Comparison of Experimental and Analytical Time Histories of Top Horizontal Acceleration for El Centro 7th Floor Motion (1 in.= 25.4 mm).

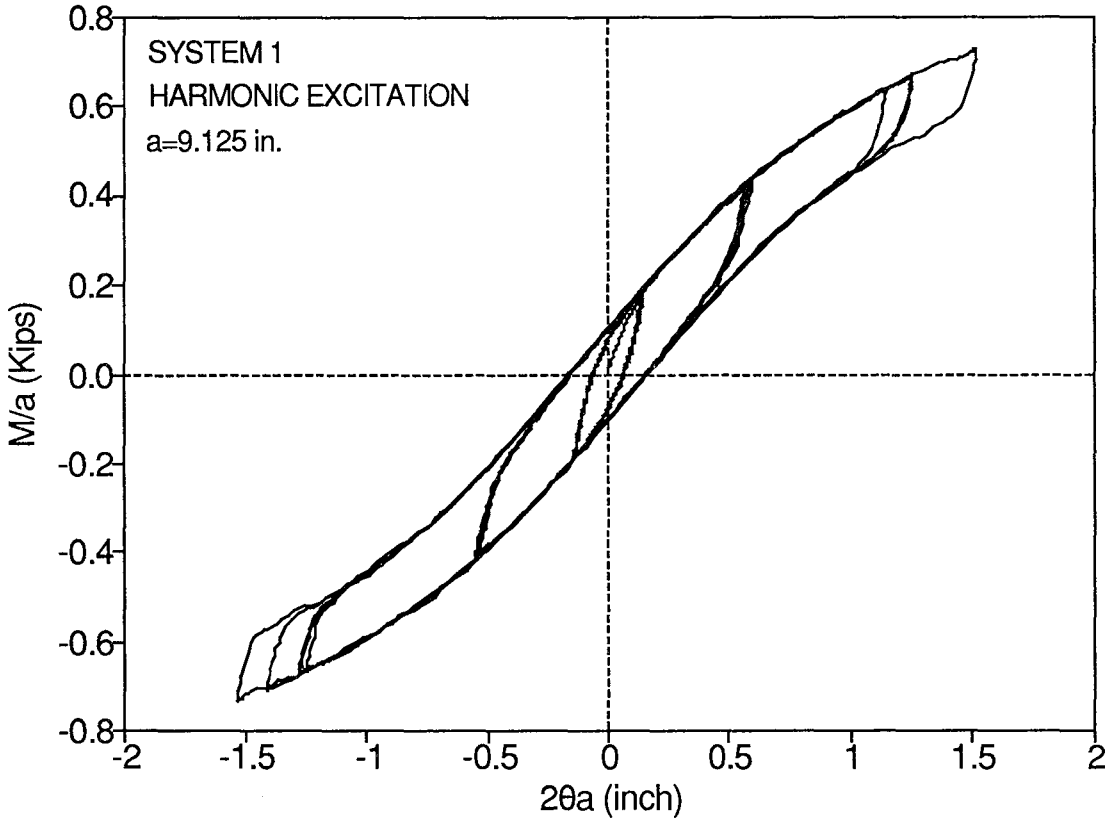

Figure 4-22 Analytical Moment - Rotation Loops of System 1 for Harmonic Excitation (1 in.= 25.4 mm, 1 Kip= 4.46 kN).

SECTION 5

COMBINED WIRE ROPE AND CASTER SUPPORT SYSTEM FOR EQUIPMENT - COMPARATIVE EXPERIMENTAL STUDY

5.1 Description of Equipment and Support System

An experimental study was performed with IBM 9370 computer equipment installed on top of a raised floor and supported by casters. Figure 5-1 shows a view of the computer equipment installed on the raised floor as it would have been in service. The casters support the weight of the equipment and allow for easy relocation on the raised floor. When in service, the casters are locked and a 90 plus degree plate angle, called the foot, is attached in the front of the body for stability. To prevent excessive displacements and overturning in earthquake excitation, positive connection of the equipment to the floor below the raised floor is normally provided by means of bungee cords or long helical steel springs. These elements run through holes on the tiles of the raised floor.

In general, earthquakes may cause effects to computer equipment which may be catastrophic when overturning occurs, or serious when damage occurs due to excessive acceleration and impact, or minor when execution is interrupted due to large accelerations or pull-out of cables. Installation methods which can reduce accelerations and displacements to acceptable levels while allowing for easy

relocation of the equipment are particularly interesting to computer manufacturers. As a part of a NCEER - IBM joint research project, various computer equipment installation methods were tested. One of them consisted of wire rope isolators.

The wire rope installation method followed the standard approach in which the equipment is supported by four locked casters with the foot installed in the front. Four helical wire rope isolators No.5 (see section 2) were connected to metal bars in sets of two isolators each as shown in Figure 5-2. The two sets of isolators were placed under the equipment and bolted to the frame above and to the tiles of the raised floor below. During testing, the isolators deformed only in their shear direction.

The IBM 9370 computer equipment has plan dimensions of 36.2 in. by 25.6 in. (920 mm by 650 mm) and height of 62.1 in. (1578 mm). Its center of mass is located at coordinates X = 12.03 in. (305.6 mm), Y = 25.08 in. (637.1 mm) and Z = 15.4 in. (391.3 mm) according to the coordinate system of Figure 5-2 at point O. Its weight is 828 lbs (3.7 kN). The fundamental frequency of the equipment when fixed at its base was experimentally determined to be 4.1 Hz in the testing (X) direction. Attempts were made to determine the coefficient of friction at the interface of locked casters and angle foot and supporting raised floor. The procedure described by Constantinou 1987 was used, however, it was not possible to

exactly determine the coefficient of friction. The coefficient was found to be in the range of 0.20 to 0.30. For such high value of friction, the ability of wire rope isolators to dissipate energy is not important and the isolators act only as restoring force devices. From the data of Table 2-II, each isolator No.5 has horizontal (shear) stiffness of 0.24 Kips/in. (0.042 kN/mm) so that the frequency of the isolated equipment is 3.4 Hz. This frequency is close to that of the equipment on top of the isolators so that the combined system doesn't behave as a rigid body.

5.2 Experimental Results and Comparison to other Installation Methods

The wire rope system was tested on the shake table with the strongest of the input motions described in section 3. Furthermore, tests were conducted with the vertical component being equal to 1/3 of the horizontal component of excitation. The horizontal component was applied in the X - direction as shown in Figure 5-2. The instrumentation diagram is shown in Figure 5-2. The displacement transducers, which are shown mounted on the equipment, measured displacements of the part just above the casters with respect to the raised floor.

The table excitation was filtered through the raised floor and arrived amplified at the supported equipment (see differences between instruments ASEX and AFEX in Table 5-I).

Response spectra of the horizontal components of excitation at the raised floor level for 0.05 damping ratio are presented in Figure 5-3. Comparison of these spectra to those of Figures 3-7 and 3-10 reveal the filtering effect of the raised floor.

The recorded peak response is presented in Table 5-I. It should be noted that the equipment responded with some torsional motion and motion in the transverse (Y) direction. This is due to asymmetry in the distribution of the equipment's weight (center of mass located close to the west side casters). At the level of the support system, this asymmetry was partially counterbalanced by additional frictional force on the east side where the foot plate angle was installed. In general, displacements are small and accelerations are at levels which can not cause any interruption of operation of the computer. This was verified in all tests by monitoring the execution of a computer program during shake table testing.

The wire rope support system performed considerably better than other commonly used installation methods for computer equipment (see section 5.1). Tables 5-II and 5-III compare peak responses of the wire rope system to those of other systems for the Taft 7th floor and El Centro 7th floor motions (both with vertical component equal to 1/3 of horizontal component). The response values included in these tables are the maximum among all of the recorded peak values. Evidently, the wire rope system reduced displacements by an

order of magnitude while maintaining accelerations at the same level as the other installation methods. Interestingly, the computer equipment sustained accelerations of more than 3g (see Table 5-III, installation method with springs) without any interruption of its operation.

Concluding, we note that the wire rope isolators used in the described installation method have a displacement capacity of about 0.5 in. prior to initiation of stiffening (see Fig. 2-8). When stiffening occurs, the equipment is prevented from further movement and uplift and impact on return may occur. This is undesirable. Tests were conducted with input motion stronger than the El Centro 7th floor and, as expected, uplift occurred and high accelerations were recorded. To avoid uplift, wire rope isolators with larger displacement capacity must be used. This, of course, requires that analyses are performed to estimate the isolator's expected displacement. Still, uplift may occur in slender equipment.

An installation method which prevents the occurrence of uplift is illustrated in Figure 5-4. The wire rope isolators are connected by two keeper bars. The top bar is bolted to the frame of the equipment. The bottom keeper bar is connected to the floor below the raised floor by two turnbuckle - toggle wing connectors. This type of connection allows for easy relocation of the equipment. A simple uplift control mechanism is included between the keeper bars. It

consists of two intersecting rectangular hooks. Two sets of keeper bars with each set including two wire rope isolators and one uplift control mechanism are placed between the four supporting casters.

5.3 Analytical Prediction of Response

The analytical prediction of the response of the caster - wire rope support system is useful in the selection of wire rope isolators and in the design of the uplift control mechanism. Spectra of peak response of frictional oscillators may be used in estimating the peak response. Such spectra were constructed for a frictional oscillator of coefficient of friction (of Coulomb type) equal to 0.2 and 0.3 and are presented in Figures 5-5 and 5-6. It should be noted that these spectra are valid for a rigid structure and, thus, the acceleration response must be viewed with caution when the equipment above the isolators is flexible and the support system exhibits characteristics of weak restoring force and strong frictional force (Constantinou 1990b and 1991). Such conditions occur when the peak frictional force is larger by at least a factor of two than the peak restoring force.

The spectra of Figures 5-5 and 5-6 were constructed by analysis of a single-degree-of freedom frictional oscillator of mass m, stiffness K, and coefficient of friction μ. The equation of motion is (Constantinou 1990a)

$$m\ddot{U} + KU + \mu mgZ = -m\ddot{u}_g \qquad (5\text{-}1)$$

where Z is again given by equation 2-2 with Y = 0.01 in. (0.25 mm), $\beta + \gamma = A = 1$ and n an integer. The period is defined as

$$T = 2\pi\left(\frac{m}{K}\right)^{\frac{1}{2}} \qquad (5\text{-}2)$$

The usefulness of these spectra is demonstrated in a comparison of analytical and experimental (average from instruments on east and west side casters, see Fig. 5-2) time histories of displacement in Figure 5-7. For the analysis, equation 5-1 was used with $\mu = 0.25$ and with the restoring force term, KU, replaced by 4F where F is given by equation 2-1 with the data of Table 2-II for isolator No.5. Almost identical results were obtained in analyses in which the term KU was maintained (linear representation of wire rope isolators) with $K = 4K_x$ (K_x = 0.24 Kip/in, see Table 2-II). The analytical results compare favorably to the experimental ones despite the uncertainties in the nature and value of the coefficient of friction. It should be noted that the large differences in experimental and analytical time histories at small displacements indicate that the coefficient of friction is velocity dependent as that of other interfaces identified in Constantinou 1990a.

Table 5-I - Recorded peak Response of IBM Equipment with Wire Rope Isolators (1 in.= 25.4 mm).

EXCITATION / INSTRUMENT		Taft Ground (H&V)	Taft 7th Floor (H&V)	Taft 7th Floor (H&V*)	El Centro 7th Floor (H&V)	El Centro 7th Floor (H&V*)
ACCELERATION (g)	ASEX	0.155	0.449	0.482	0.724	0.807
	AFEX	0.171	0.557	0.567	0.988	1.002
	ALRRX	0.198	0.888	0.791	0.947	1.060
	ALRFX	0.182	0.797	0.781	0.914	1.014
	ATRRX	0.438	0.988	0.975	1.211	1.109
	ATRFX	0.373	0.883	0.826	1.022	0.991
	ALRRY	0.043	0.129	0.138	0.223	0.266
	ATRFZ	0.155	0.225	0.313	1.063	0.875
	ATRRZ	0.130	0.198	0.258	1.079	0.876
DISPLACEMENT (in)	DSDX	0.306	0.659	0.641	0.833	0.813
	DSDZ	0.142	0.184	0.253	0.657	0.520
	DNEX	0.028	0.208	0.203	0.278	0.344
	DNWX	0.045	0.243	0.211	0.329	0.528
	DNWY	0.013	0.064	0.035	0.058	0.064
	DSWY	0.012	0.046	0.021	0.043	0.087

V* : Vertical component equal to 1/3 of horizontal component.

Table 5-II - Comparison of Peak Response of Equipment with Different Installation Methods for Taft 7th Floor Input (1 in.= 25.4 mm).

Installation System	Horizontal Top Acceleration (g)	Vertical Top Acceleration (g)	Displacement of Casters (in)
Locked Casters	0.434	0.260	6.28
Locked Casters and Bungee Cords	0.705	0.239	3.25
Locked Casters and Springs(2)	0.783	0.374	3.92
Locked Casters and Wire Rope Isolators	0.969	0.285	0.21

Table 5-III - Comparison of Peak Response of Equipment with Different Installation Methods for El Centro 7th Floor Input (1 in.= 25.4 mm).

Installation System	Horizontal Top Acceleration (g)	Vertical Top Acceleration (g)	Displacement of Casters (in)
Locked Casters	0.710	0.408	9.62
Locked Casters and Bungee Cords	1.221	0.559	5.06
Locked Casters and Springs(2)	3.079*	3.482*	8.88
Locked Casters and Wire Rope Isolators	1.056	0.876	0.53

* : Uplift and Impact

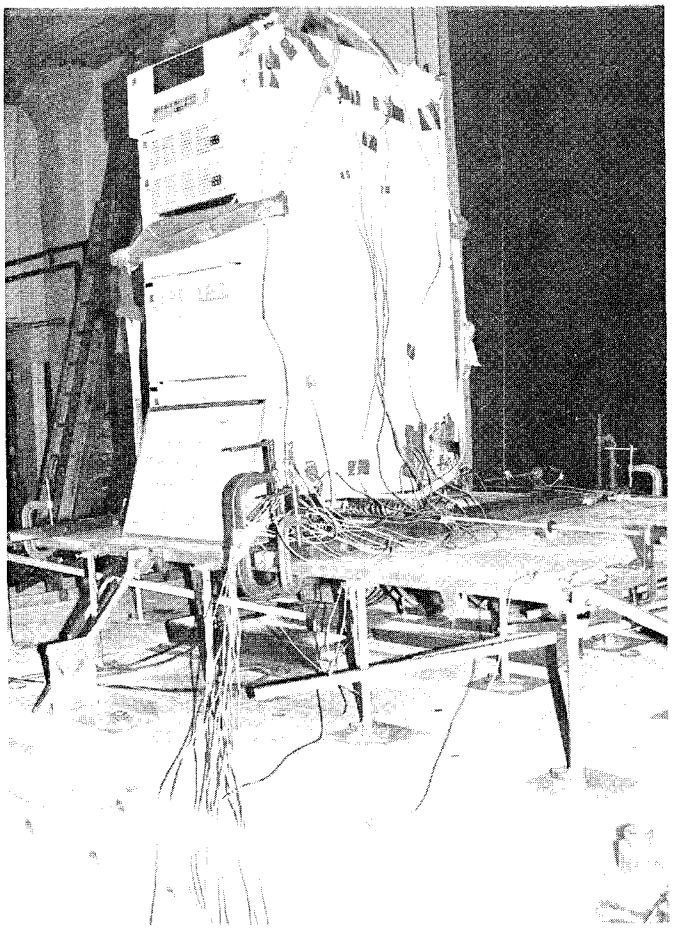

Figure 5-1 View of IBM 9370 Computer Equipment on Raised Floor and Shake Table.

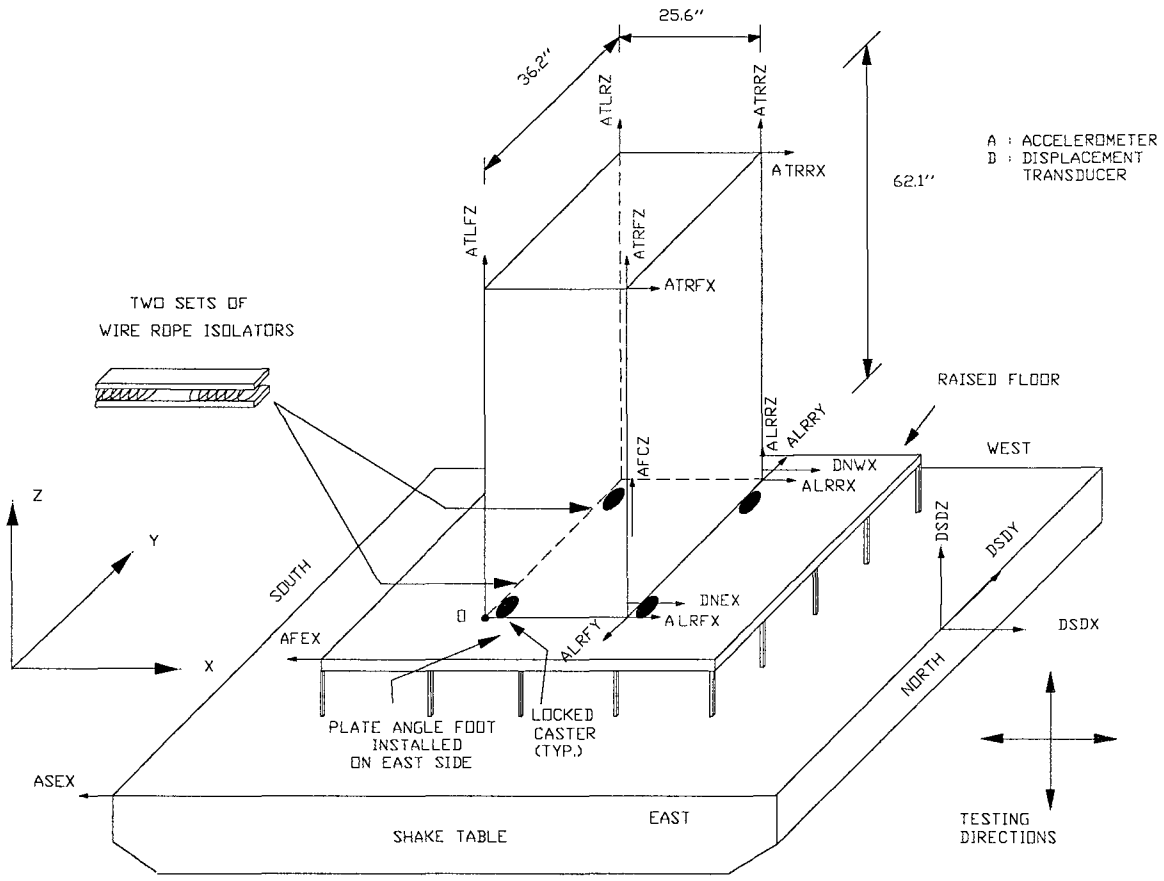

Figure 5-2 Schematic Representation of IBM 9370 Computer Equipment on Shake Table and Instrumentation Diagram.

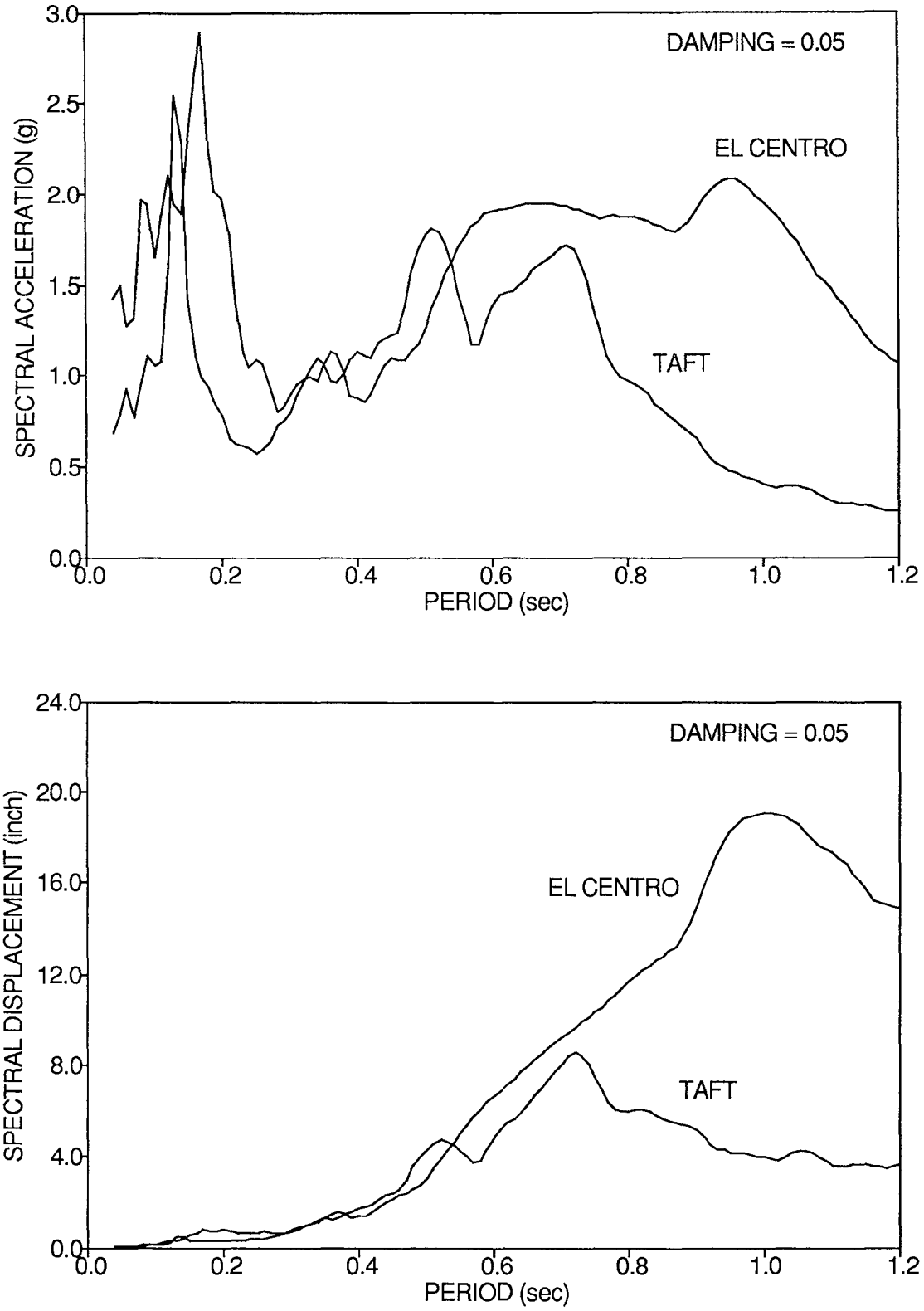

Figure 5-3 Response Spectra at Raised Floor of a 5% Damped System for Taft 7th Floor and El Centro 7th Floor Motion (1 in.= 25.4 mm).

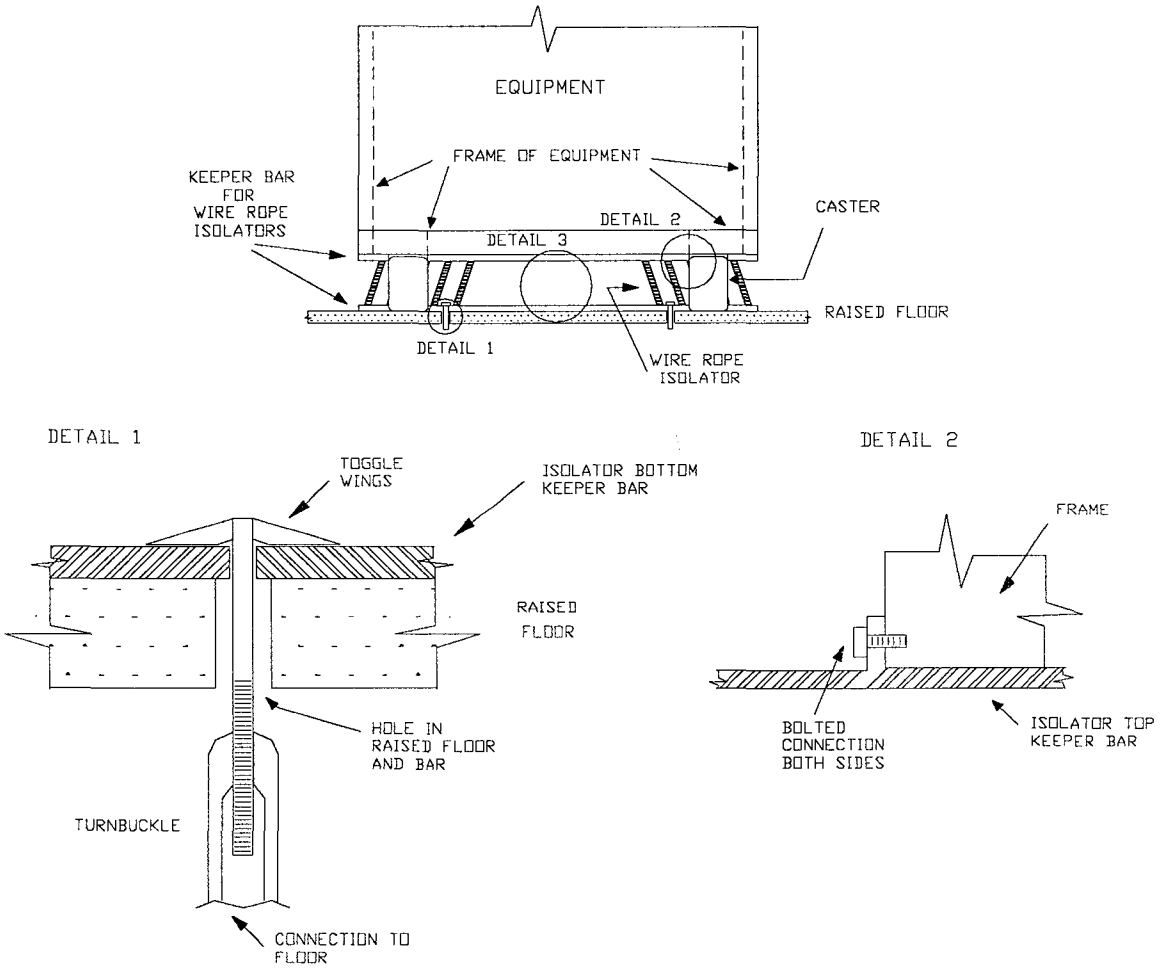

Figure 5-4 Details of Installation of Wire Rope Isolators with Uplift Restrainer.

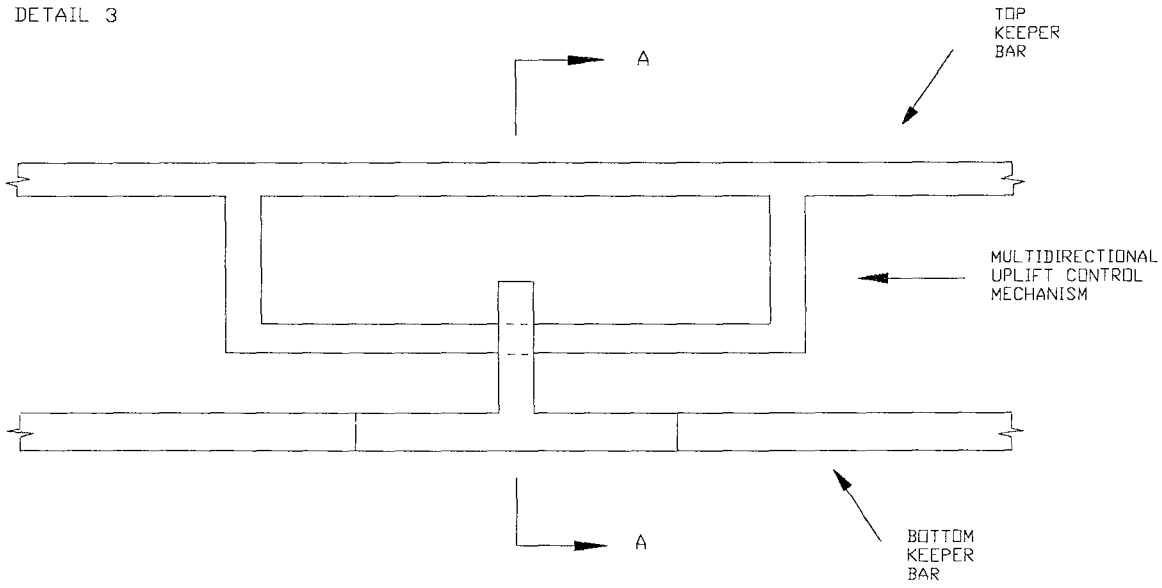

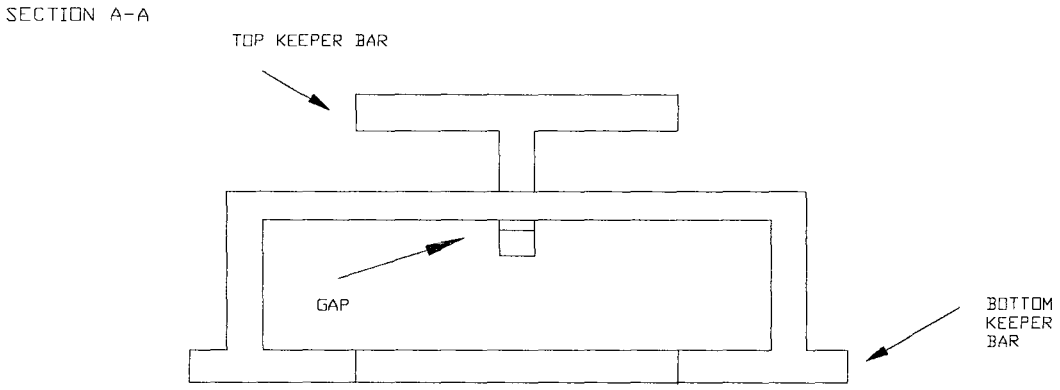

Figure 5-4 Continued.

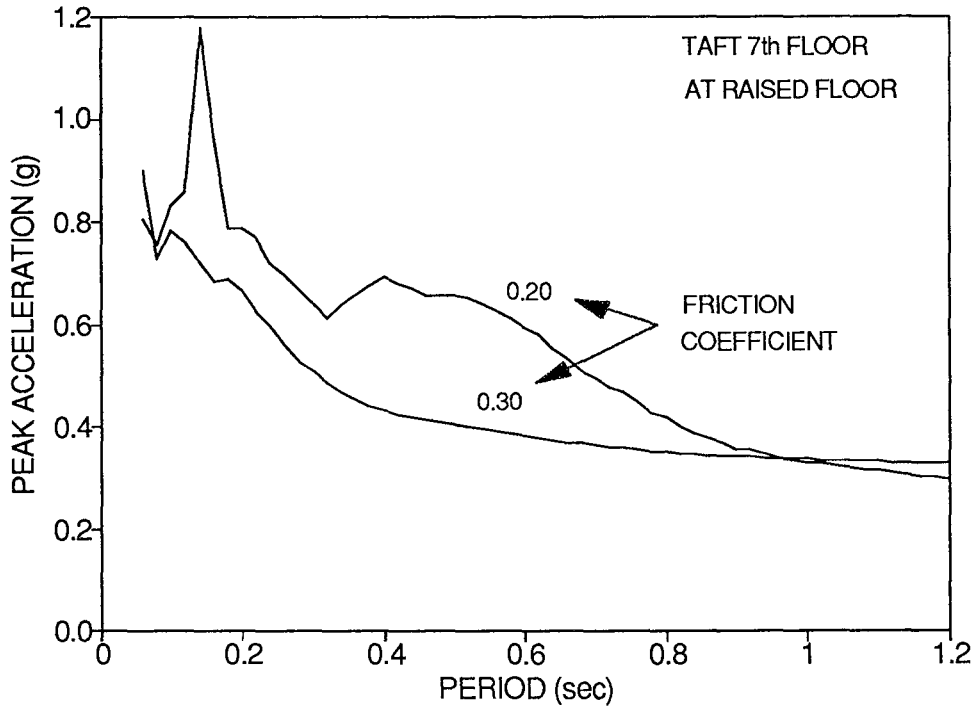

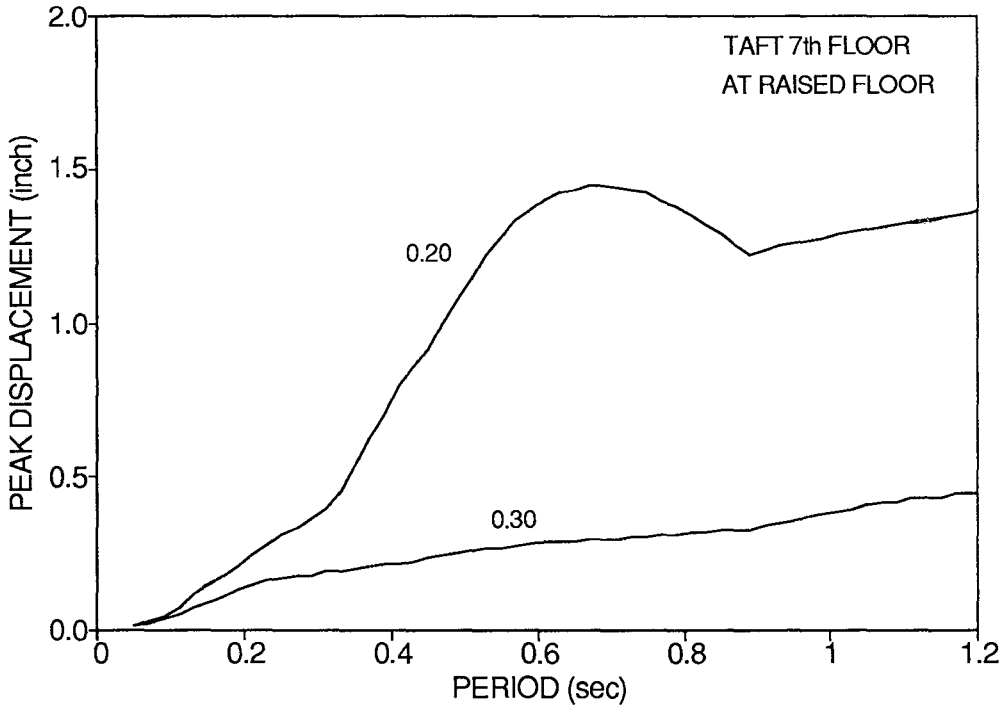

Figure 5-5 Response of Frictional Oscillator of Taft 7th Floor at Raised Floor Level (1 in.= 25.4 mm).

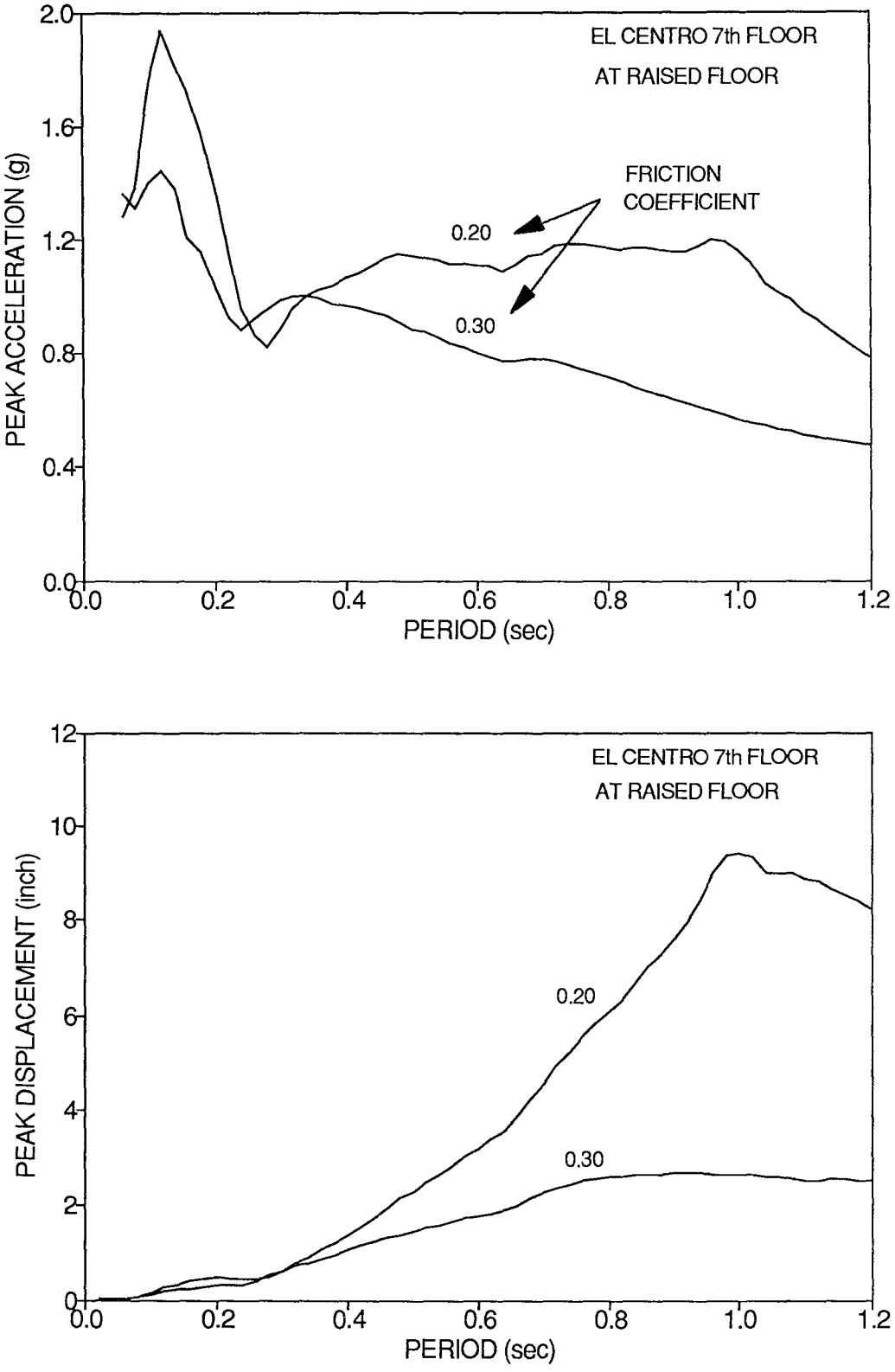

Figure 5-6 Response of Frictional Oscillator of El Centro 7th Floor at Raised Floor Level (1 in.= 25.4 mm).

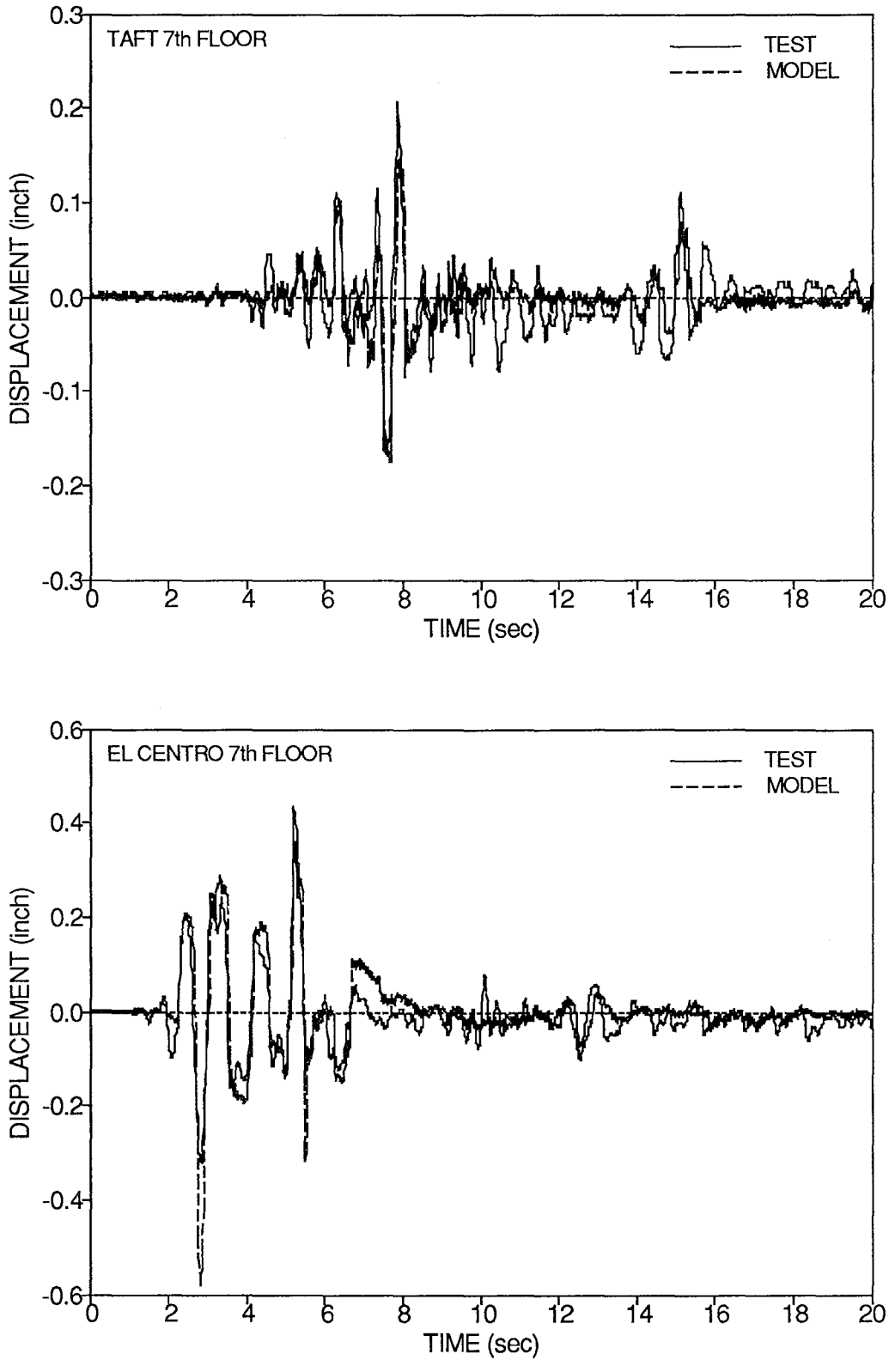

Figure 5-7 Comparison of Experimental and Analytical Time Histories of Displacement of Casters in Tested IBM Equipment (1 in.= 25.4 mm).

SECTION 6

CONCLUSIONS

Wire rope systems for the seismic protection of equipment in buildings have been studied experimentally and analytically. Two installation methods were considered: one in which the equipment is supported by wire rope isolators and one in which the equipment is supported by locked casters and wire rope isolators are used for providing restoring force.

It has been found that wire rope isolators exhibit hysteretic damping which decreases with increasing amplitude of motion. Typical values of equivalent damping ratio are about 0.1 of critical for large deformations and about 0.2 to 0.3 of critical for small deformations. These values were measured in systems which reduced the acceleration response of the tested equipment in comparison to that of a fixed equipment.

Based on these results, it was concluded that stiff wire rope systems may provide a degree of protection to equipment in buildings while allowing very small displacements. In contrast, the classical isolation approach of increasing the period of the system to values beyond the predominant period of the input motion is impractical because a) floor seismic motions are rich in long period components, and b) displacements are unacceptably large for equipment.

Analytical models for describing the hysteretic behavior of wire rope isolators have been developed and

experimentally calibrated and verified. Analytical predictions of response of an equipment supported by wire rope isolators were in good agreement with experimental results. Furthermore, a simplified analysis method was developed and shown to be capable of providing reliable estimates of the peak response of equipment supported by wire rope isolators. The method makes use of floor response spectra which is the usual design specification for equipment.

The second installation method for equipment, consisting of locked casters to support the weight and wire rope isolators, was tested with an IBM computer equipment. The equipment was placed on top of a raised floor as it would have been in service. The response of the equipment in terms of peak accelerations and displacements of the locked casters was monitored in shake table tests and compared to the response of the equipment supported by other commonly used systems. It was found that the used stiff wire rope system reduced or maintained accelerations at the same level while reducing displacements by a factor of about 10. Based on these results, an installation method using wire rope isolators and an uplift control mechanism was proposed. This installation method is not permanent but, rather, it allows for easy removal for relocation of the equipment.

SECTION 7
REFERENCES

Bouc, R. (1971). "Modele mathematique d'hysteresis." Acustica, 24(1), 16-25 (in French).

Buckle, I.G. and Mayes, R.L. (1990). "Seismic isolation history, application and performance - a world view." Earthquake Spectra, 6(2), 161-201.

Chalhoub, M. and Kelly, J.M (1988). "Theoretical and experimental studies of cylindrical water tanks in base-isolated structures." Report No. UCB/EERC-88/07, Earthquake Engineering Research Center, University of California, Berkeley, CA.

Chalhoub, M.S., and Kelly, J.M. (1990). "Sliders and tension controlled reinforced elastomeric bearings combined for earthquake isolation." Earthq. Engng. Struct. Dyn., 19, 333-344.

Chen, Y.Q., and Soong, T.T. (1988). "State-of-the-art review: Seismic response of secondary systems." Engng. Struct., 10, 218-228.

Clough, R.W. and Penzien, J. (1975), "Dynamics of Structures", McGraw-Hill Co., New York, N.Y.

Constantinou, M.C., and Adnane, M.A. (1987). "Dynamics of soil-based-isolated-structure systems : Evaluation of two models for yielding systems." Report to the National Science Foundation, Dept. of Civil Engng., Drexel Univ., Philadelphia, PA.

Constantinou, M.C., Caccese, J., and Harris, G.H. (1987). "Frictional characteristics of teflon-steel interfaces under dynamic conditions." Earthquake Engineering and Structural Dynamics, Vol. 15, 151-759.

Constantinou, M.C., Mokha, A.S. and Reinhorn, A.M.(1990a). "Teflon bearings in base isolation. II: Modeling." J. Struct. Engng., ASCE, 116 (2), 455-474.

Constantinou, M.C., Mokha, A.S., and Reinhorn, A.M. (1990b). "Experimental and analytical study of combined sliding disc bearing and helical steel spring isolation system." Report No. NCEER-90-0019, National Center for Earthquake Engineering Research, State University of New York, Buffalo, NY.

Constantinou, M.C., Mokha, A., and Reinhorn, A.M.(1991). "Study of sliding bearing and helical-steel-spring isolation system." J. Struct. Engng., ASCE, 117 (4), 1257-1275.

Fujita, T. editor (1991). "Seismic isolation and response control for nuclear and non-nuclear structures." Special Issue for the Exhibition of the 11th International Conference on Structural Mechanics in Reactor Technology (SMiRT 11), August 18-23, Tokyo, Japan.

Gear, C.W., (1971). " Numerical initial-value problems in ordinary differential equations" Prentice-Hall, Englewood Cliffs, New Jersey.

IMSL Mathematical Library (1987). "Fortran library for mathematical applications." Subroutine IVPAG.

Juhn, G., Manolis, G.D., Constantinou, M.C., and Reinhorn, A.M. (1992). "Experimental study of secondary systems in a base-isolated structure." J. Struct. Engng., ASCE, to appear.

Kamke, E. (1959). "Differentialgleichungen lösungsmethoden und lösungen." Chelsea Publishing Co., New York, NY.

Kelly, J.M. (1982). "The influence of base isolation on the seismic response of light secondary equipment." Report No. UCB/EERC - 81/17, Earthquake Engineering Research Center, University of California, Berkeley, California.

Kelly, J.M., and Tsai, H.C. (1985). "Seismic response of light internal equipment in base-isolated structures." Earthquake Engng. Struct. Dyn., 13, 711-732.

Kelly, J.M. (1988) "Base isolation in Japan, 1988", Report No. EERC 88-20, Earthquake Engineering Research Center, University of California, Berkeley, CA.

Kelly, J.M. (1991). "Base isolation: origins and development." News-Earthquake Engng. Res. Ctr., Univ. of California, Berkeley, Calif., 12(1), 1-3.

Lin, J. and Mahin, S.A.(1985). "Seismic response of light subsystems on inelastic structures." J. Struct. Engng., ASCE, 111(2), 400-417.

Makris, N.(1992a). "Theoretical and experimental investigation of viscous dampers in applications of seismic and vibration isolation." Ph.D. Dissertation, State University of New York at Buffalo, Buffalo, NY.

Makris, N. and Constantinou, M.C. (1992b). "Spring-viscous damper systems for combined seismic and vibration isolation." Earthquake Engng. and Struct. Dynamics, Vol. 21, to appear.

Manolis, G.D, Juhn, G., Constantinou, M.C., and Reinhorn, A.M. (1990). "Secondary systems in base isolated structures: Experimental investigation, stochastic response and stochastic sensitivity." Report No. NCEER-90-0013, National Center for Earthquake Engineering Research, State University of New York, Buffalo, NY.

Mokha, A., Constantinou, M.C., and Reinhorn, A.M. (1990). "Experimental study and analytical prediction of earthquake response of a sliding isolation system with a spherical surface." Report No. NCEER-90-0020, National Center for Earthquake Engineering Research, State University of New York, Buffalo, NY.

Mokha, A., Constantinou, M.C., Reinhorn, A.M., and Zayas, V. (1991). "Experimental study of friction pendulum isolation system." J. Struct. Engng., ASCE, 117(4), 1201-1217.

Okamoto, S., Nakata, S., Kitagawa, Y., Yoshimura, M., and Kaminosono, T. (1985) " Progress report on the full-scale seismic experiment of a seven-story reinforced concrete building-part of U.S. - Japan cooperative program." Research paper No. 94, Building Research Institute, Ministry of Construction, Japan.

Ozdemir, H. (1976). "Nonlinear transient dynamic analysis of yielding structures," thesis presented to the University of California, at Berkeley, Calif., in partial fulfillment of the requirements for the degree of Doctor of Philosophy.

Park, Y.J., Reinhorn, M., and Kunnath, S.K. (1987) "IDARC: inelastic damage analysis of reinforced concrete frame-shear-wall structures," Report No. NCEER-87-0008, National Center for Earthquake Engineering Research, Buffalo, NY.

Singh, M.P. (1988). "Seismic design of secondary systems" Prob. Engng. Mech., 3(3), 151-158.

Tsai, H.C., and Kelly, J.M. (1989). "Seismic response of the superstructure and attached equipment in a base-isolated building." Earthquake Engng. Struct. Dyn., 18, 551-564.

Wen, Y.K. (1976). "Method of random vibration of hysteretic systems." J. Engng. Mech. Div., ASCE, 102(2), 249-263.

Zayas, V., Low, S.S., and Mahin, S.A. (1987). "The FPS earthquake resisting system, experimental report." Report No. UCB/EERC-87/01, Earthquake Engineering Research Center, University of California, Berkeley, Calif., June.

NATIONAL CENTER FOR EARTHQUAKE ENGINEERING RESEARCH
LIST OF TECHNICAL REPORTS

The National Center for Earthquake Engineering Research (NCEER) publishes technical reports on a variety of subjects related to earthquake engineering written by authors funded through NCEER. These reports are available from both NCEER's Publications Department and the National Technical Information Service (NTIS). Requests for reports should be directed to the Publications Department, National Center for Earthquake Engineering Research, State University of New York at Buffalo, Red Jacket Quadrangle, Buffalo, New York 14261. Reports can also be requested through NTIS, 5285 Port Royal Road, Springfield, Virginia 22161. NTIS accession numbers are shown in parenthesis, if available.

NCEER-87-0001 "First-Year Program in Research, Education and Technology Transfer," 3/5/87, (PB88-134275/AS).

NCEER-87-0002 "Experimental Evaluation of Instantaneous Optimal Algorithms for Structural Control," by R.C. Lin, T.T. Soong and A.M. Reinhorn, 4/20/87, (PB88-134341/AS).

NCEER-87-0003 "Experimentation Using the Earthquake Simulation Facilities at University at Buffalo," by A.M. Reinhorn and R.L. Ketter, to be published.

NCEER-87-0004 "The System Characteristics and Performance of a Shaking Table," by J.S. Hwang, K.C. Chang and G.C. Lee, 6/1/87, (PB88-134259/AS). This report is available only through NTIS (see address given above).

NCEER-87-0005 "A Finite Element Formulation for Nonlinear Viscoplastic Material Using a Q Model," by O. Gyebi and G. Dasgupta, 11/2/87, (PB88-213764/AS).

NCEER-87-0006 "Symbolic Manipulation Program (SMP) - Algebraic Codes for Two and Three Dimensional Finite Element Formulations," by X. Lee and G. Dasgupta, 11/9/87, (PB88-219522/AS).

NCEER-87-0007 "Instantaneous Optimal Control Laws for Tall Buildings Under Seismic Excitations," by J.N. Yang, A. Akbarpour and P. Ghaemmaghami, 6/10/87, (PB88-134333/AS).

NCEER-87-0008 "IDARC: Inelastic Damage Analysis of Reinforced Concrete Frame - Shear-Wall Structures," by Y.J. Park, A.M. Reinhorn and S.K. Kunnath, 7/20/87, (PB88-134325/AS).

NCEER-87-0009 "Liquefaction Potential for New York State: A Preliminary Report on Sites in Manhattan and Buffalo," by M. Budhu, V. Vijayakumar, R.F. Giese and L. Baumgras, 8/31/87, (PB88-163704/AS). This report is available only through NTIS (see address given above).

NCEER-87-0010 "Vertical and Torsional Vibration of Foundations in Inhomogeneous Media," by A.S. Veletsos and K.W. Dotson, 6/1/87, (PB88-134291/AS).

NCEER-87-0011 "Seismic Probabilistic Risk Assessment and Seismic Margins Studies for Nuclear Power Plants," by Howard H.M. Hwang, 6/15/87, (PB88-134267/AS).

NCEER-87-0012 "Parametric Studies of Frequency Response of Secondary Systems Under Ground-Acceleration Excitations," by Y. Yong and Y.K. Lin, 6/10/87, (PB88-134309/AS).

NCEER-87-0013 "Frequency Response of Secondary Systems Under Seismic Excitation," by J.A. HoLung, J. Cai and Y.K. Lin, 7/31/87, (PB88-134317/AS).

NCEER-87-0014 "Modelling Earthquake Ground Motions in Seismically Active Regions Using Parametric Time Series Methods," by G.W. Ellis and A.S. Cakmak, 8/25/87, (PB88-134283/AS).

NCEER-87-0015 "Detection and Assessment of Seismic Structural Damage," by E. DiPasquale and A.S. Cakmak, 8/25/87, (PB88-163712/AS).

NCEER-87-0016 "Pipeline Experiment at Parkfield, California," by J. Isenberg and E. Richardson, 9/15/87, (PB88-163720/AS). This report is available only through NTIS (see address given above).

NCEER-87-0017 "Digital Simulation of Seismic Ground Motion," by M. Shinozuka, G. Deodatis and T. Harada, 8/31/87, (PB88-155197/AS). This report is available only through NTIS (see address given above).

NCEER-87-0018 "Practical Considerations for Structural Control: System Uncertainty, System Time Delay and Truncation of Small Control Forces," J.N. Yang and A. Akbarpour, 8/10/87, (PB88-163738/AS).

NCEER-87-0019 "Modal Analysis of Nonclassically Damped Structural Systems Using Canonical Transformation," by J.N. Yang, S. Sarkani and F.X. Long, 9/27/87, (PB88-187851/AS).

NCEER-87-0020 "A Nonstationary Solution in Random Vibration Theory," by J.R. Red-Horse and P.D. Spanos, 11/3/87, (PB88-163746/AS).

NCEER-87-0021 "Horizontal Impedances for Radially Inhomogeneous Viscoelastic Soil Layers," by A.S. Veletsos and K.W. Dotson, 10/15/87, (PB88-150859/AS).

NCEER-87-0022 "Seismic Damage Assessment of Reinforced Concrete Members," by Y.S. Chung, C. Meyer and M. Shinozuka, 10/9/87, (PB88-150867/AS). This report is available only through NTIS (see address given above).

NCEER-87-0023 "Active Structural Control in Civil Engineering," by T.T. Soong, 11/11/87, (PB88-187778/AS).

NCEER-87-0024 "Vertical and Torsional Impedances for Radially Inhomogeneous Viscoelastic Soil Layers," by K.W. Dotson and A.S. Veletsos, 12/87, (PB88-187786/AS).

NCEER-87-0025 "Proceedings from the Symposium on Seismic Hazards, Ground Motions, Soil-Liquefaction and Engineering Practice in Eastern North America," October 20-22, 1987, edited by K.H. Jacob, 12/87, (PB88-188115/AS).

NCEER-87-0026 "Report on the Whittier-Narrows, California, Earthquake of October 1, 1987," by J. Pantelic and A. Reinhorn, 11/87, (PB88-187752/AS). This report is available only through NTIS (see address given above).

NCEER-87-0027 "Design of a Modular Program for Transient Nonlinear Analysis of Large 3-D Building Structures," by S. Srivastav and J.F. Abel, 12/30/87, (PB88-187950/AS).

NCEER-87-0028 "Second-Year Program in Research, Education and Technology Transfer," 3/8/88, (PB88-219480/AS).

NCEER-88-0001 "Workshop on Seismic Computer Analysis and Design of Buildings With Interactive Graphics," by W. McGuire, J.F. Abel and C.H. Conley, 1/18/88, (PB88-187760/AS).

NCEER-88-0002 "Optimal Control of Nonlinear Flexible Structures," by J.N. Yang, F.X. Long and D. Wong, 1/22/88, (PB88-213772/AS).

NCEER-88-0003 "Substructuring Techniques in the Time Domain for Primary-Secondary Structural Systems," by G.D. Manolis and G. Juhn, 2/10/88, (PB88-213780/AS).

NCEER-88-0004 "Iterative Seismic Analysis of Primary-Secondary Systems," by A. Singhal, L.D. Lutes and P.D. Spanos, 2/23/88, (PB88-213798/AS).

NCEER-88-0005 "Stochastic Finite Element Expansion for Random Media," by P.D. Spanos and R. Ghanem, 3/14/88, (PB88-213806/AS).

NCEER-88-0006 "Combining Structural Optimization and Structural Control," by F.Y. Cheng and C.P. Pantelides, 1/10/88, (PB88-213814/AS).

NCEER-88-0007 "Seismic Performance Assessment of Code-Designed Structures," by H.H-M. Hwang, J-W. Jaw and H-J. Shau, 3/20/88, (PB88-219423/AS).

NCEER-88-0008 "Reliability Analysis of Code-Designed Structures Under Natural Hazards," by H.H-M. Hwang, H. Ushiba and M. Shinozuka, 2/29/88, (PB88-229471/AS).

NCEER-88-0009 "Seismic Fragility Analysis of Shear Wall Structures," by J-W Jaw and H.H-M. Hwang, 4/30/88, (PB89-102867/AS).

NCEER-88-0010 "Base Isolation of a Multi-Story Building Under a Harmonic Ground Motion - A Comparison of Performances of Various Systems," by F-G Fan, G. Ahmadi and I.G. Tadjbakhsh, 5/18/88, (PB89-122238/AS).

NCEER-88-0011 "Seismic Floor Response Spectra for a Combined System by Green's Functions," by F.M. Lavelle, L.A. Bergman and P.D. Spanos, 5/1/88, (PB89-102875/AS).

NCEER-88-0012 "A New Solution Technique for Randomly Excited Hysteretic Structures," by G.Q. Cai and Y.K. Lin, 5/16/88, (PB89-102883/AS).

NCEER-88-0013 "A Study of Radiation Damping and Soil-Structure Interaction Effects in the Centrifuge," by K. Weissman, supervised by J.H. Prevost, 5/24/88, (PB89-144703/AS).

NCEER-88-0014 "Parameter Identification and Implementation of a Kinematic Plasticity Model for Frictional Soils," by J.H. Prevost and D.V. Griffiths, to be published.

NCEER-88-0015 "Two- and Three- Dimensional Dynamic Finite Element Analyses of the Long Valley Dam," by D.V. Griffiths and J.H. Prevost, 6/17/88, (PB89-144711/AS).

NCEER-88-0016 "Damage Assessment of Reinforced Concrete Structures in Eastern United States," by A.M. Reinhorn, M.J. Seidel, S.K. Kunnath and Y.J. Park, 6/15/88, (PB89-122220/AS).

NCEER-88-0017 "Dynamic Compliance of Vertically Loaded Strip Foundations in Multilayered Viscoelastic Soils," by S. Ahmad and A.S.M. Israil, 6/17/88, (PB89-102891/AS).

NCEER-88-0018 "An Experimental Study of Seismic Structural Response With Added Viscoelastic Dampers," by R.C. Lin, Z. Liang, T.T. Soong and R.H. Zhang, 6/30/88, (PB89-122212/AS). This report is available only through NTIS (see address given above).

NCEER-88-0019 "Experimental Investigation of Primary - Secondary System Interaction," by G.D. Manolis, G. Juhn and A.M. Reinhorn, 5/27/88, (PB89-122204/AS).

NCEER-88-0020 "A Response Spectrum Approach For Analysis of Nonclassically Damped Structures," by J.N. Yang, S. Sarkani and F.X. Long, 4/22/88, (PB89-102909/AS).

NCEER-88-0021 "Seismic Interaction of Structures and Soils: Stochastic Approach," by A.S. Veletsos and A.M. Prasad, 7/21/88, (PB89-122196/AS).

NCEER-88-0022 "Identification of the Serviceability Limit State and Detection of Seismic Structural Damage," by E. DiPasquale and A.S. Cakmak, 6/15/88, (PB89-122188/AS). This report is available only through NTIS (see address given above).

NCEER-88-0023 "Multi-Hazard Risk Analysis: Case of a Simple Offshore Structure," by B.K. Bhartia and E.H. Vanmarcke, 7/21/88, (PB89-145213/AS).

NCEER-88-0024 "Automated Seismic Design of Reinforced Concrete Buildings," by Y.S. Chung, C. Meyer and M. Shinozuka, 7/5/88, (PB89-122170/AS). This report is available only through NTIS (see address given above).

NCEER-88-0025 "Experimental Study of Active Control of MDOF Structures Under Seismic Excitations," by L.L. Chung, R.C. Lin, T.T. Soong and A.M. Reinhorn, 7/10/88, (PB89-122600/AS).

NCEER-88-0026 "Earthquake Simulation Tests of a Low-Rise Metal Structure," by J.S. Hwang, K.C. Chang, G.C. Lee and R.L. Ketter, 8/1/88, (PB89-102917/AS).

NCEER-88-0027 "Systems Study of Urban Response and Reconstruction Due to Catastrophic Earthquakes," by F. Kozin and H.K. Zhou, 9/22/88, (PB90-162348/AS).

NCEER-88-0028 "Seismic Fragility Analysis of Plane Frame Structures," by H.H-M. Hwang and Y.K. Low, 7/31/88, (PB89-131445/AS).

NCEER-88-0029 "Response Analysis of Stochastic Structures," by A. Kardara, C. Bucher and M. Shinozuka, 9/22/88, (PB89-174429/AS).

NCEER-88-0030 "Nonnormal Accelerations Due to Yielding in a Primary Structure," by D.C.K. Chen and L.D. Lutes, 9/19/88, (PB89-131437/AS).

NCEER-88-0031 "Design Approaches for Soil-Structure Interaction," by A.S. Veletsos, A.M. Prasad and Y. Tang, 12/30/88, (PB89-174437/AS). This report is available only through NTIS (see address given above).

NCEER-88-0032 "A Re-evaluation of Design Spectra for Seismic Damage Control," by C.J. Turkstra and A.G. Tallin, 11/7/88, (PB89-145221/AS).

NCEER-88-0033 "The Behavior and Design of Noncontact Lap Splices Subjected to Repeated Inelastic Tensile Loading," by V.E. Sagan, P. Gergely and R.N. White, 12/8/88, (PB89-163737/AS).

NCEER-88-0034 "Seismic Response of Pile Foundations," by S.M. Mamoon, P.K. Banerjee and S. Ahmad, 11/1/88, (PB89-145239/AS).

NCEER-88-0035 "Modeling of R/C Building Structures With Flexible Floor Diaphragms (IDARC2)," by A.M. Reinhorn, S.K. Kunnath and N. Panahshahi, 9/7/88, (PB89-207153/AS).

NCEER-88-0036 "Solution of the Dam-Reservoir Interaction Problem Using a Combination of FEM, BEM with Particular Integrals, Modal Analysis, and Substructuring," by C-S. Tsai, G.C. Lee and R.L. Ketter, 12/31/88, (PB89-207146/AS).

NCEER-88-0037 "Optimal Placement of Actuators for Structural Control," by F.Y. Cheng and C.P. Pantelides, 8/15/88, (PB89-162846/AS).

NCEER-88-0038 "Teflon Bearings in Aseismic Base Isolation: Experimental Studies and Mathematical Modeling," by A. Mokha, M.C. Constantinou and A.M. Reinhorn, 12/5/88, (PB89-218457/AS). This report is available only through NTIS (see address given above).

NCEER-88-0039 "Seismic Behavior of Flat Slab High-Rise Buildings in the New York City Area," by P. Weidlinger and M. Ettouney, 10/15/88, (PB90-145681/AS).

NCEER-88-0040 "Evaluation of the Earthquake Resistance of Existing Buildings in New York City," by P. Weidlinger and M. Ettouney, 10/15/88, to be published.

NCEER-88-0041 "Small-Scale Modeling Techniques for Reinforced Concrete Structures Subjected to Seismic Loads," by W. Kim, A. El-Attar and R.N. White, 11/22/88, (PB89-189625/AS).

NCEER-88-0042 "Modeling Strong Ground Motion from Multiple Event Earthquakes," by G.W. Ellis and A.S. Cakmak, 10/15/88, (PB89-174445/AS).

NCEER-88-0043 "Nonstationary Models of Seismic Ground Acceleration," by M. Grigoriu, S.E. Ruiz and E. Rosenblueth, 7/15/88, (PB89-189617/AS).

NCEER-88-0044 "SARCF User's Guide: Seismic Analysis of Reinforced Concrete Frames," by Y.S. Chung, C. Meyer and M. Shinozuka, 11/9/88, (PB89-174452/AS).

NCEER-88-0045 "First Expert Panel Meeting on Disaster Research and Planning," edited by J. Pantelic and J. Stoyle, 9/15/88, (PB89-174460/AS).

NCEER-88-0046 "Preliminary Studies of the Effect of Degrading Infill Walls on the Nonlinear Seismic Response of Steel Frames," by C.Z. Chrysostomou, P. Gergely and J.F. Abel, 12/19/88, (PB89-208383/AS).

NCEER-88-0047 "Reinforced Concrete Frame Component Testing Facility - Design, Construction, Instrumentation and Operation," by S.P. Pessiki, C. Conley, T. Bond, P. Gergely and R.N. White, 12/16/88, (PB89-174478/AS).

NCEER-89-0001 "Effects of Protective Cushion and Soil Compliancy on the Response of Equipment Within a Seismically Excited Building," by J.A. HoLung, 2/16/89, (PB89-207179/AS).

NCEER-89-0002 "Statistical Evaluation of Response Modification Factors for Reinforced Concrete Structures," by H.H-M. Hwang and J-W. Jaw, 2/17/89, (PB89-207187/AS).

NCEER-89-0003 "Hysteretic Columns Under Random Excitation," by G-Q. Cai and Y.K. Lin, 1/9/89, (PB89-196513/AS).

NCEER-89-0004 "Experimental Study of 'Elephant Foot Bulge' Instability of Thin-Walled Metal Tanks," by Z-H. Jia and R.L. Ketter, 2/22/89, (PB89-207195/AS).

NCEER-89-0005 "Experiment on Performance of Buried Pipelines Across San Andreas Fault," by J. Isenberg, E. Richardson and T.D. O'Rourke, 3/10/89, (PB89-218440/AS).

NCEER-89-0006 "A Knowledge-Based Approach to Structural Design of Earthquake-Resistant Buildings," by M. Subramani, P. Gergely, C.H. Conley, J.F. Abel and A.H. Zaghw, 1/15/89, (PB89-218465/AS).

NCEER-89-0007 "Liquefaction Hazards and Their Effects on Buried Pipelines," by T.D. O'Rourke and P.A. Lane, 2/1/89, (PB89-218481).

NCEER-89-0008 "Fundamentals of System Identification in Structural Dynamics," by H. Imai, C-B. Yun, O. Maruyama and M. Shinozuka, 1/26/89, (PB89-207211/AS).

NCEER-89-0009 "Effects of the 1985 Michoacan Earthquake on Water Systems and Other Buried Lifelines in Mexico," by A.G. Ayala and M.J. O'Rourke, 3/8/89, (PB89-207229/AS).

NCEER-89-R010 "NCEER Bibliography of Earthquake Education Materials," by K.E.K. Ross, Second Revision, 9/1/89, (PB90-125352/AS).

NCEER-89-0011 "Inelastic Three-Dimensional Response Analysis of Reinforced Concrete Building Structures (IDARC-3D), Part I - Modeling," by S.K. Kunnath and A.M. Reinhorn, 4/17/89, (PB90-114612/AS).

NCEER-89-0012 "Recommended Modifications to ATC-14," by C.D. Poland and J.O. Malley, 4/12/89, (PB90-108648/AS).

NCEER-89-0013 "Repair and Strengthening of Beam-to-Column Connections Subjected to Earthquake Loading," by M. Corazao and A.J. Durrani, 2/28/89, (PB90-109885/AS).

NCEER-89-0014 "Program EXKAL2 for Identification of Structural Dynamic Systems," by O. Maruyama, C-B. Yun, M. Hoshiya and M. Shinozuka, 5/19/89, (PB90-109877/AS).

NCEER-89-0015 "Response of Frames With Bolted Semi-Rigid Connections, Part I - Experimental Study and Analytical Predictions," by P.J. DiCorso, A.M. Reinhorn, J.R. Dickerson, J.B. Radziminski and W.L. Harper, 6/1/89, to be published.

NCEER-89-0016 "ARMA Monte Carlo Simulation in Probabilistic Structural Analysis," by P.D. Spanos and M.P. Mignolet, 7/10/89, (PB90-109893/AS).

NCEER-89-P017 "Preliminary Proceedings from the Conference on Disaster Preparedness - The Place of Earthquake Education in Our Schools," Edited by K.E.K. Ross, 6/23/89.

NCEER-89-0017 "Proceedings from the Conference on Disaster Preparedness - The Place of Earthquake Education in Our Schools," Edited by K.E.K. Ross, 12/31/89, (PB90-207895). This report is available only through NTIS (see address given above).

NCEER-89-0018 "Multidimensional Models of Hysteretic Material Behavior for Vibration Analysis of Shape Memory Energy Absorbing Devices, by E.J. Graesser and F.A. Cozzarelli, 6/7/89, (PB90-164146/AS).

NCEER-89-0019 "Nonlinear Dynamic Analysis of Three-Dimensional Base Isolated Structures (3D-BASIS)," by S. Nagarajaiah, A.M. Reinhorn and M.C. Constantinou, 8/3/89, (PB90-161936/AS). This report is available only through NTIS (see address given above).

NCEER-89-0020 "Structural Control Considering Time-Rate of Control Forces and Control Rate Constraints," by F.Y. Cheng and C.P. Pantelides, 8/3/89, (PB90-120445/AS).

NCEER-89-0021 "Subsurface Conditions of Memphis and Shelby County," by K.W. Ng, T-S. Chang and H-H.M. Hwang, 7/26/89, (PB90-120437/AS).

NCEER-89-0022 "Seismic Wave Propagation Effects on Straight Jointed Buried Pipelines," by K. Elhmadi and M.J. O'Rourke, 8/24/89, (PB90-162322/AS).

NCEER-89-0023 "Workshop on Serviceability Analysis of Water Delivery Systems," edited by M. Grigoriu, 3/6/89, (PB90-127424/AS).

NCEER-89-0024 "Shaking Table Study of a 1/5 Scale Steel Frame Composed of Tapered Members," by K.C. Chang, J.S. Hwang and G.C. Lee, 9/18/89, (PB90-160169/AS).

NCEER-89-0025 "DYNA1D: A Computer Program for Nonlinear Seismic Site Response Analysis - Technical Documentation," by Jean H. Prevost, 9/14/89, (PB90-161944/AS). This report is available only through NTIS (see address given above).

NCEER-89-0026 "1:4 Scale Model Studies of Active Tendon Systems and Active Mass Dampers for Aseismic Protection," by A.M. Reinhorn, T.T. Soong, R.C. Lin, Y.P. Yang, Y. Fukao, H. Abe and M. Nakai, 9/15/89, (PB90-173246/AS).

NCEER-89-0027 "Scattering of Waves by Inclusions in a Nonhomogeneous Elastic Half Space Solved by Boundary Element Methods," by P.K. Hadley, A. Askar and A.S. Cakmak, 6/15/89, (PB90-145699/AS).

NCEER-89-0028 "Statistical Evaluation of Deflection Amplification Factors for Reinforced Concrete Structures," by H.H.M. Hwang, J-W. Jaw and A.L. Ch'ng, 8/31/89, (PB90-164633/AS).

NCEER-89-0029 "Bedrock Accelerations in Memphis Area Due to Large New Madrid Earthquakes," by H.H.M. Hwang, C.H.S. Chen and G. Yu, 11/7/89, (PB90-162330/AS).

NCEER-89-0030 "Seismic Behavior and Response Sensitivity of Secondary Structural Systems," by Y.Q. Chen and T.T. Soong, 10/23/89, (PB90-164658/AS).

NCEER-89-0031 "Random Vibration and Reliability Analysis of Primary-Secondary Structural Systems," by Y. Ibrahim, M. Grigoriu and T.T. Soong, 11/10/89, (PB90-161951/AS).

NCEER-89-0032 "Proceedings from the Second U.S. - Japan Workshop on Liquefaction, Large Ground Deformation and Their Effects on Lifelines, September 26-29, 1989," Edited by T.D. O'Rourke and M. Hamada, 12/1/89, (PB90-209388/AS).

NCEER-89-0033 "Deterministic Model for Seismic Damage Evaluation of Reinforced Concrete Structures," by J.M. Bracci, A.M. Reinhorn, J.B. Mander and S.K. Kunnath, 9/27/89.

NCEER-89-0034 "On the Relation Between Local and Global Damage Indices," by E. DiPasquale and A.S. Cakmak, 8/15/89, (PB90-173865).

NCEER-89-0035 "Cyclic Undrained Behavior of Nonplastic and Low Plasticity Silts," by A.J. Walker and H.E. Stewart, 7/26/89, (PB90-183518/AS).

NCEER-89-0036 "Liquefaction Potential of Surficial Deposits in the City of Buffalo, New York," by M. Budhu, R. Giese and L. Baumgrass, 1/17/89, (PB90-208455/AS).

NCEER-89-0037 "A Determinstic Assessment of Effects of Ground Motion Incoherence," by A.S. Veletsos and Y. Tang, 7/15/89, (PB90-164294/AS).

NCEER-89-0038 "Workshop on Ground Motion Parameters for Seismic Hazard Mapping," July 17-18, 1989, edited by R.V. Whitman, 12/1/89, (PB90-173923/AS).

NCEER-89-0039 "Seismic Effects on Elevated Transit Lines of the New York City Transit Authority," by C.J. Costantino, C.A. Miller and E. Heymsfield, 12/26/89, (PB90-207887/AS).

NCEER-89-0040 "Centrifugal Modeling of Dynamic Soil-Structure Interaction," by K. Weissman, Supervised by J.H. Prevost, 5/10/89, (PB90-207879/AS).

NCEER-89-0041 "Linearized Identification of Buildings With Cores for Seismic Vulnerability Assessment," by I-K. Ho and A.E. Aktan, 11/1/89, (PB90-251943/AS).

NCEER-90-0001 "Geotechnical and Lifeline Aspects of the October 17, 1989 Loma Prieta Earthquake in San Francisco," by T.D. O'Rourke, H.E. Stewart, F.T. Blackburn and T.S. Dickerman, 1/90, (PB90-208596/AS).

NCEER-90-0002 "Nonnormal Secondary Response Due to Yielding in a Primary Structure," by D.C.K. Chen and L.D. Lutes, 2/28/90, (PB90-251976/AS).

NCEER-90-0003 "Earthquake Education Materials for Grades K-12," by K.E.K. Ross, 4/16/90, (PB91-113415/AS).

NCEER-90-0004 "Catalog of Strong Motion Stations in Eastern North America," by R.W. Busby, 4/3/90, (PB90-251984)/AS.

NCEER-90-0005 "NCEER Strong-Motion Data Base: A User Manuel for the GeoBase Release (Version 1.0 for the Sun3)," by P. Friberg and K. Jacob, 3/31/90 (PB90-258062/AS).

NCEER-90-0006 "Seismic Hazard Along a Crude Oil Pipeline in the Event of an 1811-1812 Type New Madrid Earthquake," by H.H.M. Hwang and C-H.S. Chen, 4/16/90(PB90-258054).

NCEER-90-0007 "Site-Specific Response Spectra for Memphis Sheahan Pumping Station," by H.H.M. Hwang and C.S. Lee, 5/15/90, (PB91-108811/AS).

NCEER-90-0008 "Pilot Study on Seismic Vulnerability of Crude Oil Transmission Systems," by T. Ariman, R. Dobry, M. Grigoriu, F. Kozin, M. O'Rourke, T. O'Rourke and M. Shinozuka, 5/25/90, (PB91-108837/AS).

NCEER-90-0009 "A Program to Generate Site Dependent Time Histories: EQGEN," by G.W. Ellis, M. Srinivasan and A.S. Cakmak, 1/30/90, (PB91-108829/AS).

NCEER-90-0010 "Active Isolation for Seismic Protection of Operating Rooms," by M.E. Talbott, Supervised by M. Shinozuka, 6/8/9, (PB91-110205/AS).

NCEER-90-0011 "Program LINEARID for Identification of Linear Structural Dynamic Systems," by C-B. Yun and M. Shinozuka, 6/25/90, (PB91-110312/AS).

NCEER-90-0012 "Two-Dimensional Two-Phase Elasto-Plastic Seismic Response of Earth Dams," by A.N. Yiagos, Supervised by J.H. Prevost, 6/20/90, (PB91-110197/AS).

NCEER-90-0013 "Secondary Systems in Base-Isolated Structures: Experimental Investigation, Stochastic Response and Stochastic Sensitivity," by G.D. Manolis, G. Juhn, M.C. Constantinou and A.M. Reinhorn, 7/1/90, (PB91-110320/AS).

NCEER-90-0014 "Seismic Behavior of Lightly-Reinforced Concrete Column and Beam-Column Joint Details," by S.P. Pessiki, C.H. Conley, P. Gergely and R.N. White, 8/22/90, (PB91-108795/AS).

NCEER-90-0015 "Two Hybrid Control Systems for Building Structures Under Strong Earthquakes," by J.N. Yang and A. Danielians, 6/29/90, (PB91-125393/AS).

NCEER-90-0016 "Instantaneous Optimal Control with Acceleration and Velocity Feedback," by J.N. Yang and Z. Li, 6/29/90, (PB91-125401/AS).

NCEER-90-0017 "Reconnaissance Report on the Northern Iran Earthquake of June 21, 1990," by M. Mehrain, 10/4/90, (PB91-125377/AS).

NCEER-90-0018 "Evaluation of Liquefaction Potential in Memphis and Shelby County," by T.S. Chang, P.S. Tang, C.S. Lee and H. Hwang, 8/10/90, (PB91-125427/AS).

NCEER-90-0019 "Experimental and Analytical Study of a Combined Sliding Disc Bearing and Helical Steel Spring Isolation System," by M.C. Constantinou, A.S. Mokha and A.M. Reinhorn, 10/4/90, (PB91-125385/AS).

NCEER-90-0020 "Experimental Study and Analytical Prediction of Earthquake Response of a Sliding Isolation System with a Spherical Surface," by A.S. Mokha, M.C. Constantinou and A.M. Reinhorn, 10/11/90, (PB91-125419/AS).

NCEER-90-0021 "Dynamic Interaction Factors for Floating Pile Groups," by G. Gazetas, K. Fan, A. Kaynia and E. Kausel, 9/10/90, (PB91-170381/AS).

NCEER-90-0022 "Evaluation of Seismic Damage Indices for Reinforced Concrete Structures," by S. Rodriguez-Gomez and A.S. Cakmak, 9/30/90, PB91-171322/AS).

NCEER-90-0023 "Study of Site Response at a Selected Memphis Site," by H. Desai, S. Ahmad, E.S. Gazetas and M.R. Oh, 10/11/90, (PB91-196857/AS).

NCEER-90-0024 "A User's Guide to Strongmo: Version 1.0 of NCEER's Strong-Motion Data Access Tool for PCs and Terminals," by P.A. Friberg and C.A.T. Susch, 11/15/90, (PB91-171272/AS).

NCEER-90-0025 "A Three-Dimensional Analytical Study of Spatial Variability of Seismic Ground Motions," by L-L. Hong and A.H.-S. Ang, 10/30/90, (PB91-170399/AS).

NCEER-90-0026 "MUMOID User's Guide - A Program for the Identification of Modal Parameters," by S. Rodriguez-Gomez and E. DiPasquale, 9/30/90, (PB91-171298/AS).

NCEER-90-0027 "SARCF-II User's Guide - Seismic Analysis of Reinforced Concrete Frames," by S. Rodriguez-Gomez, Y.S. Chung and C. Meyer, 9/30/90, (PB91-171280/AS).

NCEER-90-0028 "Viscous Dampers: Testing, Modeling and Application in Vibration and Seismic Isolation," by N. Makris and M.C. Constantinou, 12/20/90 (PB91-190561/AS).

NCEER-90-0029 "Soil Effects on Earthquake Ground Motions in the Memphis Area," by H. Hwang, C.S. Lee, K.W. Ng and T.S. Chang, 8/2/90, (PB91-190751/AS).

NCEER-91-0001 "Proceedings from the Third Japan-U.S. Workshop on Earthquake Resistant Design of Lifeline Facilities and Countermeasures for Soil Liquefaction, December 17-19, 1990," edited by T.D. O'Rourke and M. Hamada, 2/1/91, (PB91-179259/AS).

NCEER-91-0002 "Physical Space Solutions of Non-Proportionally Damped Systems," by M. Tong, Z. Liang and G.C. Lee, 1/15/91, (PB91-179242/AS).

NCEER-91-0003 "Seismic Response of Single Piles and Pile Groups," by K. Fan and G. Gazetas, 1/10/91, (PB92-174994/AS).

NCEER-91-0004 "Damping of Structures: Part 1 - Theory of Complex Damping," by Z. Liang and G. Lee, 10/10/91.

NCEER-91-0005 "3D-BASIS - Nonlinear Dynamic Analysis of Three Dimensional Base Isolated Structures: Part II," by S. Nagarajaiah, A.M. Reinhorn and M.C. Constantinou, 2/28/91, (PB91-190553/AS).

NCEER-91-0006 "A Multidimensional Hysteretic Model for Plasticity Deforming Metals in Energy Absorbing Devices," by E.J. Graesser and F.A. Cozzarelli, 4/9/91.

NCEER-91-0007 "A Framework for Customizable Knowledge-Based Expert Systems with an Application to a KBES for Evaluating the Seismic Resistance of Existing Buildings," by E.G. Ibarra-Anaya and S.J. Fenves, 4/9/91, (PB91-210930/AS).

NCEER-91-0008 "Nonlinear Analysis of Steel Frames with Semi-Rigid Connections Using the Capacity Spectrum Method," by G.G. Deierlein, S-H. Hsieh, Y-J. Shen and J.F. Abel, 7/2/91, (PB92-113828/AS).

NCEER-91-0009 "Earthquake Education Materials for Grades K-12," by K.E.K. Ross, 4/30/91, (PB91-212142/AS).

NCEER-91-0010 "Phase Wave Velocities and Displacement Phase Differences in a Harmonically Oscillating Pile," by N. Makris and G. Gazetas, 7/8/91, (PB92-108356/AS).

NCEER-91-0011 "Dynamic Characteristics of a Full-Sized Five-Story Steel Structure and a 2/5 Model," by K.C. Chang, G.C. Yao, G.C. Lee, D.S. Hao and Y.C. Yeh," to be published.

NCEER-91-0012 "Seismic Response of a 2/5 Scale Steel Structure with Added Viscoelastic Dampers," by K.C. Chang, T.T. Soong, S-T. Oh and M.L. Lai, 5/17/91 (PB92-110816/AS).

NCEER-91-0013 "Earthquake Response of Retaining Walls; Full-Scale Testing and Computational Modeling," by S. Alampalli and A-W.M. Elgamal, 6/20/91, to be published.

NCEER-91-0014 "3D-BASIS-M: Nonlinear Dynamic Analysis of Multiple Building Base Isolated Structures," by P.C. Tsopelas, S. Nagarajaiah, M.C. Constantinou and A.M. Reinhorn, 5/28/91, (PB92-113885/AS).

NCEER-91-0015 "Evaluation of SEAOC Design Requirements for Sliding Isolated Structures," by D. Theodossiou and M.C. Constantinou, 6/10/91, (PB92-114602/AS).

NCEER-91-0016 "Closed-Loop Modal Testing of a 27-Story Reinforced Concrete Flat Plate-Core Building," by H.R. Somaprasad, T. Toksoy, H. Yoshiyuki and A.E. Aktan, 7/15/91, (PB92-129980/AS).

NCEER-91-0017 "Shake Table Test of a 1/6 Scale Two-Story Lightly Reinforced Concrete Building," by A.G. El-Attar, R.N. White and P. Gergely, 2/28/91.

NCEER-91-0018 "Shake Table Test of a 1/8 Scale Three-Story Lightly Reinforced Concrete Building," by A.G. El-Attar, R.N. White and P. Gergely, 2/28/91, to be published.

NCEER-91-0019 "Transfer Functions for Rigid Rectangular Foundations," by A.S. Veletsos, A.M. Prasad and W.H. Wu, 7/31/91, to be published.

NCEER-91-0020 "Hybrid Control of Seismic-Excited Nonlinear and Inelastic Structural Systems," by J.N. Yang, Z. Li and A. Danielians, 8/1/91.

NCEER-91-0021 "The NCEER-91 Earthquake Catalog: Improved Intensity-Based Magnitudes and Recurrence Relations for U.S. Earthquakes East of New Madrid," by L. Seeber and J.G. Armbruster, 8/28/91, (PB92-176742/AS).

NCEER-91-0022 "Proceedings from the Implementation of Earthquake Planning and Education in Schools: The Need for Change - The Roles of the Changemakers," by K.E.K. Ross and F. Winslow, 7/23/91, (PB92-129998/AS).

NCEER-91-0023 "A Study of Reliability-Based Criteria for Seismic Design of Reinforced Concrete Frame Buildings," by H.H.M. Hwang and H-M. Hsu, 8/10/91.

NCEER-91-0024 "Experimental Verification of a Number of Structural System Identification Algorithms," by R.G. Ghanem, H. Gavin and M. Shinozuka, 9/18/91, (PB92-176577/AS).

NCEER-91-0025 "Probabilistic Evaluation of Liquefaction Potential," by H.H.M. Hwang and C.S. Lee," 11/25/91.

NCEER-91-0026 "Instantaneous Optimal Control for Linear, Nonlinear and Hysteretic Structures - Stable Controllers," by J.N. Yang and Z. Li, 11/15/91, (PB92-163807/AS).

NCEER-91-0027 "Experimental and Theoretical Study of a Sliding Isolation System for Bridges," by M.C. Constantinou, A. Kartoum, A.M. Reinhorn and P. Bradford, 11/15/91, (PB92-176973/AS).

NCEER-92-0001 "Case Studies of Liquefaction and Lifeline Performance During Past Earthquakes, Volume 1: Japanese Case Studies," Edited by M. Hamada and T. O'Rourke, 2/17/92.

NCEER-92-0002 "Case Studies of Liquefaction and Lifeline Performance During Past Earthquakes, Volume 2: United States Case Studies," Edited by T. O'Rourke and M. Hamada, 2/17/92.

NCEER-92-0003 "Issues in Earthquake Education," Edited by K. Ross, 2/3/92.

NCEER-92-0004 "Proceedings from the First U.S. - Japan Workshop on Earthquake Protective Systems for Bridges," 2/4/92, to be published.

NCEER-92-0005 "Seismic Ground Motion from a Haskell-Type Source in a Multiple-Layered Half-Space," A.P. Theoharis, G. Deodatis and M. Shinozuka, 1/2/92, to be published.

NCEER-92-0006 "Proceedings from the Site Effects Workshop," Edited by R. Whitman, 2/29/92.

NCEER-92-0007 "Engineering Evaluation of Permanent Ground Deformations Due to Seismically-Induced Liquefaction," by M.H. Baziar, R. Dobry and A-W.M. Elgamal, 3/24/92.

NCEER-92-0008 "A Procedure for the Seismic Evaluation of Buildings in the Central and Eastern United States," by C.D. Poland and J.O. Malley, 4/2/92.

NCEER-92-0009 "Experimental and Analytical Study of a Hybrid Isolation System Using Friction Controllable Sliding Bearings," by Q. Feng, S. Fujii and M. Shinozuka, 2/15/92, to be published.

NCEER-92-0010 "Seismic Resistance of Slab-Column Connections in Existing Non-Ductile Flat-Plate Buildings," by A.J. Durrani and Y. Du, 2/1/92, to be published.

NCEER-92-0011 "The Hysteretic and Dynamic Behavior of Brick Masonry Walls Upgraded by Ferrocement Coatings Under Cyclic Loading and Strong Simulated Ground Motion," by H. Lee and S.P. Prawel, 5/11/92, to be published.

NCEER-92-0012 "Study of Wire Rope Systems for Seismic Protection of Equipment in Buildings," by G.F. Demetriades, M.C. Constantinou and A.M. Reinhorn, 5/20/92.